The Role of Intestinal Glucocorticoid Synthesis in the Development of Colorectal Tumors

Doctoral thesis for obtaining the

academic degree of Doctor of Natural Science

(Dr. rer. nat.)

presented by

Ahmed Hassan Elshiekh, Asma

at the

Universität Konstanz

Faculty of Sciences
Department of Biology

Konstanz, 2019

Date of the oral examination: 09.04.2019

1. Reviewer: Prof. Dr. Thomas Brunner

2. Reviewer: Prof. Dr. Daniel Legler

Table of Contents

Table of Contents

Abstract

Colorectal cancer (CRC) is the third leading cause of cancer death worldwide. Despite extensive studies that resulted in many treatment and preventive measures, the overall CRC survival is still very low. Therefore, there is an urgent need for the identification of new therapeutic targets.

Liver receptor homolog-1 (LRH-1) is an important transcriptional regulator of developmental, metabolic and inflammatory pathways. In the intestinal mucosa, LRH-1 regulates intestinal homeostasis by regulation of epithelial barrier regeneration as well as inducing local glucocorticoid (GC) synthesis under immunological stress. LRH-1 is also associated with CRC development via controlling tumor cell proliferation. Recently it has been shown that tumor-derived GCs suppress the activation of T cells, and thus could contribute to suppression of immune surveillance resulting in tumor immune escape.

Although GC synthesis is demonstrated in the intestinal mucosa and colorectal tumors, it remains unknown whether local GCs play a role in the tumor onset. Moreover, the functional relevance of tumor-derived GC is hardly investigated. Nevertheless, we provide the first functional *in vivo* study for investigating the role of GC in the initiation and progression of CRC.

In this study we used the azoxymethane (AOM) and dextran sodium sulphate (DSS)-induced mouse model of inflammation-driven colon carcinogenesis, to induce tumors in mice with intestine-specific deletion of the enzyme that catalyzes the last step in the synthesis of bioactive GC, Cyp11b1, to study the direct role of GC in CRC development. Tumors were also induced in intestine-specific LRH-1 knockout mice and mice deficient of the nuclear receptor and the potent inhibitor of LRH-1, small heterodimer partner (SHP), to study the role of LRH-1 in CRC development.

We could show that intact local GC synthesis regulates intestinal epithelium homeostasis and attenuates the initiation of CRC, whereas enhanced GC synthesis abrogates CRC development. Moreover, we were able to show that LRH-1-induced proliferation and tumor-derived GCs are critical for the progression of CRC. Furthermore, we could show an unexpected role of SHP deficiency in the control of CRC development, not via the control of LRH-1-promoted tumor proliferation, but rather via the regulation of intestinal inflammation and associated tumorigenesis. Additionally, we report a possible role of LRH-1-mediated GC synthesis in CRC tumors as an important immune escape mechanism.

Taken together, our data provide the first evidence for the role of local GC synthesis in the initiation and progression of CRC development. Additionally, we identified the nuclear receptors LRH-1 and SHP as important therapeutic targets for the treatment of CRC. Furthermore, we could show a critical role of tumor-derived GCs in the regulation of anti-tumor immune responses that could possibly represent an important immune escape mechanism.

Zusammenfassung

Darmkrebs ist weltweit die dritthäufigste Krebserkrankung. Obwohl durch umfangreiche Forschung zahlreiche Behandlungs- und Präventionsmaßnahmen entwickelt wurden, ist die Überlebensrate von Darmkrebspatientin nach wie vor sehr niedrig. Daher ist es wichtig weitere therapeutisch relevante Proteine zu identifizieren, um erfolgreichere Behandlungsansätze zu entwickeln.

Liver receptor homolog-1 (LRH-1) ist entscheidend an der Regulation verschiedener Entwicklungs-, Stoffwechsel- und Entzündungsprozesse beteiligt. In der Darmschleimhaut reguliert LRH-1 die Regeneration der Epithelbarriere sowie die lokale Glucocorticoid-Synthese und trägt somit zur intestinalen Homöostase bei. Durch die Steuerung der Tumorzellproliferation wird LRH-1 jedoch außerdem mit der Entwicklung von kolorektalem Krebs (KRK) assoziiert. Erst kürzlich konnte gezeigt werden, dass von Krebszellen gebildete Glucocorticoide (GCs) die Aktivierung von T-Zellen unterdrücken. Dies führt zur Unterdrückung einer lokalen Immunantwort und damit zur Tumor-Immun-Escape.

Obwohl die GC-Synthese in der Darmschleimhaut sowie in kolorektalen Tumoren nachgewiesen werden konnte, ist bisher unklar, ob lokale GCs eine Rolle in der Entstehung von Darmkrebs spielen. Auch über die funktionelle Relevanz Tumor gebildeter GCs ist bisher wenig bekannt.

Diese Thesis ist die erste *in vivo* Studie, die die Rolle von GCs als Auslöser und die Fortschreitung von Darmkrebs untersucht. In einer Mauslinie, in der darmspezifisch Cyp11b1, das Enzym, welches für den letzten Syntheseschritt zur Bildung aktiver GCs, deletiert ist, wurde mittels Azoxymethan (AOM) und Natrium-Dextransulfat (DSS) entzündungsvermittelte Kolonkarzinogese ausgelöst. Dieses Modell wurde verwendet um die direkte Rolle von GCs in der Entstehung von KRK zu untersuchen. Um die direkte Rolle von LRH-1 in der KRK-Entstehung zu untersuchen, wurden Tumore ebenso in Mäusen mit einem darmspezifischen LRH-1 Knockout sowie in Mäusen mit einer Deletion des nukläeren Rezeptors und potenten LRH-1 Inhibitors small heterodimer partner (SHP) induziert.

Es konnte gezeigt werden, dass eine intakte lokale GC-Synthese die intestinale Homöostase reguliert und die Entstehung von KRK vermindert, während eine erhöhte Produktion von GCs die Entwicklung von Darmkrebs komplett verhindert. Darüberhinaus wurde eine kritische Beteiligung von LRH-1 induzierter Proliferation und von Tumor gebildeter GCs am Fortschreiten von Darmkrebs nachgewiesen. Die Deletion des SHP Gens offenbarte eine

unerwartete Rolle von SHP in der Kontrolle der KRK-Entwicklung durch die Regulation der Entzündungsprozesse, die zur Tumorgenese im Darm führen und nicht über die Hemmung LRH-1-vermittelter Tumorproliferation. Weitere Ergebnisse sprechen außerdem für eine mögliche Funktion der LRH-1-vermittelten GC-Synthese in Darmkrebstumoren als wichtiger Immun-Escape-Mechanismus.

Zusammengenommen liefert diese Thesis den ersten Beweis für eine Rolle der lokalen GC-Synthese bei der Initiation und dem Fortschritt von KRK. Es konnte außerdem gezeigt werden, dass die beiden nukleären Rezeptoren LRH-1 und SHP wichtige therapeutische Targets für die Behandlung von Darmkrebs sind. Darüber hinaus wurde eine entscheidende Funktion Tumor gebildeter GCs für die Regulation der Tumor gerichteten Immunabwehr aufgezeigt, die möglicherweise einen bedeutenden Immun-Escape-Mechanismus darstellt.

Abbreviations

aa	amino acids
ACTH	adrenocorticotropic hormone
APC	adenomatous polyposis coli
AF	activation function
AOM	azoxymethane
AP-1	activator protein 1
bp	base pair
BME	basement membrane extract
BSA	bovine serum albumin
CD	Cluster of differentiation
CDK	cyclin-dependent kinase
cDNA	complementary DNA
CRC	colorectal cancer
CRH	corticotropin releasing hormone
CTL	cytotoxic T lymphocyte
CO_2	carbon dioxide
CYP	cytochrome P450
DAX-1	dosage-sensitive sex reversal and adrenal hypoplasia congenital critical region on chromosome X gene
DBD	DNA-binding domain
DLPC	dilauroyl phosphatidylcholine
DMEM	Dulbecco's Modified Eagle's Medium
DNA	deoxyribonucleic acid
DSS	dextran sodium sulphate
FBS	fetal bovine serum
FTZ-F1	*fushi tarazu* factor 1
GAPDH	glyceraldehyde-3-phosphate dehydrogenase
GCs	glucocorticoids
GR	glucocorticoid receptor
HPA	hypothalamic-pituitary-adrenal
HSD	hydroxysteroid dehydrogenase
Hsp	heat shock protein

IECs	intestinal epithelial cells
IELs	intraepithelial lymphocytes
IFNγ	Interferon gamma
IHC	immunohistochemistry
IL	interleukin
i.p.	intraperitoneal
JNK	c-Jun N-terminal kinase
kb	kilobase
kDa	kilodalton
KO	knockout
LBD	ligand binding domain
LPS	lipopolysaccharide
loxP	floxed allele
LRH-1	liver receptor homolog-1
MAPK	mitogen-activated protein kinase
mh	myc-his tagged
mRNA	messenger RNA
NF-κB	nuclear factor 'kappa-light-chain-enhancer' of activated B-cells
NR	nuclear receptor
NR0B2	nuclear receptor subfamily 0, group B, member 2
NR5A1	nuclear receptor subfamily 5, group A, member 1
NR5A2	nuclear receptor subfamily 5, group A, member 2
PBS	phosphate buffered saline
PCR	polymerase chain reaction
pH	potential of hydrogen
PMA	phorbol 12-myristate 13-acetate
PPARγ	peroxisome proliferator-activated-receptor-gamma
qPCR	quantitative real-time polymerase chain reaction
ROCK	Rho kinase
RNA	ribonucleic acid
RT	room temperature
SF-1	steroidogenic factor 1
SDS	sodium dodecyl sulfate
SHP	small heterodimer partner

TF	transcription factor
TGFß	transforming growth factor beta
Th	T helper
TNF	tumor necrosis factor alpha
Treg	regulatory T cells

1 Introduction

Glucocorticoids (GCs) are steroid hormones synthesized in response to stress in order to mediate a wide range of activities, primarily anti-inflammatory and immunosuppressive (Liberman et al., 2018; Rhen and Cidlowski, 2005). GCs secretion was classically thought to be exclusively confined to the adrenal glands. However, it has been shown that various other extra-adrenal organs are capable of producing GCs, including the primary lymphoid organs, the skin, the brain, the vascular system as well as the intestine (reviewed in (Taves et al., 2011)). Evidence for local GCs synthesis comprises the detection of steroidogenic enzymes and high levels of local GCs, even upon adrenalectomy (Cima et al., 2004; Croft et al., 2008; Hostettler et al., 2012; Taves et al., 2011). The locally synthesized GCs regulate immune cells activation and result in a highly specific action. Whereas, systemic adrenal-derived GCs coordinate multiple organ functions (Reichardt and Schütz, 1998).

In the intestinal mucosa, GCs are synthesized in response to immunological stress to regulate local immune responses (Cima et al., 2004; Kostadinova et al., 2014). Interestingly, colorectal cancer cells as well as primary colon tumors were also reported to synthesize GCs (Sidler et al., 2011). The synthesis of GCs in the intestine as well as colorectal tumors is regulated by the nuclear receptor Liver Receptor Homolog-1 (LRH-1) (Mueller et al., 2007; Sidler et al., 2011).

Nuclear receptors are important regulators of gene transcription and therefore their dysfunction is linked to pathological conditions such as obesity, diabetes and cancer (Bookout et al., 2006; Zhang and Wang, 2011). There is increasing evidence for a role of LRH-1 in the development of several human cancers (Benod et al., 2011; Schoonjans et al., 2005; Thiruchelvam et al., 2011; Wang et al., 2008), thus LRH-1 is emerging as an important therapeutic target for cancer treatment (Nadolny and Dong, 2015).

In the intestinal epithelium, LRH-1 is highly expressed in the proliferating cells at the bottom of the crypts. LRH-1 regulates epithelial cell renewal, by inducing cell proliferation through the induction of cell cycle proteins, namely cyclin D1 and E1 (Botrugno et al., 2004). Furthermore, LRH-1 regulates intestinal immune homeostasis by regulating intestinal steroidogenesis (Mueller et al., 2007; Noti et al., 2010a).

Although LRH-1 was extensively studied in the field of cancer, the relevance of LRH-1-mediated GC synthesis in the development of colorectal tumors awaits further

investigation. Furthermore, although Sidler et al. described for the first time a novel LRH-1-dependent GCs production by colorectal tumors (Sidler et al., 2011), it remains unknown whether tumor derived GCs play a role in tumor progression.

In this introduction GCs will be discussed with regards to the synthesis, functions, as well as extra-adrenal production. Furthermore, intestinal immune homeostasis as well as intestinal GCs synthesis and its role in inflammatory conditions will be discussed. Moreover, an introduction to colorectal cancer including etiology, development and treatment will be deliberated. The introduction will also consider nuclear receptors conferring their mechanism of action, functions and regulation, focusing on LRH-1 and its transcriptional regulation, especially by small heterodimer partner (SHP), and LRH-1 as a potential therapeutic target.

1.1 Glucocorticoids

Glucocorticoids (GCs) are immunoregulatory hormones that regulate essential body functions in mammals, such as control of cell metabolism, growth, differentiation, immune function, and apoptosis (Bereshchenko et al., 2018; Oakley and Cidlowski, 2013). GCs are predominantly produced in the adrenal glands. Emotional, physical and immunological stress induces the production and release of GCs from the adrenal glands, which mediate immunoregulatory, mostly immunosuppressive, activities on distant target tissues and cells. GCs have an important immunosuppressive activity on T cells and T cell-mediated immune responses (Cima et al., 2004), thus synthetic GCs are used therapeutically for the treatment of autoimmune and inflammatory diseases (reviewed in (Rhen and Cidlowski, 2005)).

1.1.1 Synthesis

GCs are synthesized and released by the *zona fasciculata* of the adrenal cortex in a circadian manner and in response to environmental as well as immunological stress. The secretion of these hormones is controlled by the hypothalamic-pituitary-adrenal (HPA) axis (Nicolaides et al., 2017). Stress signals trigger the hypothalamus to release corticotropin releasing hormone (CRH), which acts on the anterior pituitary to stimulate the synthesis and secretion of adrenocorticotropic hormone (ACTH). ACTH then acts on the adrenal cortex to stimulate the production and secretion of GCs. Afterwards, GCs target the hypothalamus and anterior pituitary to inhibit the production and release of CRH and ACTH, thereby limit both the

magnitude and duration of the GC increase in a negative feedback loop (Oakley and Cidlowski, 2013; Rhen and Cidlowski, 2005).

1.1.2 Mechanism of action

GCs play a fundamental role in the maintenance of basal and stress-related homeostasis (Nicolaides et al., 2017). The GCs act via genomic (transcriptional) and non-genomic (transcription-independent) mechanisms. Most cellular actions of GCs are mediated by binding to the glucocorticoid receptor (GR), a transcription factor of the nuclear receptors (NR) superfamily which is expressed in virtually all cells and it is essential for life (Bereshchenko et al., 2018; Oakley and Cidlowski, 2013; Rhen and Cidlowski, 2005; Vandewalle et al., 2018).

The GR is sequestered predominantly in the cytoplasm in a complex formed by chaperonic molecules, such as heat shock proteins Hsp90, 70, 23 and immunophilins (Baschant and Tuckermann, 2010; Lazarus et al., 2012a). Upon binding to endogenous or synthetic GC, the GR undergoes a structural rearrangement resulting in conformational changes that allow an efficient and rapid translocation of the GR to the nucleus. Following translocation to the nucleus, the GR positively or negatively regulates the transcriptional responses of target genes, either by direct DNA-binding or by interaction with other proteins (Bereshchenko et al., 2018; Oakley and Cidlowski, 2013).

GCs are acting on nearly every tissue and organ in the body and their function is to maintain physiological homeostasis both in response to normal diurnal changes in metabolism, as well as under stress conditions (Oakley and Cidlowski, 2013). GC effector function involve a wide variety of fundamental processes, such as metabolic homeostasis, blood pressure regulation, mental health, cognition, reproduction, cell proliferation, development and inflammation (reviewed in (Vandewalle et al., 2018)). Another mechanism of action of GC includes induction of proteins with anti-inflammatory activities, such as glucocorticoid-induced leucine zipper (GILZ) (Bereshchenko et al., 2018). Non-genomic pathway of GCs signaling is through direct interaction with membrane-associated receptors and second messengers (Rhen and Cidlowski, 2005).

1.1.3 Anti-inflammatory actions of GCs

Inflammation is a physiological response of the body to tissue injury, pathogen invasion and irritants. During inflammation, immune cells of the innate and adaptive immune system are

activated and recruited to the site of inflammation (Schonthaler et al., 2011). Although categorically distinct, the innate (the relatively non-specific immediate host defense system that provides a rapid reaction to infection and tissue damage) and adaptive (the more slowly acquired, highly antigen-specific response) immune systems interact and often overlap during an inflammatory response. Indeed, although acute inflammation is largely mediated by the innate immune system, the adaptive immune system often plays a major role in chronic inflammatory disease, with deregulated lymphocyte responses (Coutinho and Chapman, 2011).

The activation and recruitment of immune cells is mediated via cytokines and chemokines, that are regulated by inflammatory transcription factors (TFs) including the nuclear factor 'kappa-light-chain-enhancer' of activated B-cells (NF-κB), Signal transducer and activator of transcription proteins (STATs) and activator protein 1 (AP-1) (Schonthaler et al., 2011). The aforementioned TFs are crucial regulators of a variety of cellular functions comprising cell survival, proliferation, differentiation and apoptosis (Ameyar et al., 2003; Hankey et al., 2018; Pasparakis, 2012; Rawlings et al., 2004). Upon inflammation these TFs trigger activation of pro-inflammatory genes, such as tumor necrosis factor alpha (TNF) among others, to induce inflammation and promote cell survival (McEwan et al., 1997).

GR was reported to interact directly with NF-κB (McEwan et al., 1997), STAT3 (Zhang et al., 1997), STAT5 and AP-1 leading to their inhibition, hence repressing the expression of pro-inflammatory genes. Furthermore, GC-mediated induction of GILZ exerts anti-inflammatory actions comprising inhibition of mitogen-activated protein kinase (MAPK) pathway activity (Bereshchenko et al., 2018). MAPK activation is associated with cell proliferation, differentiation, migration, senescence and apoptosis (reviewed in (Sun et al., 2015)). GILZ also inhibits NF-κB and AP-1 activities (Bereshchenko et al., 2018; Vandevyver et al., 2013). The inhibition of these important inflammatory pathways by GCs results in the resolution of inflammation (Baschant and Tuckermann, 2010).

1.1.4 Modulation of immune responses by GCs

GCs mediate immunosuppressive functions by acting on almost all types of immune cells (Liberman et al., 2018). They control the function of various innate immunity cells, such as neutrophils (the major infiltrating cell type in acute inflammation), macrophages, natural killer cells and dendritic cells (DCs) (Bereshchenko et al., 2018). GCs can regulate the phenotype, survival, and functions of monocytes and macrophages, thereby playing crucial

roles in tissue homeostasis and innate immunity (Liberman et al., 2018). GCs efficiently suppress classical pro-inflammatory macrophage (M1) activation, as evidenced by the inhibition of the pro-inflammatory cytokines TNF, interferon gamma (IFNγ) and interleukin 1β (IL-1β) (Ehrchen et al., 2007). The mentioned cytokines were reported to be highly upregulated in many inflammatory disorders, suggesting a role in these pathophysiologies (Bode et al., 1998). Upon GC treatment an alternative anti-inflammatory macrophage (M2) phenotype was observed, evident by the induced expression of the immunomodulatory cytokine IL-10 (Ehrchen et al., 2007). Moreover, GCs promote the survival of anti-inflammatory macrophages via prolonged activation of the MAPK pathway resulting in inhibition of caspase activities, the central executers of apoptotic cell death, and expression of anti-apoptotic genes (Barczyk et al., 2010).

Furthermore, GCs potently inhibit DCs functions via different mechanisms including promoting apoptosis (Baschant and Tuckermann, 2010), disturbing maturation demonstrated by strong reduction in the capacity of GC-treated DCs to stimulate T cells (Woltman et al., 2000). In addition to inducing a tolerogenic DCs phenotype via downregulation of major histocompatibility complex class II (MHCII), of co-stimulatory molecules, and of cytokine expression (Baschant and Tuckermann, 2010), such effects on DCs are associated with reduced proliferative and T helper 1 (Th1) responses and an increase in immunosuppressive regulatory T cells (Treg) (Chen et al., 2017).

Effects of GC on adaptive immune cells include induction of apoptosis in developing thymocytes as well as circulating and tissue resident T cells, mediated by the pro-apoptotic proteins Puma and Bim (Brunner et al., 2001; Erlacher et al., 2006; Mittelstadt et al., 2018). GCs were also reported to promote the shift from Th1 to Th2 immune responses by differentially regulating apoptosis of Th1 and Th2 cells (Ashwell et al., 2000; Ramírez et al., 1996). Moreover, GCs upregulate the expression of the master regulator of Treg cells, FoxP3, thereby leading to expansion of immunosuppressive Treg population (Chen et al., 2006; Ugor et al., 2018).

The resulting immune reaction in pathophysiological conditions depends on the balance between effector cells producing inflammation and its modulation by regulatory mechanisms (Souza et al., 2016). In this context, the discussed anti-inflammatory and immunosuppressive properties of GCs are necessary to restore homeostasis following successful elimination of the injurious agent, ultimately leading to the resolution of inflammation and tissue repair by preventing tissue damage caused by excessive inflammation (Coutinho and Chapman, 2011).

1.2 Adrenal GC synthesis and regulation

Adrenal GC synthesis is substantially regulated by the transcriptional control of steroidogenic enzymes of the cytochrome P450 gene family (CYP), as well as hydroxysteroid dehydrogenase (HSD) enzymes (Bouguen et al., 2015a). GCs are synthesized from the precursor cholesterol, and the pathway is depicted in Figure 1. Briefly, side-chain cleavage cytochrome P450; P450scc (CYP11A1) converts cholesterol to pregnenolone, which is the first and rate-limiting step in steroid synthesis. Type I 3β hydroxysteroid dehydrogenase (HSD3B1) converts pregnenolone to progesterone. Next, 21-hydroxylase (CYP21) converts progesterone into 11-deoxycortisol, and 11β-hydroxylase encoded by the CYP11B1 gene catalyzes the last step in GC synthesis. The last step comprises the conversion of 11- deoxycortisol to cortisol in humans, while 11- deoxycorticosterone to corticosterone in rodents due to the lack of Cyp17 enzyme in the rodents adrenals (Miller, 2008; Noti et al., 2009).

Most of the secreted cortisol in the blood (approximately 90%) is bound to corticosteroid-binding globulins, this binding regulates the general availability of steroids to tissues, and/or direct the delivery of hormones to specific sites (Breuner and Orchinik, 2002).

GC metabolism is regulated by the isoenzymes of 11ß-hydroxysteroid dehydrogenase (11β-HSD encoded by HSD11B gene). Free cortisol, the biologically active form, is converted from the inactive cortisone via HSD11B1, while HSD11B2 converts active cortisol to inactive cortisone. These enzymes regulate the target cell adjustment between the active and the inactive form of GCs. Thus, HSD11B1, which is expressed in a wide range of tissues mainly in the liver, facilitates GC hormone action, whereas the major role of HSD11B2 is to prevent cortisol from gaining access to high-affinity mineralocorticoid (MC) receptors. Hence, the enzyme is predominantly expressed in the MC responsive cells of the kidney and other MC target tissues (colon, salivary glands) and the placenta (Nicolaides et al., 2000). Variations in the 11β-HSD enzyme system in relation to levels of expression and regulation has been shown to play a role in the pathogenesis of inflammatory bowel disease (IBD) (Hussey et al., 2017).

Adrenal GC synthesis is regulated by the NR steroidogenic factor 1 (SF-1 encoded by the NR5A1 (nuclear receptor subfamily 5, group A, member 1) gene), which is an essential regulator of endocrine development and function via induction of the expression of steroidogenic enzymes, such as CYP11A1, CYP17, CYP21, CYP11B1 and HSD3B2 (Schimmer and White, 2010).

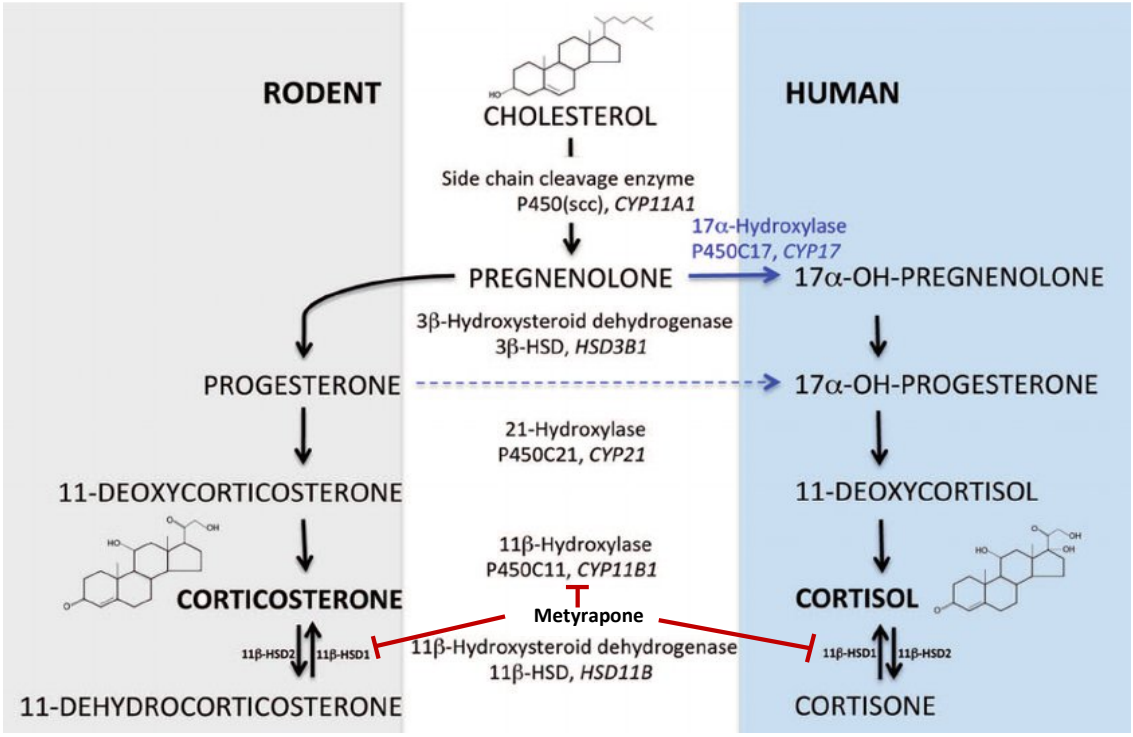

Figure 1 Glucocorticoid synthesis pathway in rodents and humans
Glucocorticoids are synthesized from cholesterol by cytochrome P450 (CYP) as well as hydroxysteroid dehydrogenase (HSD) enzymes. Rodents do not express CYP17 gene in the adrenals, therefore the active GC in rodents is corticosterone while in humans it is cortisol. Red lines indicate inhibition of the enzymes by metyrapone. The name of the protein and the corresponding gene are indicated for each step and the GC synthesis steps are explained in the text (Modified from Kostadinova et al. 2014).

1.3 Therapeutic uses of GC

Natural and synthetic GCs are used either locally or systemically for the treatment of both endocrine and non-endocrine disorders (Busillo and Cidlowski, 2013; Nicolaides et al., 2000). Endocrine indications via systemic GCs are mainly two: as replacement therapy in patients with primary or secondary adrenal insufficiency, and as adrenal suppression therapy in congenital adrenal hyperplasia and GC resistance (Nicolaides et al., 2000).

As a result of their potent anti-inflammatory and immunosuppressive properties, synthetic GCs are widely used in anaphylaxis (Liyanage et al., 2017), autoimmune and chronic inflammatory diseases, such as rheumatoid arthritis (Bijlsma et al., 2015), asthma (Alangari, 2014), sepsis (Annane et al., 2009), lupus erythematosus, dermatitis (Nicolaides et al., 2000), in immunosuppressive regimes following organ transplant (Coutinho and Chapman, 2011),

multiple sclerosis (Ciccone et al., 2008), as well as IBD (De Iudicibus et al., 2011). Furthermore, in hematology, GCs are used, along with chemotherapy, for the treatment of lymphomas and leukemias (Nicolaides et al., 2000).

1.4 Extra-adrenal GC synthesis

There is now increasing evidence that GCs are not only produced by the adrenal glands, but also by other tissues. In the past two decades the thymus (Gomez-Sanchez, 2009; Lechner et al., 2000; Vacchio et al., 1994), the skin (Nikolakis and Zouboulis, 2014; Slominski et al., 2013), the brain (Croft et al., 2008; Gomez-Sanchez, 2009), the vasculature (Takeda et al., 1994), the lung (Hostettler et al., 2012) and the intestine (Cima et al., 2004; Mueller et al., 2006, 2007) have been reported to produce substantial amounts of GCs and thereby, regulate local immunological responses. Unlike systemic GCs which regulate multiple organ functions, local GCs have been described to act with a high spatial specificity to regulate distinct organ functions (Taves et al., 2011). Supporting this notion, the ability to therapeutically target local GC synthesis could be of advantage to avoid systemic side effects. This is exemplified by the improvement of skin wound healing following local administration of the GC synthesis inhibitor, metyrapone (Talabér et al., 2013).

1.5 Intestinal epithelium

The epithelium of the small and large intestine (colon) represents the largest mucosal surface of the human body with a surface area of broadly 300 m^2 (Walter and Ley, 2011). This surface is in constant contact with harmless commensal bacteria and food antigens as well as potential harmful pathogens (Hooper and Macpherson, 2010). The main function of the intestinal epithelium is the absorption of nutrients and water, as well as the maintenance of barrier function (physical and biochemical barrier) in order to prevent luminal microorganisms from invading the body (Delgado et al., 2016; Peterson and Artis, 2014).

The intestinal epithelium comprises of several distinct layers: the mucosa, submucosa, muscularis propria and connective tissue-composed serosa (Gaifulina et al., 2016; Humphries and Wright, 2008). The intestinal mucosa is composed of a single layer of columnar epithelial cells, in addition to the underlying lamina propria and muscularis mucosa (Turner, 2009). The architecture of the intestine is organized into crypts of Lieberkühn and villi in the small intestine, whereas the colon consists only of crypts but does not display villi (Spit et al., 2018). The villi in the small intestine are specialized units for the absorption of nutrients, while the

function of the colon is largely dedicated to the compaction of stool (Clevers and Batlle, 2013). The different layers of the colon are depicted in Figure 2 (Gaifulina et al., 2016).

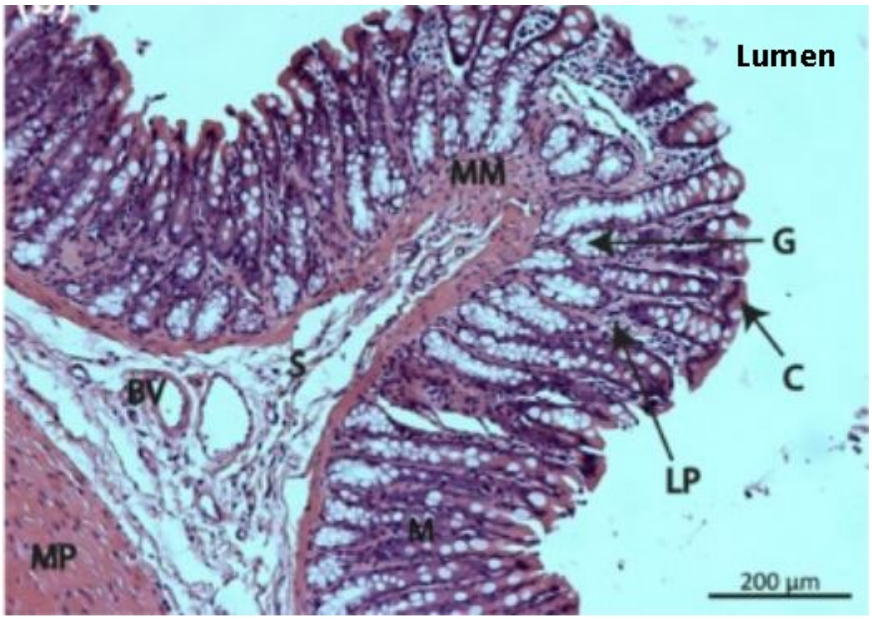

Figure 2 Histology of the colon
Structure of transversely cut H&E-stained colon section showing the different layers of the colon epithelium; M: mucosa (composed of; C: crypt columnar cells containing G: goblet cells, LP: lamina propria and MM: muscularis mucosa), S: submucosa that contains BV: blood vessels, and MP: muscularis propria (Modified from Gaifulina et al. 2016).

The intestinal barrier function is mediated by the single layer of intestinal epithelial cells (IECs), composed of different cell types that cover the main functions of the intestine (Delgado et al., 2016). IECs are constantly and rapidly newly generated from the intestinal stem cells (ISCs) residing at the bottom of the crypt columnar cells (Haegebarth and Clevers, 2009). With a turnover of less than 5 days, the entire epithelial layer is constantly renewed (Clevers and Batlle, 2013; Sato and Clevers, 2013). ISCs are able to replenish the whole crypt-villus axis, generating all differentiated cell types required for the physiological function of the intestine in the crypts (Spit et al., 2018). Intestinal epithelium structure is depicted in Figure 3.

ISCs give rise to rapidly proliferating subset of progenitor cells, also known as transient amplifying (TA) cells, that occupy the crypts and migrate upwards while differentiating into

one of the specialized epithelial lineages. Among the differentiated cells, absorptive epithelial cells, or enterocytes, constitute the majority of the IECs (van der Flier and Clevers, 2009).

Other major lineages comprise secretory cell types such as mucus producing goblet cells, that generate a protective barrier from luminal bacteria (Johansson et al., 2013), and enteroendocrine cells that secrete various hormones to coordinate digestion and metabolism (Gerbe et al., 2012). Other epithelial cell types are the pyramidal-shaped Paneth cells, which are present at the bottom of the small intestine crypt and absent in the colon. These cells escape the upward migration and instead, they migrate downwards to constitute the niche for ISCs at the crypt base (Sato et al., 2011a). Paneth cells secrete anti-microbial peptides, such as lysozymes and defensins to prevent bacterial infection (Sato et al., 2009). Furthermore, two more rare cell types are produced in the epithelium, including secretory tuft cells that act as sensor for luminal contents (Gerbe et al., 2012), and microfold (M) cells that reside in specialized epithelium overlying Peyer's patches to communicate with the gut immune system (Spit et al., 2018). The continuous proliferation and migration of the IECs is ultimately balanced by cell death resulting from loss of attachment at the tip of the villus and subsequent shedding into the lumen. This process of apoptotic cell death is known as anoikis (Haegebarth and Clevers, 2009).

Moreover, a very interesting population of cells that reside within the epithelium are the so-called intraepithelial lymphocytes (IELs). These cells are one of the main branches of the local immune system, a unique population of mostly $CD8^+$ T cells. Upon encountering antigen, IELs immediately release immunoregulatory cytokines or mediate killing of infected target cells. They are involved in the host defense, while maintaining tolerance to innocuous antigens from the diet or resident non-invasive commensals (Cheroutre et al., 2011). Additionally, the lamina propria also contains immune cells, including resident macrophages, DCs, plasma cells, lamina propria lymphocytes, and neutrophils (Rakoff-Nahoum et al., 2004; Turner, 2009).

Contributing to the effective epithelium barrier function are the Tight Junctions (TJs) proteins, which are junctional complexes that connect epithelial cells to each other, supporting the polarity of the epithelial layer by forming tight intercellular seals. Disturbance of intestinal epithelial TJs is implicated in the pathogenesis of IBD (Boivin et al., 2007).

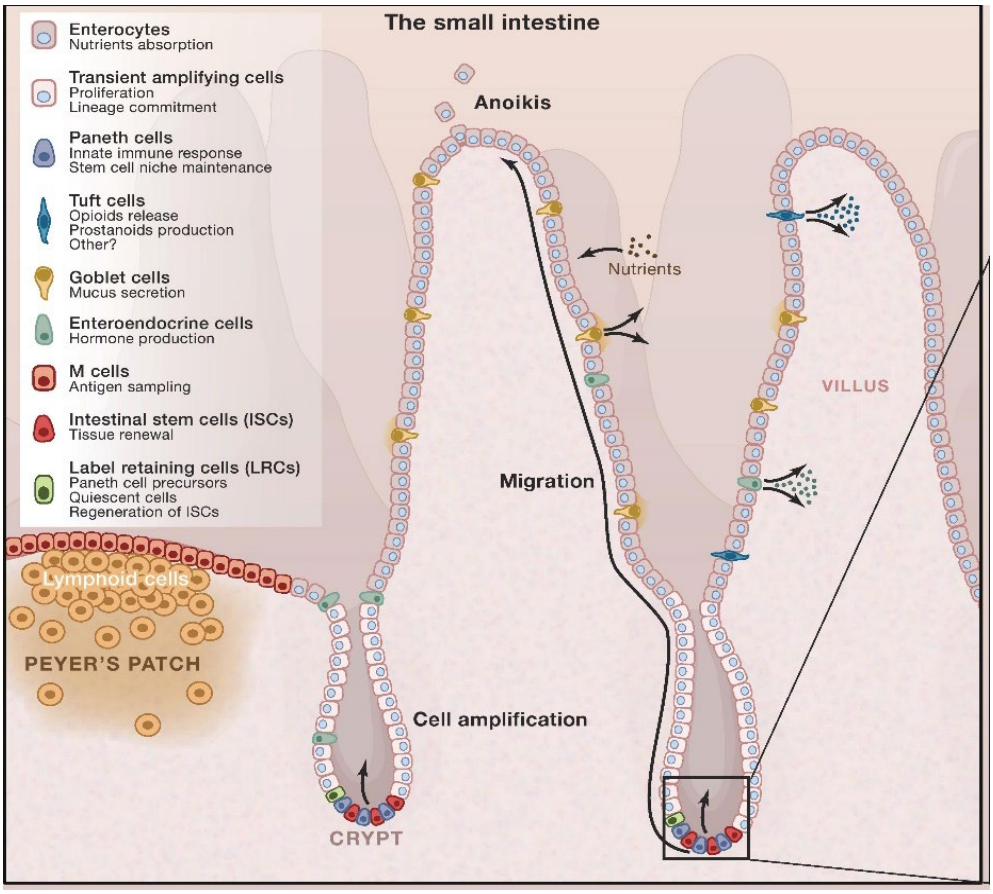

Figure 3 The intestinal epithelium
Epithelial cell types of both the small intestine and colon are organized following a bottom-to-top axis into three compartments: the stem cell compartment, the transient-amplifying (TA) compartment, and the differentiation zone. Different cell types of intestinal epithelial cells and their functions are explained in the text. The colon consists mainly of crypts (Modified from Clevers and Battle 2013).

1.5.1 Intestinal stem cell niche

Several populations of ISCs have been described based on their location in the crypts and expression of markers. Among these cells are the crypt base columnar stem cells, marked by leucine-rich-repeat containing G-protein coupled receptor 5 (Lgr5) (Barker et al., 2007). Additionally, a slow dividing, reserve stem cell population was identified, the so-called position 4/+4 cells or label-retaining cells (LRCs). These cells account for the plasticity of the ISCs (Tian et al., 2011). Furthermore, several secretory progenitors showed the ability to de-differentiate and revert to stem-like cells to replenish the crypt upon extensive tissue damage, as recently shown for Paneth cells following irradiation (Yu et al., 2018).

The complex and tightly regulated process of intestinal renewal and homeostasis is governed by a variety of signaling pathways that maintains the balance between cell proliferation and differentiation through maintaining the ISC niche. Signaling in ISCs include Wnt/β-catenin, Notch, hedgehog, bone morphogenetic protein (BMP), epidermal growth factor (EGF) and Ephephrin signaling cascades (reviewed in (Spit et al., 2018)).

In the intestine, Wnt signaling is the main driving force for crypt proliferation (Haegebarth and Clevers, 2009; Kuhnert et al., 2004; Pinto et al., 2003). Wnt ligands, such as R-spondin, produced by Paneth cells and surrounding stromal cells, and following binding to their cognate Frizzled receptor, leads to activation of canonical Wnt pathway. This results in the nuclear translocation and accumulation of β-catenin (Clevers, 2013). Wnt-induced stabilization of β-catenin involves the inactivation of a large multi-protein destruction complex composed of the scaffold proteins Axin and adenomatous polyposis coli (APC), as well as the kinases glycogen synthase kinase 3β (GSK3β) and casein kinase 1 (Ikeda et al., 1998). In the nucleus, β-catenin binds to the TF T-cell factor (TCF4), thus induces expression of Wnt target genes involved in proliferation of cells (Nusse and Clevers, 2017).

EGF signals exert strong mitogenic effects on stem and TA cells (Wong et al., 2012). The EGF receptor (EGFR) is expressed on all epithelial and stromal cells. EGFR signaling has pleiotropic effects, including mitogenesis or apoptosis, enhanced cell motility, protein secretion, and differentiation or dedifferentiation, in addition to morphogenesis and repair. EGFR executes these functions by activation of multiple signaling pathways including the MAPK pathways (reviewed in (Wells, 1999)).

BMPs are a class of signaling molecules. They belong to the transforming growth factor-β (TGF-β) superfamily of proteins. BMP signaling is mediated via the canonical SMAD-dependent pathway (Heldin et al., 1997). TGF-β signaling through SMAD proteins regulates a wide range of biological processes, including cellular proliferation, migration, differentiation, apoptosis and extracellular matrix deposition (Zhang et al., 2010a). In the intestine, BMP pathway negatively regulates intestinal epithelial proliferation and restrict the number of stem cells in the crypt (Kosinski et al., 2007). Noggin, the BMP antagonist, sequester BMP ligands resulting in crypt proliferation (Haramis et al., 2004).

1.5.2 Intestinal organoids

Recently, Sato et al. utilized the knowledge about ISC niches, and successfully employed it in the long-term culture of three-dimensional (3D) intestinal organoids *in vitro,* from a single

small ISC. They referred to these organ-like structures as mini-guts. Interestingly, these mini-guts retain the hallmarks and cellular composition of the *in vivo* epithelium (Sato et al., 2009). The growth requirements of the 3D organoids include the addition of several growth factors to imitate the niche for epithelium development, such as R-spondin, EGF, and noggin. Furthermore, since isolated intestinal cells undergo anoikis outside the normal tissue context, it is critical to grow the organoids in a laminin and collagen-rich matrix that mimics the basal lamina (Grabinger et al., 2014; Sato and Clevers, 2013; Sato et al., 2009).

This breakthrough technology opened the door for an exciting new field of research. Of higher interest is the application in the stem cell research especially in the field of cancer.
Extensive research resulted in the optimization of the culture conditions for colon organoids as well. It has been shown that, colon organoids require additionally N-acetylcysteine, A83-01 (TGF-β inhibitor), and Rho kinase (Rock) inhibitor (O'Rourke et al., 2016; Sato et al., 2011b). The rationale of using Rock inhibitor in organoid culture emerged from the reports that it extends the life span of epithelial cells (Liu et al., 2012).
The great success in the culture of small intestinal and colonic organoids (O'Rourke et al., 2016; Sato et al., 2009, 2011b), stimulated further research to optimize and extend the culture conditions to primary colon tumors.
Indeed, further studies applied this state-of-the-art organoid technology in the isolation and culture of organoids from primary mouse and human tumors (O'Rourke et al., 2016; Sato et al., 2011b; Xue and Shah, 2013). The advantage of growing tumor organoids would be of great importance in cancer diagnostics and therapeutics. Furthermore, the use could be extended to personalized medicine.
Recent advances in the exciting technology of tumor organoids field was followed by extensive research to better understand the molecular mechanisms of colorectal tumor initiation and progression, in an attempt to identify new therapeutic targets (Canli et al., 2017; Melo et al., 2017; O'Rourke et al., 2017; Roper et al., 2017; Xie and Wu, 2016).

1.5.3 Intestinal GC synthesis and regulation

The Brunner lab was the first to describe and characterize the *de novo* synthesis of immunoregulatory GCs in the intestinal mucosa that occurs in response to immunological stress. They used adrenalectomized mice to exclude the role of systemic GCs (Cima et al., 2004). Corticosterone synthesis was proven to be *in situ*, since the GC release from the tissue was blocked by metyrapone; a potent inhibitor of CYP11B1 and HSD11B1 enzymes (Cima et

al., 2004; Kaminski and Rogawski, 2011; Sampath-Kumar et al., 1997). Cima et al. demonstrated that, the murine intestinal mucosa strongly upregulates the steroidogenic enzymes (Cyp11b1, Cyp11a1, and Hsd11b1), and release the GC corticosterone in response to anti-CD3- or viral-activated T cells (Cima et al., 2004). Likewise, stimulation of the innate immune system with lipopolysaccharide (LPS), induces intestinal GC synthesis in a macrophage-dependent manner (Noti et al., 2010b). Local GCs in turn provide a negative feedback on the activation of local immune cells and inflammatory processes to avoid tissue damage (Cima et al., 2004; Kostadinova et al., 2014; Noti et al., 2010b). Inhibition of intestinal GC synthesis results in accelerated expansion of intestinal antigen-specific cytotoxic T lymphocytes (CTL) during viral infection, further confirming the immunosuppressive role of locally produced GCs (Cima et al., 2004; Huang et al., 2018).

Furthermore, intestinal GC synthesis was also shown to control colonic peroxisome proliferator-activated-receptor-gamma (PPARγ) expression. PPARγ plays an important role in the regulation of intestinal immune homeostasis and was reported to be impaired in inflammatory bowel disease (Bouguen et al., 2015b).
Additionally, *In vitro* data suggested the importance of GCs in the maturation of the IECs (Lu et al., 2011). GCs were also implicated in the regulation of the expression of TJ proteins and maintaining the intestinal epithelial barrier, especially antagonizing the TJ-destructing effect of TNF during inflammation (Boivin et al., 2007).

Interestingly, intestinal GC synthesis is dependent on TNF, since it was absent in TNF or TNF receptor-deficient mice treated with the inflammatory agent DSS or the hapten 2,4,6-trinitrobenzenesulphonic acid (TNBS). Furthermore, oxazolone, a hapten that promotes a Th2 cytokine-mediated intestinal inflammation with no TNF, fails to promote intestinal GC synthesis (Cima et al., 2004; Noti et al., 2010b, 2010a). This clearly indicates that inflammation *per se* is not sufficient to promote intestinal steroidogenesis, but rather the type of inflammation appears to be critical (Kostadinova et al., 2012). In this regard, TNF plays an anti-inflammatory action, by the induction of GC synthesis, in addition to its apoptosis-inducing effect in immune cells (Noti et al., 2010a).

In contrast to the regulation of GC in the adrenals via SF-1, SF-1 expression was absent in the intestinal epithelium (Mueller et al., 2007). Interestingly, SF-1 activity in the intestine was replaced by its close homolog, the NR liver receptor homolog-1 (LRH-1, NR5A2) (Atanasov et al., 2008; Botrugno et al., 2004; Mueller et al., 2007).

The expression of CYP11B1 and CYP11A1 is linked to cell cycle, thus implicating a restriction of the intestinal GC synthesis to the proliferating cells at the bottom of the crypts (Atanasov et al., 2008; Bouguen et al., 2015a). Similar to steroidogenic enzymes, LRH-1 expression is confined to the proliferating cells of the crypts, suggesting a cell cycle-dependent regulation of intestinal GC synthesis (Atanasov et al., 2008; Botrugno et al., 2004; Mueller et al., 2006). Thus far, the importance of locally synthesized GCs has been reflected by the impairment of cortisol production as well as decreased LRH-1 expression in colonic epithelial cells from ulcerative colitis patients (Bouguen et al., 2015b).

1.5.4 Intestinal immune homeostasis

Intestinal mucosal epithelium functions as a barrier to maintain the balance between nutrient absorption while preventing the entry of pathogens and responding to harmful contents of the lumen, in order to maintain tissue homeostasis (Salim and Söderholm, 2011).
A single layer of IECs provides the physical barrier that separates from the underlying lamina propria and the rest of the body, 10^{14} microorganisms (mostly commensal bacteria) living in the intestinal lumen. These lumen-resident microorganisms are termed gut microbiota (Cario, 2008; Mukherji et al., 2013).

Under steady-state conditions, the microbiota provides constitutive signals to the innate immune system through the activation of Toll-like receptors (TLRs), a family of pattern-recognition receptors that detect conserved molecular products of microorganisms such as LPS. TLRs expressed on macrophages and DCs play a crucial role in host defense against microbial infection (Rakoff-Nahoum et al., 2004). Activation of TLRs by commensal microflora is critical to maintain a healthy inflammatory tone within the intestinal mucosa, thus enhancing the resistance to infection with enteric pathogens (Cario, 2008; Hooper and Macpherson, 2010).

This direct contact of intestinal epithelium with a large number of immune cells (about 70% of all lymphocytes in the body, in addition to B cells, macrophages and DCs) (Lee et al., 2008a) and microbiota, with great potential to stimulate these immune cells, requires the intestinal epithelium to find the appropriate balance between protective immune responses against pathologic microorganisms and tolerance towards microbiota. The synthesis of immunoregulatory GCs seems to play a novel and important role in the maintenance of intestinal immune homeostasis under physiological as well as pathological conditions (Ballegeer et al., 2018; Noti et al., 2009).

Several other immune mechanisms were described to limit contact between the dense luminal microbial community and the IEC surface, including secretion of mucus by goblet cells. Furthermore, epithelial cells such as enterocytes, Paneth cells and goblet cells secrete anti-microbial proteins that further help to eliminate bacteria that penetrate the mucus layer. Additionally, Lamina propria plasma cells secrete IgA across the epithelial layer to limit the numbers of mucosa-associated bacteria and prevent bacterial penetration to the host tissue (Hooper and Macpherson, 2010).

The intestinal mucosa has also been described to contain high levels of the immunosuppressive cytokines TGF-β and IL-10 produced by the Tregs, DCs and even epithelial cells. The importance of these immunoregulatory cytokines is illustrated by the fact that TGF-β and IL-10-deficient mice develop spontaneous inflammation (Nagamine et al., 2008; Powrie, 1995).

Inappropriate activation of immune cells from either the innate and/or adaptive immune system may result in chronic inflammatory reactions and associated tissue destruction, as observed in IBD (Cario, 2008; McGuckin et al., 2009).

1.5.5 Inflammatory bowel disease

IBD comprises ulcerative colitis (UC) and Crohn's disease (CD) (Roda et al., 2010; Zhang and Li, 2014). UC causes inflammation of the mucosa of the colon and rectum, whereas CD causes inflammation of the full thickness of the bowel wall and may involve any part of the digestive tract from the mouth to the anus (Haggar and Boushey, 2009).

Although the etiology of IBD remains largely unknown, it involves a complex interaction between the genetic, environmental or microbial factors and the immune system (Roda et al., 2010; Shaw et al., 2018; Zhang and Li, 2014). These diseases are characterized by chronic relapsing inflammation of the intestine thought to be caused by inappropriate activation of the immune system (Rakoff-Nahoum et al., 2004). IBD result from disruption of the intestinal epithelium barrier integrity, thus leading to permeability defects and subsequent interaction between environmental factors in the intestinal lumen and cells of the immune system. The epithelium barrier breach exacerbate inflammation leading to severe tissue damage, which impairs the reconstitution of the intestinal epithelial barrier resulting in increased exposure to products of the microbiota, ultimately prolonging intestinal inflammation (Kinnebrew and Pamer, 2012; Salim and Söderholm, 2011).

Chronic inflammation is emerging as one of the hallmarks of cancer. Many cancers arise following prolonged inflammation or display inflammatory characteristics throughout progression (Hanahan and Weinberg, 2011; Lasry et al., 2016). In fact, the relative risk of colorectal cancer in patients with IBD has been estimated to increase by up to 20 folds (Gillen et al., 1994; Haggar and Boushey, 2009; Levin, 1992). The risk correlates directly with the duration and extent of inflammation (Eaden et al., 2001; Jess et al., 2012).

1.5.6 Tumor necrosis factor alpha

TNF is a pro-inflammatory cytokine, which presents a wide range of pleiotropic functions, including induction of inflammation, cell survival, proliferation, and cell death (Wang et al., 2017). In the intestinal epithelium, TNF demonstrates variable and very complex functions in physiological and pathological conditions (Leppkes et al., 2014). On the one hand, it drastically promotes epithelial cell death and hence is implicated in the pathogenesis of IBD (Grabinger et al., 2017). Moreover, it promotes intestinal inflammation and therefore drives colon tumor formation after sustained chronic colitis (Popivanova et al., 2008). On the other hand, TNF regulates intestinal GCs synthesis, which represents an important mechanism for intestinal immune homeostasis (Noti et al., 2010a). In this regard, TNF plays an anti-inflammatory role, that could also be through sensitizing activated T cells to undergo apoptosis resulting in accelerated resolution of the inflammation (Zhou et al., 1996).

Immune cells, such as monocytes, macrophages, natural killer (NK) and T cells are the main sources of TNF. Additionally, TNF is produced by fibroblasts and epithelial cells (Roulis et al., 2011). Macrophage and T cell activation results in massive release of TNF, which contributes to the damage of the epithelial layer (Marini et al., 2003). Therefore TNF-neutralizing antibodies have a strong therapeutic effect in the treatment of IBD (Bradley, 2008; Fries et al., 2008). This is mainly due to inhibition of IEC cell death, but also due to the downregulation of pro-inflammatory processes that might contribute to local tissue damage (Delgado et al., 2016).

TNF has also been shown to suppress LRH-1 and thereby reduce local GC synthesis resulting in a sustained chronic colitis (Huang et al., 2014). Interestingly, the significant increase in TNF mRNA levels in colon tumors was reported to be inversely correlated with a decrease in LRH-1 mRNA (Schoonjans et al., 2005). However, the relevance of this inverse correlation is so far unknown and requires further investigation.

1.6 Colorectal cancer (CRC)

Cancer is a leading cause of death worldwide, and half of all deaths caused by cancer are due to lung, stomach, liver, colorectal and female breast cancer (Ferlay et al., 2010; Lascorz et al., 2011). Colorectal cancer (CRC) is the most common malignant cancer in the gastrointestinal tract, with more than 1.2 million patients diagnosed every year globally (Brenner et al., 2014; Granados-Romero et al., 2017).

1.6.1 CRC epidemiology: incidence, mortality and etiology

CRC is the third most prevalent malignancy and the fourth leading cause of cancer death worldwide (Bray et al., 2018; Haggar and Boushey, 2009; Mármol et al., 2017). Incidence considerably varies globally, it is higher in developed countries and in males than in females. In addition, incidence strongly increases with age. The 5-year prognosis ranges between 50–65%, and drastically reduces in advanced disease stages reaching 10% in patients diagnosed for distant metastasis (Arnold et al., 2017; Brenner et al., 2014; Haggar and Boushey, 2009). Metastases represent the main cause of CRC-related mortality, and the most common metastatic sites are the liver and the lungs (Vatandoust et al., 2015).

Although the etiology and pathogenic mechanisms underlying CRC development appear to be complex and heterogeneous, several line of evidence identified various risk factors that are associated with CRC development (Fearon, 2011; Fleet, 2014). These include family history of CRC, IBD, smoking, excessive alcohol intake, high consumption of red and processed meat, obesity, and diabetes (Erhardt et al., 2002; Huxley et al., 2009; Larsson et al., 2005; Marchand et al., 1997). Moreover, overexpression of EGFR is common in 60–80% of CRC and it is associated with poor prognosis (Pabla et al., 2015). Of interest, EGF activates LRH-1, a NR that emerged as an oncogene and is a major focus of this study (Lee et al., 2006; Schoonjans et al., 2005).

CRC symptoms include abdominal pain, bloody diarrhea, weight loss, anorexia and abdominal distension (Granados-Romero et al., 2017).

Carcinogenesis is a multistep process starting with the formation of a benign adenoma that progresses over a course of several decades to malignant carcinoma (Fearon and Vogelstein, 1990; Fleet, 2014).

Genomic instability is an important feature underlying CRC development. The pathogenic mechanisms leading to this situation can be included in three different pathways: namely

i) chromosomal instability (CIN), characterized by imbalances in the number of chromosomes, thus leading to aneuploidic tumors and loss of heterozygosity (LOH), ii) microsatellite instability (MSI), and iii) CpG island methylator phenotype (CIMP) (Mármol et al., 2017).
CRC progresses due to the sequential acquisition of genetic mutations in pluripotent stem cells in the intestinal epithelial crypts (Davies et al., 2005). These include loss of function mutations of tumor suppressor genes, such as APC, TP53, DCC, BRAF, AKT, TGFβ, and SMAD4, as well as activating mutations of oncogenes such as KRAS, β-catenin, and c-myc (Fearon and Vogelstein, 1990; Granados-Romero et al., 2017; He et al., 1998; Markowitz et al., 1995; Mármol et al., 2017; Melo et al., 2017). CRC also develops from epigenetic changes in DNA such as methylation (Ilyas et al., 1999; Smith et al., 2002). In addition, CRC arises following chronic inflammation in the intestine as in patients with IBD (Lasry et al., 2016; Rowan et al., 2000). Although CRC is often sporadic with unknown hereditary basis, nevertheless hereditary cases account for 20–30% of all CRC cases (Kerber et al., 2005; Rustgi, 2007).

1.6.2 Hereditary colorectal cancer

The most common forms of hereditary CRC are familial adenomatous polyposis (FAP), and hereditary nonpolyposis colon cancer (HNPCC) or Lynch syndrome (Fearon, 2011).

FAP is an autosomal dominant inherited syndrome characterized by the progressive development of hundreds to thousands of small adenomatous polyps throughout the colon, some of which inevitably progress to cancer (Powell et al., 1993; Rustgi, 2007). FAP is caused by germline nonsense mutation in the APC gene (a component of the Wnt signaling pathway) at chromosome 5q21, that lead to premature truncation of APC protein synthesis (Kinzler et al., 1991). APC is affected by CIN that leads to LOH (Mármol et al., 2017).

The APC protein, together with GSK3β, phosphorylates cytoplasmic β-catenin, thereby leading to its degradation (Korinek et al., 1997). However, germline or somatic APC mutations render cytoplasmic β-catenin stable, resulting in its nuclear translocation, where β-catenin binds TCF4 and thereby activates transcription of Wnt target genes including c-myc and cyclin D1. These genes are implicated in cell proliferation (Korinek et al., 1997; Rustgi, 2007). Accumulating evidence has shown that c-myc is often overexpressed in colorectal tumors (He et al., 1998).
Another mechanism by which APC dictates its tumor suppressor function is the transcription-independent acceleration of apoptosis-associated caspase 3 activity (Qian et al., 2007; Steigerwald et al., 2005).

Progression of FAP to CRC occurs by mutations or epigenetic deregulation of KRAS and TP53 genes (Fearon and Vogelstein, 1990; Lynch and de la Chapelle, 2003).

HNPCC syndrome is marked by an autosomal dominant mode of inheritance. Multiple generations are affected with CRC at an early age, approximately 45 years, with an 80% lifetime risk to develop CRC. HNPCC is characterized by germline mutations in DNA mismatch repair (MMR) genes (Lynch and de la Chapelle, 2003; Rustgi, 2007). MLH1, MSH2, MSH6, and PMS2 are among the genes that produce MMR proteins. An estimated 70–90% of Lynch syndrome is attributable to deleterious mutations in MLH1 and MSH2, with the remaining 10–30% distributed approximately equally between MSH6 and PMS2 (Cohen and Leininger, 2014).

1.6.3 Sporadic colorectal cancer

Approximately 70% of sporadic CRC cases follow a specific succession of mutations. As shown in Figure 4A, the first mutation occurs in APC gene and triggers the formation of non-malignant adenomas, also called polyps (Brenner et al., 2014; Fearon, 2011; Powell et al., 1992). The APC mutation is followed by mutations in KRAS and TP53, that further promote these adenomas to the carcinoma state (Fearon, 2011; Mármol et al., 2017; Smith et al., 1994; Yamashita et al., 1995). DNA damage in cycling cells induces stabilization of p53 which then activates genes such as the cell cycle inhibitor, p21, to cause cell cycle arrest in G1 phase (the phase after which the cells are committed to undergo cell cycle progression). This allows for repair of the DNA before proceeding to S-phase. However, if the damage is too great for effective repair, p53 mediated activation of genes such as BAX results in apoptosis. Consequently, mutation of TP53 leads to apoptosis resistance (Harris and Levine, 2005; Ilyas et al., 1999).

These characteristic gene mutations are frequently accompanied by MSI (Lengauer et al., 1997). Nearly 70–80% of sporadic colorectal adenomatous polyps harbor somatic APC mutations (Ilyas et al., 1999; Powell et al., 1992, 1993).

CRC with high rates of MSI has been demonstrated to harbor inactivation mutations in the type II TGFβ receptor gene (Markowitz et al., 1995). This mutation render tumors insensitive to the growth suppression mediated by TGFβ (Kinzler and Vogelstein, 1996).

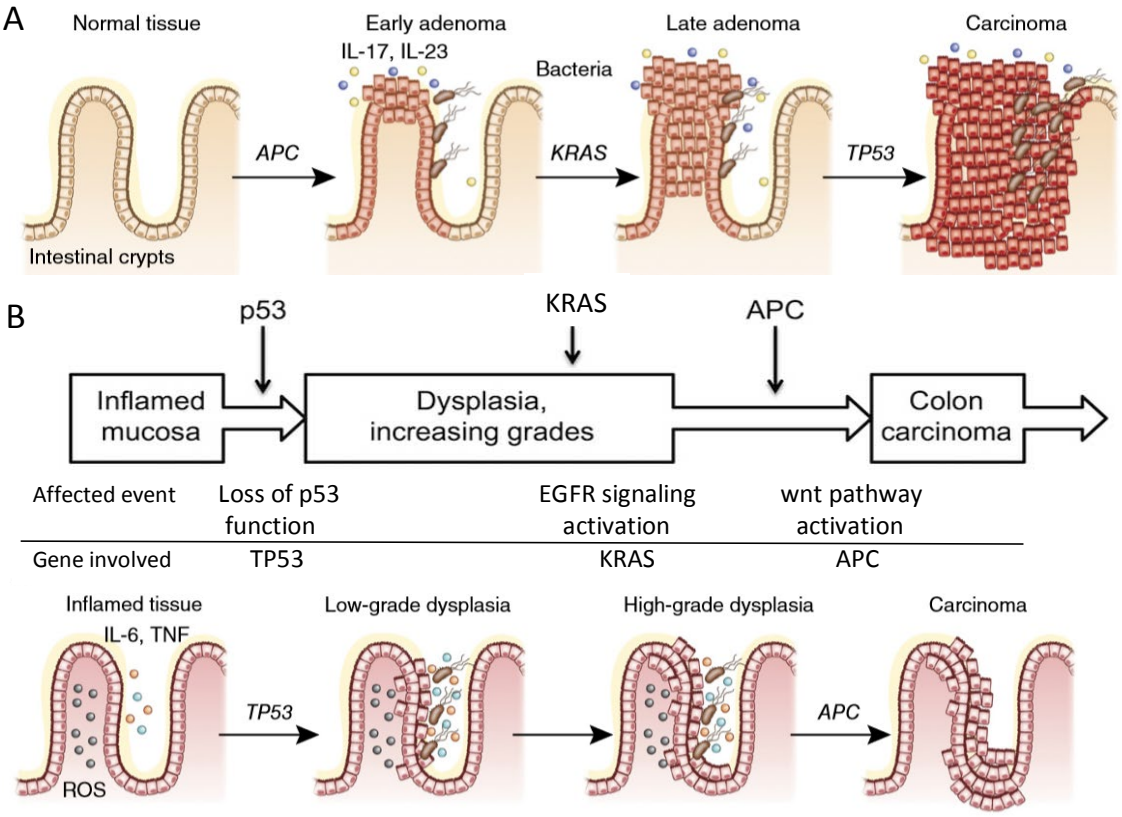

Figure 4 Molecular genetics of colorectal cancer
(A) Sporadic colorectal cancer follows the adenoma-carcinoma sequence, an early event is mutation of the tumor suppressor gene APC triggering adenoma formation, accompanied by loss of cell polarity and tight junctions, which enables bacteria invasion and the production of proinflammatory cytokines IL-17 and IL-23. Followed by mutations in the oncogene KRAS and loss of function mutation of TP53, which enable the progression of adenoma to carcinoma. **(B)** Colitis-associated colon carcinogenesis follows the inflammation-dysplasia-carcinoma sequence, an early event is the mutation in p53 as a result of inflammation and the associated production of proinflammatory cytokines TNF and IL-6 and reactive oxygen species (ROS). Which leads to prolonged activation of NF-κB and enhanced inflammation. Barrier dysfunction enables the invasion of bacteria, which further promotes inflammation. The inflammatory environment generates ROS and subsequent DNA damage, finally resulting in mutation of KRAS and APC and the development of carcinoma (Modified from Lasry et al. 2016 and De Lerma Barbaro et al. 2014).

1.6.4 Colitis-associated colorectal cancer (CAC)

CRC has long been described as one of the cancers tightly linked to chronic inflammation. Strikingly, even hereditary cases that are not often preceded by inflammation can be prevented by treatment with anti-inflammatory drugs suggesting an important role of inflammation in the tumor onset (Burn et al., 2011; Lasry et al., 2016).

Inflammation can function in all three stages of tumorigenesis: initiation, promotion, and progression (Hanahan and Weinberg, 2011; Korniluk et al., 2017).

Inflammation disturbs the normal wound healing process, resulting in a vicious interplay between excessive mucosal injury and tissue remodeling through sustained immune cell recruitment, proliferation, and migration (Cario, 2013). It involves interaction between various immune cells, chemokines, cytokines, reactive oxygen and nitrogen species (ROS and RNS) produced by neutrophils and macrophages, and pro-inflammatory mediators, such as cyclooxygenase (COX) and lipoxygenase (LOX) pathways. These collaborate to signaling towards tumor cell proliferation, growth, and invasion (Janakiram and Rao, 2014; Mármol et al., 2017; Meira et al., 2008).

Moreover, inflammation may directly damage cells and promote malignant transformation by inducing CIN and MSI, CIMP, epigenetic alterations, and posttranslational modifications (Cario, 2013; Meira et al., 2008; Philip et al., 2004). Additionally epithelial barrier breach further enhances inflammation and malignant transformation due to invasion of luminal bacteria, suggesting that the gut microbiota may have a role in CRC development (Lasry et al., 2016). Indeed, accumulating evidence confirmed that, under germ-free conditions, genetically engineered mice predisposed to CRC showed a lower tumor incidence (reviewed in (Kostic et al., 2013)).

Once a tumor is initiated, intra-tumoral immune cells and their secreted growth factors and proteases can contribute to tumor progression, invasion, and metastasis by preventing malignant cells from undergoing apoptosis (Grivennikov and Karin, 2010; Kostic et al., 2013).

Remarkably, the sequence of mutations that occurs in CAC is in sharp contrast with that of familial or sporadic CRC. CAC follows the inflammation-dysplasia-carcinoma pathway as depicted in Figure 4B. Interestingly, APC mutation occurs at a later stage preceded by TP53 and followed by KRAS mutations (De Lerma Barbaro et al., 2014; Waldner and Neurath, 2014). The reason for early selection of TP53 mutations is unknown, but one possibility is that it represents a means of escaping from apoptotic stresses imposed by the inflammatory cytokines and cells during the periods of inflammation (Ilyas et al., 1999).

NF-κB has been identified as one of the main participants in the transition from intestinal inflammation to malignancy (Greten et al., 2004; Shaked et al., 2012). NF-κB activation induces the pro-inflammatory cytokines TNF and IL-6. (Lasry et al., 2016). The role of these cytokines in CRC will be discussed in more details below.

1.6.5 NF-κB activation and the IL-6-STAT3 axis in CRC

Inflammatory signals activates pro-survival and proliferative pathways such as NF-κB and STAT3 (Lee et al., 2009a; Waldner and Neurath, 2014). Activation of either NF-κB or STAT3 is demonstrated in over 50% of all cancers (Grivennikov and Karin, 2010).
Tissue injury, resulting in DNA damage, is the initial step required for neoplastic transformation (Hoesel and Schmid, 2013). Loss of p53 has been shown to activate NF-κB in IECs, as well as in surrounding stromal cells, due to loss of barrier function and invasion of bacteria. It also induces epithelial-mesenchymal transition, in addition to promotion of CRC invasion and metastasis (Lasry et al., 2016; Schwitalla et al., 2013).

Activation of NF-κB in IEC leads to induction of TNF expression, that is required for the initial growth of the resulting neoplastic cells and thereby activates an oncogenic immune response (Burstein and Fearon, 2008). Subsequent NF-kB activation in myeloid cells regulates the expression of multiple inflammatory and tumor-promoting cytokines, including TNF, IL-6 and IL-1β (Grivennikov and Karin, 2010; Wang et al., 2009a). Which in turn activates NF-kB in malignant cells. Much of the growth stimulating cross-talk between immune and malignant cells is mediated by TNF and IL-6 that activate the oncogenic transcription factors NF-κB and STAT3, respectively (Grivennikov, 2013). In line with this, reduced NF-kB activity in myeloid cells or IECs *in vivo* alters the expression of the anti-apoptotic genes Bcl-xL and Bcl2, resulting in increased levels of apoptosis and decreased tumor load (Kostic et al., 2013). Moreover, TNF has been shown to be upregulated in the colons of mice after CAC. Consequently, mice lacking the TNF receptors or treated with etanercept, a specific pharmacological inhibitor for TNF, were protected from CAC (Popivanova et al., 2008).

Additionally, NF-κB-induced IL-6 enhances the development of CRC *in vivo* (Becker et al., 2005). IL-6 has been shown to drive STAT3 activation in IECs, leading to the upregulation of Bcl-xL and Bcl2, cell-cycle regulators cyclin D1 and c-myc, and the angiogenic factors basic fibroblast growth factor (bFGF) and vascular endothelial growth factor (VEGF). Thereby, promoting CAC development through the activation of MAPK and phosphoinositide 3-kinase (PI3K)-Akt pathways (Bollrath et al., 2009; Kostic et al., 2013; Yu et al., 2009). MAPK can activate downstream TFs including LRH-1, and thus could contribute to its tumorigenic effects (Mueller et al., 2007; Schoonjans et al., 2005). Indeed, STAT3 IEC-specific ablation results in profound reduction of CAC tumor growth and multiplicity (Grivennikov et al., 2009). Interestingly, persistent STAT3 activation has been shown to maintain constitutive NF-κB activation in both, tumors as well as tumor associated immune cells (Lee et al., 2009a).

1.6.6 CRC tumor immunology

CRC are infiltrated by diverse cell types that form the tumor microenvironment (TME) including stromal cells, fibroblasts, endothelial cells, cytokines and chemokines as well as innate and adaptive immune cells (Grizzi et al., 2018; Sica et al., 2008a; Vinay et al., 2015). Many cancer cells overexpress cellular proteins or neoantigens, which can be recognized by the immune system and provoke anti-tumor immune responses (Sidler et al., 2011).

A vast number of cytokines were reported to infiltrate CRC including TNF, IL-6, IL-1β, IL11, IL-17, IL23, IL-8, IL-10 and TGFβ, among others (Ferrone and Dranoff, 2010; Lasry et al., 2016; Waldner and Neurath, 2014). The immune cells infiltrating CRC tumors include tumor infiltrating lymphocytes (TILs), such as $CD8^+$ CTLs and the $CD4^+$ helper subpopulation; Th1, Th2, Th17 and $FoxP3^+$ Treg cells, as well as DCs, NK cells and tumor associated macrophages (TAMs) (Ferrone and Dranoff, 2010; Grizzi et al., 2018; Tosolini et al., 2011).
TAMs closely resemble M2 phenotype and represent the most abundant immune cells at the TME. Although their role in CRC is controversial, recent studies provide strong evidence that TAMs promote CRC tumor growth (reviewed in (Zhong et al., 2018)). In addition, $FoxP3^+$ Tregs has been shown to antagonize anti-tumor toxicity and thereby foster tumor growth (Ferrone and Dranoff, 2010).

In a large CRC patients' cohort, it has been demonstrated that absence of signs of early metastasis and increased survival is markedly correlated with high expression of $CD8^+$ effector memory cells particularly of Th1 and CTL types (Pagès et al., 2005). Camus et al. also observed that increased densities of CTLs and effector memory T cells within the primary tumor of CRC patients were associated with a significant protection against tumor recurrence (Camus et al., 2009). Moreover, another patient cohort has shown that patients with high expression of the Th17 responses have a poor prognosis, whereas patients with high expression of the Th1 responses and CTLs have prolonged disease-free survival (Tosolini et al., 2011). Taken all together, it is conceivable that the type of immune responses at the TME is a major determinant of CRC development and progression. Thus, modulation of these responses represents a promising therapeutic approach.

1.6.7 CRC prevention and treatment

The choice of first-line treatment in CRC follows a multimodal approach based on tumor-related characteristics and usually comprises surgical resection followed by chemotherapy

(e.g. 5-fluorouracil and irinotecan) and combined with monoclonal antibodies against VEGF (e.g. Bevacizumab), and EGFR (e.g. Cetoximab or Panitumumab). In advanced stages, radiotherapy is also included in the treatment regimen (Granados-Romero et al., 2017; Mármol et al., 2017; Pabla et al., 2015). Strikingly, several line of evidence have proven the efficiency of nonsteroidal anti-inflammatory drugs (NSAIDs) in the prevention and treatment of CRC even in advanced disease stages (Gupta and Dubois, 2001; Ng et al., 2015; Sandler et al., 2003; Williams et al., 1999). NSAIDs such as sulindac and aspirin are non-selective inhibitors of COX-2 (Hawkey, 1999). It is conceivable that the anti-carcinogenic effect of NSAIDs stems at least in part from their anti-inflammatory properties (Lasry et al., 2016). Supporting this notion, expression of COX-2 was reported to be markedly elevated in 85-90% of human colorectal adenocarcinomas, reflecting the inflammatory state at the TME (Williams et al., 1999).

The preventive effect of NSAIDs was first demonstrated in reduced polyp formation in FAP patients treated with sulindac for 1 year (Waddell et al., 1989). Furthermore, another study has shown an overall reduction of 40-50% in the risk of CRC in patients following long-term use (more than 5 years) of low-dose aspirin (Sandler et al., 2003). Herein, aspirin also shows a positive effect in patients with advanced CRC, evidenced by reduced tumor recurrence (Ng et al., 2015).

An emerging therapeutic strategy for solid tumors, is to target the anti-tumor immunity by reactivating the adaptive immune system against tumors. The negative regulators of the immune system called immune checkpoints play a key role in limiting anti-tumor immunologic responses. For this reason, immune checkpoint inhibitors, such as those targeting cytotoxic T-lymphocyte antigen 4 (CTLA-4) and programmed death-1 receptor (PD1) and its ligand PD-L1, have been developed for CRC treatment. However, whereas preliminary clinical trial results on PD1 and PD-L1 blockade appear promising, CTL-4 inhibitors fail to show any significant activity (reviewed in (Passardi et al., 2017)).

Despite all these treatment and preventive measures, the overall CRC survival is still very low, especially in advanced disease stages. In addition, due to the high toxicity of the currently used therapies, there is an urgent need for the elucidation of the molecular mechanisms for CRC development, in order to identify new therapeutic targets that could ultimately lead to the development of more effective therapies while minimizing the side effects.

1.6.8 Mouse models of CRC

In order to mimic the features of colon carcinogenesis and to study the mechanisms underlying the initiation and progression of CRC, several mouse models have been developed that recapitulate the adenoma-carcinoma sequences that occurs in humans (Rosenberg et al., 2009; Tong et al., 2011). These can be classified into genetically engineered, chemically induced and xenoplant models (Tong et al., 2011). Among the transgenic mice, the APC/ multiple intestinal neoplasia (Apc^{Min}) mouse model has been used to recapitulate the human sporadic CRC. These mice develop numerous adenomas in the small intestine while few in the colon (Leclerc et al., 2004; McCart et al., 2008). One of the most widely used chemically induced CRC model is the azoxymethane/dextran sodium sulphate (AOM/DSS) model (Fazio et al., 2011; Neufert et al., 2007; Tanaka et al., 2003).

1.6.9 AOM/DSS inflammation-driven CRC model

In order to elucidate the molecular mechanisms of inflammation induced CRC, a highly reliable and reproducible chemically induced mouse model of colon carcinogenesis was developed (Tanaka et al., 2003). Based on a single dose of the mutagenic agent, AOM, followed by repeated administration of the inflammatory agent, DSS, in the drinking water. AOM/DSS model rapidly shortened the time to CRC induction and recapitulated the aberrant crypt foci-adenoma-carcinoma sequence that occurs in human CRC. Consequently, causing rapid growth of multiple colon tumors per mouse within 8 - 10 weeks of exposure (Fazio et al., 2011; Neufert et al., 2007; Tanaka et al., 2003).

AOM is a pro-carcinogen that exerts its mutagenic action after activation, it can initiate cancer by alkylation of DNA, thus leading to base mispairing. Stepwise activation of AOM following intraperitoneal injection includes a hydroxylation step in the liver mediated by CYP2E1 enzyme resulting in methylazoxymethanol (Neufert et al., 2007; Sohn et al., 2001). Methylazoxymethanol is transported via the bile to the intestine, where further activation to methyldiazonium occurs promoted by factors of the bacterial flora (Neufert et al., 2007).

DSS is an inflammatory agent that acts as a tumor promoter after AOM injection. After administration of DSS, it induces alterations in intestinal barrier function leading to a macrophage/granulocyte-driven type of intestinal inflammation. Consequently, mice exhibit weight loss, diarrhea and sometimes rectal bleeding and colon shortening paralleled by increased mRNA expression of pro-inflammatory cytokines with acute inflammatory

properties such as IL-1β, IL-6 and TNF, interestingly the immunomodulatory cytokine, IL-10, was also reported to be upregulated (Egger et al., 2000; Kim et al., 2012; Kostadinova et al., 2014). Histopathological analysis of the inflamed colons revealed frequent formation of lymphoid follicles as well as multiple erosions and inflammatory changes including crypt abscesses, a phenotype that mimic the characteristics of UC in human patients (Okayasu et al., 1990; Viennois et al., 2013). Tumor development after DSS-induced inflammation strongly confirm that chronic inflammation in IBD plays a critical role in CRC as mentioned earlier.

1.7 Nuclear receptors

NRs are a superfamily of ligand-activated TFs that utilize lipophilic ligands to mediate their function (Crowder et al., 2017). NRs regulate the expression of genes involved in reproduction, development and metabolism. They play critical roles in mammalian physiology and regulation of immune responses (Bookout et al., 2006). Therefore, it comes as no surprise that NRs signaling dysfunction leads to pathological conditions such as diabetes, obesity and cancer (Zhang and Wang, 2011).

The most important distinction of NRs from other TFs is their ability to function as ligand-dependent sensors of fat-soluble hormones, vitamins and dietary lipids. Members of this group includes receptors of endocrine steroids, fat soluble vitamins, thyroid hormones, fatty acids, oxysterols, bile acids and xenobiotic lipids (Bookout et al., 2006). The NR superfamily comprise of 48 members in the human genome, approximately half of the superfamily have well characterized endogenous ligands (Burris et al., 2012). Whereas the remaining half composed of a distinct subset of NRs called “orphans”, lacking a defined endogenous ligand (Huang et al., 2010).

The NRs can be broadly classified into three sub-groups based on their physiologic ligands and potential functions: i) The classical, also called endocrine NRs, with well-known hormone ligands such as the receptors for androgen (AR), estrogen (ER), GR, thyroid hormone (TR) and progesterone (PR). ii) The adopted orphan NRs: whose ligand has been identified as a natural compound or an endogenous metabolic product, however the functional relevance of the ligand is still unclear. This sub-group include the farnesoid X receptor (FXR), retinoid X receptor (RXR), pregnane X receptor (PXR), liver X receptor (LXR), PPAR, SF-1 and LRH-1. iii) The true orphan NRs, with no defined ligand, and these include SHP, dosage-sensitive sex reversal and adrenal hypoplasia congenital critical region gene on the X chromosome gene-1 (DAX-1), chicken ovalbumin upstream promoter transcription factor (COUP-TF), and nerve

growth factor-inducible protein B (NGFI-B, also called Nurr77) (Lee et al., 2007; Sonoda et al., 2008).

1.7.1 Structure

All NRs share a common structure consisting of five to six distinct domains denoted A to F, starting from the N- to C-terminus of the protein as depicted in figure 5 (Zhang et al., 2011).

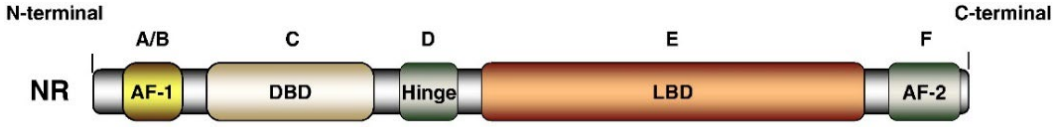

Figure 5 Nuclear receptors common structure
Classical nuclear receptor (NR) contains five major functional domains: The N-terminal ligand-independent transactivation domain (AF-1 or A/B domain), the DNA-binding domain (DBD or C domain), hinge region (D domain), the C-terminal ligand-binding domain (LBD or E domain), and the ligand-dependent transactivation domain (AF-2 or F domain) (Modified from Zhang et al. 2011).

NR structure consists of a highly variable N-terminal region that contains a ligand-independent activation function-1 (AF-1, A/B). The central DNA-binding domain (DBD, C), represents the most conserved domain consisting of two highly conserved zinc-finger motifs unique to NRs, that targets the receptor to specific DNA sequences called hormone response elements (HRE). The hinge region (D) confers structural flexibility in the receptor dimers allowing a single receptor dimer to interact with multiple HRE sequences. The C-terminal ligand-binding domain (LBD, E) is functionally very unique to NRs and responsible for: i) receptor dimerization, ii) ligand recognition and iii) cofactor interaction. The LBD consists of approximately 12 helices; the last helix is called the ligand-dependent activation function-2 (AF-2, F) or Helix12 and it is structurally dynamic (Kojetin and Burris, 2013; Sonoda et al., 2008; Zhang et al., 2011).

1.7.2 Mechanism of action

NRs interact with a wide family of co-regulator molecules (coactivators and corepressors). Coactivators are generally recruited to ligand bound NRs and enhance gene expression. Corepressors fulfill the opposite role and mainly bind to un-liganded NRs and repress transcription (Wang et al., 2009b). In the absence of ligand, NRs are either present in the cytoplasm forming a complex with Hsp and immunophilin chaperones (Pratt and Toft, 1997).

Or in the nucleus bound to the respective HRE, forming a repressive complex with a corepressor such as silencing mediator of retinoid and thyroid hormone receptors (SMRT) and nuclear receptor corepressor (NCoR) complexed with histone deacetylase enzymes (HDAC) (Rosenfeld et al., 2006; Watson et al., 2012). Binding of ligand in the ligand-binding pocket induces conformational changes in the AF-2, which mechanistically facilitates the release of corepressors and HDAC complexes and the recruitment of coactivators and histone acetyltransferases (HAT) complexes. In some cases, the AF-2 peptide is fixed in an active conformation, resulting in constitutive receptor activation. In these cases, the activity of the NR is regulated by nuclear availability of the receptor itself or coactivators, or by signal-induced receptor modifications such as phosphorylation or acetylation (Sonoda et al., 2008). NRs can act through i) direct activation or repression of their target genes by binding to the HRE in the promoter region via DBD. ii) binding to specific activating molecules via LBD and thereby interact with other coactivators and corepressors to exert transcriptional regulation (Bookout et al., 2006; Zhang and Wang, 2011).

1.7.3 Nuclear receptors in intestinal immune homeostasis

Anatomical profiling of NR expression revealed that a subset is abundantly expressed in different areas of the gastrointestinal tract. These NR include the GR, PPARγ, LRH-1, SHP, FXR and LXR (Bookout et al., 2006). Many of these NRs have been described before to play regulatory functions in metabolism and immune homeostasis of the gut (Bayrer et al., 2018; Bouguen et al., 2015b; Coste et al., 2007) and some of these receptors are established therapeutic targets for the treatment of IBD (Fernandez-Marcos et al., 2011). For example the use of GCs to activate the GR (De Iudicibus et al., 2011; Raddatz et al., 2004) and the use of 5-aminosalicylic acid to activate PPARγ (Dubuquoy et al., 2006) have a known therapeutic benefit in IBD.

Recently, Huang et al. investigated the role of the NRs SHP and LRH-1 in the regulation of local intestinal GC synthesis and its relevance in intestinal immune homeostasis in the context of viral infection. They could show that systemic deficiency of SHP results in increased intestinal GC synthesis during viral infection that suppressed the expansion and altered the activation of virus-specific T cells. In contrast, intestinal-specific deletion of LRH-1 reduced intestinal GC synthesis and accelerated the expansion of cytotoxic T cells upon viral infection (Huang et al., 2018). Furthermore, another recent study has shown that LRH-1 mitigates

intestinal inflammatory disease using intestinal organoids as a model system (Bayrer et al., 2018).

1.8 Liver receptor homolog 1

The nuclear receptor LRH-1, also known as nuclear receptor subfamily 5, group A, member 2 (NR5A2), is a member of the NR superfamily (Fayard et al., 2004). Due to the identification of LRH-1 independently by different research groups, different names are assigned to LRH-1, including fetoprotein transcription factor (FTF), since it was characterized as a NR related to the *Drosophila fushi tarazu* factor 1 (FTZ-F1) receptor (Galarneau et al., 1996), CYP7A promotor-binding factor (CPF) (Nitta et al., 1999), and human B1-binding factor (hB1F) (Li et al., 1998), among others.
LRH-1 is expressed in tissues derived from endoderm including intestine, liver and exocrine pancreas, as well as in the ovary (Fayard et al., 2004). Additionally, LRH-1 is expressed in macrophages (Lefèvre et al., 2015) and T cells (Schwaderer et al., 2017).

LRH-1 plays vital roles in early embryonic development as evidenced by the embryonic lethal phenotype of the LRH-1-null mice (Paré et al., 2004). This phenotype results from the loss of LRH-1-maintained octamer-binding transcription factor 4 (Oct4) expression, which is required to sustain the pluripotency of embryonic stem cells (Gu et al., 2005). LRH-1 is also important for cholesterol and bile acid homeostasis, glucose metabolism and steroidogenesis in adulthood (Cobo et al., 2018; Lazarus et al., 2012b). The human gene encoding LRH-1 spans more than 150 kb of chromosome 1q32.11 and has eight exons (Lazarus et al., 2012a).

1.8.1 LRH-1 signaling and regulation

LRH-1 structure follows the classic NR structure as described in 1.7.1. The Ftz-F1 box in the C-terminus of the DBD dictates LRH-1 binding. It binds the DNA as a monomer (Lazarus et al., 2012a). Activation of LRH-1 induces conformational change that results in the dissociation of corepressor complexes and the recruitment of coactivator complexes. The coactivator complexes typically contain proteins that inhibit or induce the initiation of transcription (Fayard et al., 2004). As LRH-1 is constitutively active, its function must be regulated by several mechanisms. Those include, interactions with coactivators and corepressors, as well as posttranslational modifications such as phosphorylation and SUMOylation (Lazarus et al., 2012a; Nadolny and Dong, 2015). Additionally, LRH-1 has been shown to be activated by phospholipids as potential endogenous ligands (Crowder et al., 2017; Krylova et al., 2005).

Coactivators of LRH-1 contain an LXXLL motif in the receptor interaction domain that binds to LRH-1 LBD (Lazarus et al., 2012a). These include PPAR-γ-co-activator-1 alpha (PGC-1α) in the ovary (Yazawa et al., 2010), FXR (Hoeke et al., 2014), and multi-protein bridging factor (MBF-1) in the liver (Brendel et al., 2002), as well as steroid receptor coactivators (SRC-1 and SRC-3) (Lazarus et al., 2012a). Interestingly, β-catenin was also reported to activate LRH-1 (Yumoto et al., 2012).

Several corepressors were reported to inhibit LRH-1 transcriptional activity. For instance, interactions with other NRs such as SHP (Lee and Moore, 2002) and DAX-1 inactivates LRH-1. Furthermore, prospero-related homeobox 1 (Prox-1), protein inhibitor of activated signal transducer and activator of transcription-γ PIASy and SMRT also repress LRH-1 activity (Fernandez-Marcos et al., 2011; Lazarus et al., 2012a).

LRH-1 activity is also regulated by posttranslational modification such as phosphorylation of the serine residues 238 and 243 located within the hinge region by phorbol 12-myristate 13-acetate (PMA) via MAPK/ERK (extracellular-signal regulated kinase) pathway. Phosphorylation was shown to be important for transactivation of LRH-1 (Lee et al., 2006), whereas SUMOylation of the hinge region inhibits LRH-1 (Benod et al., 2013).

1.8.2 LRH-1 in intestinal immune homeostasis

In the intestinal epithelium, LRH-1 is predominantly expressed in the proliferating crypt cells, where it regulates epithelial cell proliferation as well as barrier integrity and immune homeostasis via induction of cell cycle proteins on the one hand (Botrugno et al., 2004), and the transcriptional regulation of steroidogenic enzymes and intestinal steroidogenesis on the other hand (Mueller et al., 2006; Noti et al., 2010b) (Figure 6).

LRH-1 induces cell proliferation through the concomitant induction of cyclin D1 and E1, which is further potentiated by its interaction with β-catenin. Whereas β-catenin coactivates LRH-1 after direct binding of LRH-1 to the cyclin E1 promoter, LRH-1 acts as a coactivator for β-catenin/TCF4 on the cyclin D1 promoter (Botrugno et al., 2004).

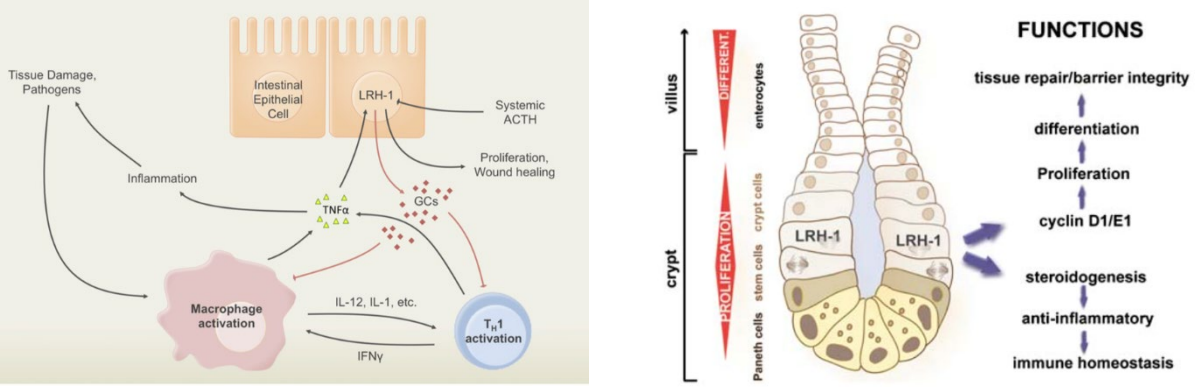

Figure 6 Dual roles of LRH-1 in the regulation of intestinal epithelium homeostasis
Right panel: A simplified scheme illustrates the dual role of LRH-1 in the intestine by promoting cell proliferation to maintain epithelial barrier integrity and by inducing intestinal steroidogenesis. Left panel: local GC synthesis regulation and function; activated macrophages and Th1 cells secrete the proinflammatory cytokine TNF, which upregulates the transcription factor LRH-1 in epithelial cells of the intestinal crypt. LRH-1 induces local production of glucocorticoids, which down- regulate immune cell activation and resulting inflammation (Modified from Noti et al. 2009 and Taves et al 2011).

In humans, LRH-1 transcriptionally regulates the expression of the steroidogenic enzymes CYP11A1, CYP17, HSD3B2, and CYP11B1 as well as steroid acute regulator (StAR), the transporter of cholesterol with in the cell, hence supplying the steroid synthesizing machinery with the substrate for GC synthesis (Sirianni et al., 2002).

LRH-1-mediated local GC synthesis in the intestine is promoted in response to inflammation and subsequent immune cell stimulation in mice. GCs then exert anti-inflammatory effects on the activated immune cells in order to suppress inflammation (Cima et al., 2004; Huang et al., 2018; Noti et al., 2010b, 2010a). In line with these important functions, it has been shown that haplodeficiency or intestinal-specific deletion of LRH-1 results in defective intestinal GC synthesis and renders mice more susceptible to experimental colitis (Coste et al., 2007; Mueller et al., 2006). And more recently evidence for reduced control of anti-viral immune responses was provided (Huang et al., 2018). Furthermore, colon biopsies from IBD patients showed reduced expression of LRH-1 and genes involved in steroidogenesis (Coste et al., 2007), implicating an important role of defective local GC synthesis in the etiology of IBD.

Moreover, restoration of LRH-1 restored epithelium homeostasis in organoids and protected mice from T-cell-induced colitis (Bayrer et al., 2018). Taken all together, these findings provide convincing evidence that LRH-1 is an essential mediator of epithelial homeostasis and thereby represent an attractive therapeutic target in intestinal disease.

1.8.3 LRH-1: an oncogene

LRH-1 has been identified as an oncogene implicated in the development of a variety of cancers due to its role in proliferation and maintenance of pluripotency. These include breast (Chand et al., 2010; Thiruchelvam et al., 2011), pancreatic (Benod et al., 2011), prostate (Xiao et al., 2018), gastric (Wang et al., 2008) and colorectal cancer (Kramer et al., 2016; Schoonjans et al., 2005). LRH-1 has also been shown to contribute in the development of metastasis in pancreatic cancer (Benod et al., 2011). LRH-1 exhibited an increased expression pattern in high-grade prostate cancer, and has been reported to promote prostate cancer growth by inducing intra-tumoral steroidogenesis (Xiao et al., 2018).

In the intestinal mucosa, LRH-1 promotes epithelial cell proliferation and crypt cell renewal by the induction of cell cycle proteins such as cyclin D1 and E1, thus postulated to play a role in the development of colon carcinoma (Botrugno et al., 2004).
LRH-1 aberrant activity is associated with tumorigenesis by affecting cell cycle control and proliferation in synergy with the β-catenin/TCF4 signaling pathway (Botrugno et al., 2004; Schoonjans et al., 2005). Additionally, LRH-1 drives colon cancer cell growth by repressing the expression of p21 in a p53-dependent manner (Kramer et al., 2016). The importance of LRH-1 in CRC development has been demonstrated by the fact that heterozygous LRH-1 mice developed significantly less tumors compared to wild type, using two different models of CRC: $APC^{min/+}$ mice and AOM-induced (Schoonjans et al., 2005). Contrary to the expectation and the known role of LRH-1 in intestinal tumorigenesis, LRH-1 expression has been shown to be significantly downregulated in adenoma tissue compared to adjacent normal mucosa in mice (Modica et al., 2010; Schoonjans et al., 2005). The expression of LRH-1 gene was reduced in tumors that express elevated levels of the proinflammatory cytokine TNF. Reciprocally, decreased LRH-1 expression in heterozygous LRH-1 mice attenuates TNF expression (Schoonjans et al., 2005).

As predicted in humans, positive LRH-1 expression determined by IHC was drastically enhanced in colon cancer samples compared with adjacent non-cancerous tissue from the same patients. That was correlated with a more advanced disease stage. Furthermore, the overall survival rate of patients with positive LRH-1 expression was significantly lower than that of patients with low expression (Wu et al., 2018). Elsewhere, another patient study confirmed the marked overexpression of LRH-1 in CRC tissue compared to paired non-cancerous tissue (Qu et al., 2018). Wu et al. suggested LRH-1 as a possible prognostic marker in CRC patients and a novel therapeutic target for the treatment of CRC (Wu et al., 2018).

1.8.4 LRH-1 as a therapeutic target

Since LRH-1 is an important regulator of pathways involved in metabolism, steroidogenesis, cancer and regulation of pluripotency, it has recently emerged as a novel therapeutic target. Accumulating evidence from extensive research has shown the therapeutic potential of LRH-1 modulators (Lazarus et al., 2012a). These include the antidiabetic and lipotropic effects of the *in vitro* and *in vivo* LRH-1 agonist dilauryl phosphatidylcholine (DLPC) in mice. In this study, DLPC treatment increased bile acid levels and lowered hepatic triglyceride and serum glucose. Furthermore, DLPC decreased steatosis and improved glucose homeostasis in two mouse models of insulin resistance. All these effects were LRH-1-dependent (Lee et al., 2011; Musille et al., 2012).

Further confirming the role of LRH-1 in intestinal homeostasis, it has been shown recently that LRH-1 restoration mitigates inflammatory damage in murine and human intestinal organoids, including organoids derived from IBD patients. Moreover, LRH-1 greatly reduces disease severity in T-cell mediated murine colitis (Bayrer et al., 2018). Indicating the therapeutic potential of LRH-1 in the treatment of IBD.

Additionally, since LRH-1 was shown to be upregulated in many tumors and to contribute in tumor formation as mentioned previously, suppression of LRH-1 activity in tumors would potentially exert anti-proliferative effects. This has been shown by the impaired proliferation of the CRC cell lines HT29 and Caco2 upon LRH-1 knockdown (Bayrer et al., 2015). Similarly, knockdown of LRH-1 inhibits pancreatic cancer cell proliferation *in vitro* (Benod et al., 2011). Furthermore, it has been shown that targeting LRH-1 using microRNA *in vitro* inhibits proliferation and invasion of the colon cancer cell lines HCT116 and SW480, an effect that was abolished by LRH-1 overexpression (Qu et al., 2018).
Taken all together, LRH-1 represents a novel and promising therapeutic target for the treatment of cancer.

1.9 Small heterodimer partner

The orphan nuclear receptor SHP, also known as nuclear receptor subfamily 0, group B, member 2 (NR0B2), is a unique NR that contains the dimerization and LBD but lacks the highly conserved DBD present in all other NR superfamily as shown in Figure 7 (Seol et al., 1996). SHP exerts its regulatory function through protein-protein interaction with a wide variety of NRs and TFs in a tissue-specific manner (reviewed in (Zhang et al., 2011)).

SHP represses other NRs via at least three suggested mechanisms: i) Inhibition of DNA binding via heterodimerization, ii) Direct antagonism of coactivator function via competition, and iii) Transrepression via recruitment of putative corepressors (Johansson et al., 2000).
The ability of SHP to bind directly to other NRs is critical for its function as an inhibitor of gene expression (Lee and Moore, 2002; Zhang and Wang, 2011). In contrast to its repressive function, SHP has been described as a novel coactivator of NF-κB in macrophages treated with oxidized low-density lipoprotein (Kim et al., 2001). SHP also enhances the transcriptional activity of PPARγ (Nishizawa et al., 2002).

1.9.1 SHP gene structure and function

The genomic structure of SHP consists of two exons interrupted by a single intron spanning approximately 1.8 kb in humans and 1.2 kb in mouse. Human SHP gene is located at chromosome 1p36.1, while mouse and rat SHP reside in chromosome 4 and 5 respectively (Chanda et al., 2008; Zhang et al., 2011). SHP binds to AF-2 domain of other NRs through two functional LXXLL-related motifs called NR-boxes, which are located in the putative N-terminal helix 1 of the LBD and in the C-terminal region of helix 5 as shown in Figure 7 (Johansson et al., 2000).

The NRs SF-1 and LRH-1 have been shown to transactivate SHP (Lee et al., 1999).
SHP is predominantly expressed in the gallbladder and liver and at lower levels in the pancreas, adrenal, brain, heart, ovary, kidney and gastrointestinal tract (Bookout et al., 2006). SHP expression was also reported in the spleen and bone marrow-derived macrophages (Yuk et al., 2011).

SHP regulates diverse physiological and pathological functions via interacting with other NRs and TFs. These include gluconeogenesis, insulin secretion, bile acid and cholesterol metabolism, lipid metabolism, steroidogenesis, and cancer (Chanda et al., 2008; Zhang et al., 2011).

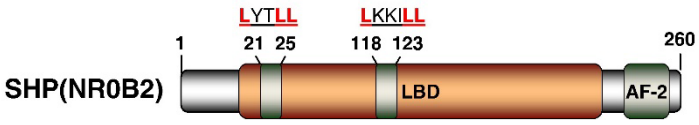

Figure 7 SHP domain structure
SHP contains the ligand binding domain (LBD) and the ligand-dependent transactivation domain (AF-2) but lacks the conserved DNA binding domain (DBD) commonly present in other nuclear receptors. SHP represses target genes by utilizing two functional LXXLL-related motifs, which are located in the putative N-terminal helix 1 of the LBD and in the C-terminal region of helix 5 (Modified from Zhang et al. 2011).

1.9.2 SHP as an inhibitor of LRH-1

SHP is a direct target and at the same time a potent inhibitor of LRH-1 (Chanda et al., 2010; Lee et al., 1999). The repressive effect of SHP on LRH-1-mediated transcriptional activation has been extensively studied. Structural studies have shown that SHP preferentially inhibits LRH-1 over other NRs, including its close homolog SF-1 (Li et al., 2005; Ortlund et al., 2005). SHP inhibits LRH-1 via interacting with the AF-2 transactivation domain of LRH-1, thereby competing with coactivators binding. In addition, the C-terminal domain in SHP represses LRH-1 via direct transcriptional repression (Lee and Moore, 2002; Zhang and Wang, 2011). Furthermore, SHP inhibits LRH-1 transactivation via recruiting HDAC. Consistent with this, inhibition of either SHP or HDAC drastically diminished the strong SHP repressive effect on LRH-1 (Chanda et al., 2010).

In the liver, it has been shown that binding of bile acids to FXR leads to transcriptional activation of SHP. Elevated SHP protein results in the inactivation of LRH-1 by forming a heterodimer complex, hence repressing the LRH-1-mediated expression of CYP7A1, the rate limiting enzyme in bile acid biosynthesis. This heterodimer complex leads to promoter specific repression of SHP in an autoregulatory negative feedback loop in order to maintain hepatic cholesterol catabolism (Goodwin et al., 2000; Lu et al., 2000).

Interestingly, SHP inhibits LRH-1-induced CYP11A1 and CYP11B1 expression and GC synthesis in the intestinal epithelial cell line mICcl2 (Mueller et al., 2007). Indicating a potential role of SHP in the regulation of intestinal immune homeostasis.
Furthermore, SHP is a potent inhibitor of LRH-1-induced aromatase transcription and estrogen production in breast adipose tissue (Clyne et al., 2002; Kovacic et al., 2004). Downregulation of SHP in the adrenocortical cell lines H295R, ACC-T36 and Y-1 increases LRH-1 expression and its target cyclin E1 leading to increased proliferation (França et al., 2015).

1.9.3 SHP in disease and Cancer

Because SHP is implicated in the regulation of a wide array of biological processes as discussed previously, its dysfunction is associated with the development of many diseases. For example, loss of function mutation in the SHP gene is demonstrated to influence the risk of metabolic diseases such as obesity, diabetes (Hung et al., 2003; Nishigori et al., 2001), and fatty liver disease (Zou et al., 2015). Moreover, due to the inhibitory effect of SHP on angiotensin II-stimulated plasminogen activator inhibitor-1 expression in vascular smooth muscle cells (a major effector molecule in the development of cardiovascular disease (Lee et al., 2009b)), loss of SHP protects mice from atherosclerosis (Kim et al., 2013).

Interestingly, SHP has been described to play a rather controversial role in the regulation of NF-κB function. Whereas it activates NF-κB in macrophages treated with oxidized low-density lipoprotein (Kim et al., 2001), SHP has been shown to play a previously unrecognized role in regulating innate immune responses after LPS-induced septic shock. In this regard, SHP acts as a negative regulator of systemic inflammation triggered by TLRs-mediated activation of NF-κB (Yang et al., 2013; Yuk et al., 2011). These facts suggest that the regulatory function of SHP on NF-κB might be context and stimulus dependent.

Accumulating evidence suggested that SHP acts as a potent tumor suppressor, by inhibiting tumorigenesis and cell proliferation through suppressing transcription of cyclin D1 (Zhang et al., 2008) and activating apoptosis (Zhang et al., 2010b). In line with this, it has been shown that SHP expression is diminished in HCC pathologic specimens and cell lines due to epigenetic silencing that leads to decreased LRH-1 binding to the SHP promoter (He et al., 2008). Similarly, SHP expression was downregulated in lung, stomach and renal tumor tissues compared to adjacent healthy mucosa from the same patients (Kudryavtseva et al., 2018; Prestin et al., 2016).

SHP demonstrated antitumor role in HCC by playing pleiotropic role in regulating cell proliferation, apoptosis, DNA methylation and inflammation (reviewed in (Zou et al., 2015)). In contrast, SHP has been implicated in the initiation and progression of cancer, particularly breast and liver cancer (Zhang et al., 2011). In line with this, inhibition of SHP *in vivo* causes regression of hepatoma (Zhang and Wang, 2011).

Taken all together, tissue-specific modulation of SHP activity represents an attractive area of research for potential clinical application in the treatment of cancer, inflammatory diseases, and several metabolic diseases.

1.10 Tumor immune escape mechanisms in cancer

The concept that the immune system can recognize and destroy nascent transformed cells is known as cancer immunosurveillance. However, recently it was replaced by the term cancer immunoediting to describe the immune system dual roles in promoting host protection against cancer and facilitating tumor escape from immune destruction (Dunn et al., 2002; Smyth et al., 2006).

Cancer cells exploit several mechanisms to evade the immune system. Those include: i) Immune suppression in the TME, mostly mediated by $FoxP3^+$ Tregs, myeloid-derived suppressor cells, modulated DCs and M2 macrophages. Immune suppression seems to be the major mechanism of tumor immune escape. ii) Defective antigen presentation, thus CTLs can no longer recognize target antigens on the tumor cells. iii) Immunosuppressive mediators such as TGFβ and IL-10. iv) Tolerance and immune deviation. Most tumor cells fail to express costimulatory molecules and can thereby induce anergy or tolerance in T cells. Moreover, tumors can shift the balance from Th1 to Th2 (immune deviation) in a TGFβ- and IL-10-dependent manner. Additionally, tumor expression of inhibitory molecules like PD-L1 and CTLA-4 has been shown to cause deletion or anergy on tumor reactive cells. v) Deletion of tumor-specific CTLs through apoptosis (reviewed in (Vinay et al., 2015)).

Accumulating evidence suggests that TGFβ produced by tumor cells, among other cells, causes conversion of $CD4^+$ T cells into suppressive Tregs *in situ.* Tregs dampen T-cell immunity to tumor-associated antigens and represent the main obstacle tempering successful immunotherapy and active vaccination (reviewed in (Zou, 2006)). In addition, M2 macrophages produce high levels of TGFβ, IL-10, and VEGF and thereby promote tumor progression and metastasis (Qian and Pollard, 2010; Sica et al., 2008b).
These facts clearly indicate that the immune reactions at the TME play a critical role in determining the fate of cancer. Interactions at the TME can either induce anti-tumor immune responses and thereby limit the tumor development or shape the TME to create an immunosuppressive microenvironment that fosters the tumor growth.

1.11 GC synthesis in colorectal tumor: a potential immune escape mechanism

Due to the immunogenic nature of CRC, anti-tumor immune responses may significantly limit tumor development and growth. In particular in CRC, a strong correlation between anti-tumor immune responses and patient survival has been demonstrated (Camus et al., 2009; Pagès et al., 2005). On the other hand, immune escape mechanisms have been recognized as one of the hallmarks of cancer by significantly limiting the efficacy of anti-tumor immune responses (Finn, 2008; Hanahan and Weinberg, 2011).

Of interest, it has been shown that colon cancer cells express steroidogenic enzymes and synthesize immunoregulatory GCs. Remarkably, primary tumors from CRC patients maintained the capability to synthesize GCs, regulated by LRH-1 (Sidler et al., 2011). Considering the immunomodulatory activities of GCs discussed in section 1.1.4, it is stimulating to postulate that, CRC synthesize GCs as a mechanism to control anti-tumor immune responses.

While the immunoregulatory role of GCs in the intestinal mucosa is well investigated (reviewed in (Kostadinova et al., 2012)), its role in CRC is studied only indirectly. The immunosuppressive activities of CRC-derived GCs have been shown by the inhibitory effect of CRC supernatant on the activation of T cells. Likewise, CRC-derived supernatant promoted apoptosis in murine T cells. These effects were GC-dependent, since they could be reversed by GR inhibition (Sidler et al., 2011). Taken together, LRH-1-mediated synthesis of immunoregulatory GCs in CRC could represent a novel immune escape mechanism.

2 Aims of the study

The nuclear receptor LRH-1 promotes colorectal tumor formation through affecting cell cycle control and proliferation via induction of cyclin D1 and E1 in synergy with β-catenin (Bayrer et al., 2015; Botrugno et al., 2004; Schoonjans et al., 2005). In addition to its repressive activity on the expression of the cell cycle inhibitor p21 (Kramer et al., 2016). LRH-1 also regulates intestinal homeostasis by inducing local GC synthesis (Coste et al., 2007; Mueller et al., 2006). Nevertheless, it remains unknown whether local GCs play a role in tumor initiation and/or progression. Furthermore, interesting data from Sidler et al. described for the first time LRH-1-dependent GC production in colorectal tumors (Sidler et al., 2011). However, the functional relevance of tumor-derived GCs remains to be elucidated. In this study we hypothesized that tumor-derived GCs could serve as an important immune escape mechanism by suppressing anti-tumor immune responses.

Therefore, to address these so far not answered questions about GCs in colorectal cancer, we aimed at investigating the role of intestinal GC synthesis in inflammation-derived tumorigenesis. For this purpose, we employed an inflammation-driven colon carcinogenesis model.

Consequently, colorectal cancer was first induced in LRH-1 intestine-specific knockout mice to confirm the role of LRH-1 in colorectal tumor development.

Next, since SHP has been shown to potently inhibit the transcriptional activity of LRH-1 (Lee and Moore, 2002), a second aim was to study the effect of unleashing LRH-1 activity in carcinogenesis. For this reason, colorectal cancer was induced in SHP-deficient mice, hypothesizing that, SHP deficiency will increase LRH-1-induced tumor formation.

Moreover, to study the direct effect of GC synthesis in colorectal tumor development, colorectal cancer was induced in Cyp11b1 intestine-specific knockout mice.

Another aim of this study was to dissect the proliferation phase of carcinogenesis from the inflammation phase, and to test the immunosuppressive activity of tumor-derived GCs. For this purpose, the growth capacity of tumor organoids derived from all the above-mentioned three genotypes was investigated after subcutaneous injection in immunocompetent wild type mice.

3 Material and Methods

3.1 Material

Culture media and additives

Product	Supplier	Cat. No
A83-01 (TGFβ inhibitor)	Sigma Aldrich	SML0788
N-acetyl cysteine	Sigma Aldrich	A9165
Bovine serum albumin (BSA)	Sigma Aldrich	8076-3
Dulbecco's Modified Eagle's Medium (DMEM)- high glucose	Sigma Aldrich	D0572
DMEM/F12	Sigma Aldrich	D6421
Fetal Bovine Serum (FBS)	Sigma Aldrich	032M3395
Gentamicin solution	Sigma Aldrich	G1272
L-Glutamine solution	Sigma Aldrich	G7513
Nicotinamide	Sigma Aldrich	N0636
PBS	Sigma Aldrich	RNBF0297
RPMI 1640 Medium	Sigma Aldrich	R8758
Trypsin-EDTA solution	Sigma Aldrich	T3924
B-27 Supplement (50X) serum free	Fisher Scientific	17504044
Chir99021 (GSK-3 inhibitor)	Axon Medchem	1386
Cultrex Pathclean Reduced Growth factor BME	Trevigen & R&D	3533-010-02
N-2 Supplement (100X)	Fisher Scientific	17502048
Penicillin/Streptomycin (100X)	PAA laboratories	P11-010
Recombinant murine EGF	Peprotech	315-09
Recombinant murine Noggin	Peprotech	250-38
TrypLE™ Express (1X), no phenol red (gibco)	Thermo Fisher	12604-021
Y-27632 Dihydrochloride (Rho kinase inhibitor)	Selleckchem	S1049

Reagents

Product	Supplier	Cat. Number
1,4-Dithiothreitol (DTT)	Roth	6908.2
6x DNA Loading Dye	Thermo Fisher	R0611
2-Mercaptoethanol	Sigma Aldrich	M-6250
Acetone	VWR	UN1090
Ammonium persulfate (APS)	Roth	9592.2
Aqua Ad Iniectabilia Braun	Braun	V07AB
Azoxymethane (AOM)	Sigma Aldrich	A5486
Biozym LE Agarose	Biozyme	840004
Calciumchlorid	Merck	2379

Charcoal, activated	Riedel-de Haen	18002
Chloroform	Sigma Aldrich	SZBD1630V
Cotricostertone	Sigma Aldrich	C2505-500MG9
D (+)-Glucose	Sigma Aldrich	16325
Dextran	Sigma Aldrich	D-1390
Dextran sulphate sodium salt (DSS)	MP Biomedicals	0216011090-500g
Diethylpyrocarbonate (DEPC)	Sigma Aldrich	D-5758
Dispase 5000U (Corning)	Fisher scientific	11553550
Dimethyl sulfoxide (DMSO)	Roth	A994-1
dNTP Solution Mix	NEB	N0447S
Ethanol	VWR Chemicals	
Eosin	Roth	X883.1
Fast SYBR®Green Master Mix	Applied Biosystems by Thermo Fisher	10447494
Formaldehyde solution 37%	Roth	7398.1
GeneRuler 1 kb Plus DNA Ladder	Thermo Scientific	SM1331
Glycerol	VWR	
Glycine	Roth	3908.2
Glycyl-glycine	Roth	HN74.2
Goat Serum	Sigma Aldrich	G9023
HDGreen+ DNA Stainer	Intas	ISII-HD Green Plus
Hematoxylin solution	Sigma Aldrich	51275
HEPES	Sigma Aldrich	9105.3
Hot corticosterone	Perkin Elmer	NET399250UC
Hydrogen peroxide 30%	Merck	8597
ImmPACT DAB	Biozol	SK-4105
Isopropanol	Fisher Scientific	1288393
Magnesium chloride hexahydrate	Merck	5833
Methanol	Sigma Aldrich	32213-1l
Metyrapone	Sigma Aldrich	856525
MicroScint 40 (scintillation liquid)	Perkin Elmer	6013641
Organo/Limonene Mount™ (mounting medium)	Sigma Aldrich	08015
PageRuler™ Prestained Protein Ladder	Thermo Scientific	26616
peqGOLD Tri FastTM	VWR	30-2010
Potassium chloride	Roth	6781.1
Potassium phosphate dibasic	Merck	A877573
Proteinase K	Sigma Aldrich	P2308
RedSafe™ Nucleic Acid Staining Solution	Hiss Diagnostic	21141
Rotiphorese® Gel 30 (37,5:1)	Roth	3029.1
Sodium azide	Riedel-de Haen	13412
Sodium chloride	Roth	3957.2
Sodium citrate tribasic dihydrate	Riedel-de Haen	32320
Sodium dodecyl sulfate (SDS)	Bio-Rad	161-0302
Sodium phosphate dibasic dihydrate	Sigma Aldrich	4272

Sucrose	Roth	4661.2
Taq DNA Polymerase	NEB	M0267X
Tetramethylethylenediamine (TEMED)	Sigma Aldrich	1766
Thermopol Reaction buffer (10X)	NEB	B9004S
Tris	BRL	
Tris Base	Sigma	T1503
Tris hydrochloride	Roth	9090-2
TritonX-100	Sigma Aldrich	X-100
Trypan Blue Solution	Sigma Aldrich	93395
Tween 20	Sigma Aldrich	P-1379
Xylene	Roth	4436.1

Plastic ware

Product	**Supplier**
0.2 ml PCR SingleCap soft stripes	Biozyme
0.2 ml 96-well PCR plate, semi-skirted, AB1 FAST systems (qPCR plates)	STARLAB
1.5 ml tube	Sarstedt
2 ml tube	Sarstedt
15 ml falcon tube	Sarstedt
50 ml falcon tube	Sarstedt
60 x 15 mm Petri dishes	Greiner Bio-one
EASYstrainer™ Cell Strainer (40 µm)	VWR
EASYstrainer™ Cell Strainer (70 µm)	VWR
Pipet tips	Sarstedt
PVDF Western Blotting Membranes	Roche
Scintillation tubes	Sarstedt
Serological pipettes (5ml, 10ml, 25 ml)	Sarstedt
StarSeal Advanced Polyolefin Film	STARLAB
Syringe (Inject 20 ml)	Braun
Syringe-Filter 0.45 µm	TPP
TC Flask T175, Stand.,Vent. Cap	Sarstedt
TC Plate 24 Well, Standard, F	Sarstedt
TC Plate 96 Well, Standard, F	Sarstedt
Tissue embedding cassettes (blue, white, green)	Medite

Glass ware

Product	**Supplier**
Object slide Histobond+ blue	Roth
Object slide microscope cover glasses	Marienfeld
Object slides superfrost plus	Thermo Scientific

Antibodies

Antibody (clone)	Supplier	Cat. No	Dilution	Species
Immunohistochemistry primary Antibodies				
anti-mouse CD3 (ab5690)	abcam	ab5690	1:100 1:400	Rabbit
anti-mouse F4/80 (IgG2a)	eBioscience	14-4801	1:100	Rat
anti-mouse Ki-67	Cell Signaling	12202	1:400	Rabbit
Immunohistochemistry secondary Antibodies				
biotinylated goat anti-rabbit	Jaksons immunoresearch	111-095-144	1:100	Goat
biotinylated goat anti-rat	Biozol	PK-6104	1:100	Goat
Immunohistochemistry isotype control Antibodies				
anti-rabbit IgG isotype	Cell signaling	3900S	1:400	Rabbit
anti-rat IgG2a isotype (eBR2a)	eBioscience	14-4321-85	1:100	Rat
Western blot primary Antibodies				
anti-Myc	-	-	1:1000	Mouse
anti-tubulin	Sigma	T5168	1:4000	Mouse
Western blot secondary Antibody				
anti-mouse IgG (HRP)	Jakson ImmunoResearch	115-035-146	1:5000	Goat
RIA antibody				
anti-corticosterone	Millipore	AB1297	1:60 000	Sheep

Primer sequences

The following primers were provided by metabion international AG.

Product		Sequence (5' → 3')
• **Primer for qPCR**		
mβ-actin	forward	TAT TGG CAA CGA GCG GTT CC
	reverse	GCA CTG TGT TGG CAT AGA GG
mCyclin D1	forward	GAG CGT GGT GGC TGC GAT GCA A
	reverse	GGC TTG ACT CCA GAA GGG CTT CAA T
mCyclin E1	forward	TTC TGC AGC GTC ATC CTC TC
	reverse	TGT GCC AAG TAG AAC GTC TC
mCyp11a1	forward	CTT TGA GTC CAT CAG CAG TGT T
	reverse	TGG TAG ACA GCA TTG ATG AAC C
mGAPDH	forward	CGT CCC GTA GAC AAA ATG GT
	reverse	TCT CCA TGG TGG TGA AGA CA
mHsd11b1	forward	GCC AGC AAA GGG ATT GGA AG
	reverse	CGA GTT CAA GGC AGC GAG AC
mIL-6	forward	CACAAGTCCGGAGAGGAGAC
	reverse	TTGCCATTGCACAACTCTTT
mIL-10	forward	GACTTTAAGGGTTACTTGGGTTGC
	reverse	GCCTGGGGCATCACTTCTAC
mLRH-1	forward	TCA TGC TGC CCA AAG TGG AGA
	reverse	TGG TTT TGG ACA GTT CGC TT
mTNF	forward	TAGCCCACGTCGTAGCAAAC
	reverse	ACAAGGTACAACCCATCGGC
• **Primer for genotyping**		
Villin-Cre	forward	GAA CCT GAT GGA CAT GTT CAG G
	reverse	AGT GCG TTC GAA CGC TAG AGC CTG T
Myogenin	forward	TTA CGT CCA TCG TGG ACA GC
	reverse	TGG GCT GGG TGT TAG CCT TA
SHP	1	TTGAGTCATCCGATAAAGGGCATCC
	2	AACCTTGACTCCAGAAGTCACGTTC
	3	TAGTTGCTTGTGGAAAGGACCAACC
	4	CTAGGAAGTGAAGTGGCCTTGTCTG

The following Quantitect primers were provided by Qiagen.

Product	Sequence (5' → 3')
• **Primer for qPCR**	
mCyp11b1	
mCyp21	-
mHsd11b2	

Plasmid

Plasmid name	Backbone	Insert
pcDNA3.1 (+) hRspoI mh (kl.9)	pcDNA3.1 (+) C myc/his	h RspondinI

Kits

Product	Supplier	Cat. No
FastPlasmid™ Mini Kit	Eppendorf	2300000
High capacity cDNA Reverse Transcription Kit	Applied Biosystems by Thermo Fischer	10400745
ImmPACT DAB Peroxidase Substrate kit	Biozol	SK-4105
Pure Yield Plasmid Midiprep System	Promega	A2495
SV Total RNA isolation system	Promega	Z3100
Thermo scientific Pierce BCA Protein Assay	Thermo scientific	23225
Vectastain ABC Kit (vector laboratories)	Biozol	PK-4000

Devices

Device	Supplier
AXIO Observer.Z1 Microscope, Laser Capture microdissection (LCM) Microscope	Zeiss
AxioCamICcl1 camera	Zeiss
BD Plasticpak™ 1 ml sub-Q with 26G needle	BD Biosciences
Electronic balance AE 240	Mettler
Image Quant LAS 4000	GE Healthcare
Infinite® 200 PRO series (i.control 1.10 software)	TECAN
Nanodrop 2000 spectrophotometer	Thermo Scientific
peQStar 2X Gradient PCR (thermocycler)	peQLab
StepOnePlus™ Real- Time PCR System Thermal Cycling Block	Applied Biosystems
Tissue lyser II	Qiagen
Rotor microtome Hyrax M40	Zeiss
Scintillation and Luminescence Counter	Perkin Elmer
Sliding caliper	-
Spin Tissue Processor Microm STP 120	Thermo Scientific
Stainless steel surgical blades	Swann Motion

Buffers

Buffer	Content
1x PBS	137 mM NaCl, 2.7 mM KCl, 10 mM Na_2HPO_4, 1.8 mM KH_2PO_4 in H_2O
20x Proteinase K solution	400 µg/ml proteinase K in TE buffer (pH 8.0)
12% resolving gel	4 ml Rotiphorese® Gel 30, 2.5 ml 1.5 M Tris (pH 8.8), 100 µl 10% SDS, 100 µl 10% ammonium persulfate, 12 µl TEMED, 3.3 ml H_2O
1x TAE	40 mM Tris acetate, 1 mM EDTA (pH 8.0)
1x TBS	8 g/l NaCl, 0.2 g/l KCl, 3 g/l Tris base in H_2O
1x TBS-T	8 g/l NaCl, 0.2 g/l KCl, 3 g/l Tris base, 0.1% Tween in H_2O
2x HEPES-buffered saline (HBS)	280 mM NaCl, 10 mM KCl, 1.5 mM $Na_2HPO_4*2H_2O$, 50 mM HEPES, 12 mM glucose in H_2O (pH 7.0)
5% stacking gel	830 µl Rotiphorese® Gel 30; 630 µl 1.0 M Tris (pH 6.8), 50 µl 10% SDS, 50 µl 10% ammonium persulfate, 12 µl TEMED, 3.4 ml H_2O
5x loading buffer	250 mM Tris-Cl (pH 6.8), 500 mM DTT, 10% SDS, 50% glycerol, 0.5% bromophenol blue
Antibody dilution buffer (IHC)	5% goat serum, 5% mouse serum in 1x TBS (F4/80) 5% goat serum, 5% BSA in 1x TBS (CD3) 5% goat serum in 1x TBST (Ki67)
ECL solution (pH 8.5)	2.5 mM Luminol, 0.4 mM p-Coumaric acid, 10 mM Tris in H_2O (add fresh: 0.015% H_2O_2)
NP-40 lysis buffer	150 mM NaCl, 50 mM Tris (pH 7.6), 1mM EDTA, 1% NP-40
Radioimmunoassy (RIA) buffer	50 mM Tris-Hcl, 0.1 M NaCl, 0.1% NaN_3 in H_2O (pH 8.0)
SDS Running buffer (pH 8.3)	25 mM Tris, 250 mM glycine, 0.1% SDS (w/v) in H_2O
Sodium citrate buffer	10 mM $C_6H_5Na_3O_7*2H_2O$ in H_2O (pH 6.0)
Tail lysis buffer	50 mM KCl, 1.5 mM $MgCl_2$, 10 mM Tris-HCl (pH 8.3), 0.45% NP-40, 0.45% Tween 20, 100 µg/ml Proteinase K in H_2O
TE buffer	50 mM tris, 1 mM EDTA in H_2O (pH 8.0)
Transfer Buffer	192 mM glycine, 25 mM Tris base, 0.1% SDS, 21.5% methanol

3.2 Methods

3.2.1 Mice

Mice were bred at the animal facility of the University of Konstanz. All animal experiments were performed in compliance with the German laws and guidelines of the Care and Use of Laboratory Animals and approved by local ethics committee (Regierungspräsidium Freiburg).

Mice were group housed and accustomed to a 12 h- light/dark cycle under specific pathogen-free conditions with free access to standard chow and water *ad libitum*. Pathogen-free 7-11 weeks old, age and sex-matched mice were used for the experiments. All mice lines were kept under C57BL/6 genetic background.

3.2.1.1 SHP-deficient mice

SHP-deficient mice (SHP -/-) were described previously (Volle et al., 2007). The mice were kindly provided by Prof. Dr. K. Schoonjans (EPFL Lausanne, Switzerland).

SHP -/- mice were kept under C57BL/6 genetic background, and wild-type C57BL/6 mice (SHP +/+) were used as controls.

3.2.1.2 LRH-1 intestine specific knockout mice

Mice with a floxed LRH-1 gene (LRH-1 L2L2) (Coste et al., 2007) and villin-Cre transgenic mice (El Marjou et al., 2004) have been described previously. The mice were kindly provided by Prof. Dr. K. Schoonjans (EPFL Lausanne, Switzerland).

LRH-1 Intestinal epithelial cell conditional knockout (IEC KO) mice were generated using the Cre-mediated recombination (El Marjou et al., 2004). Therefore, LRH-1 L2L2 mice were crossed with villin-Cre transgenic mice; offspring mice harboring the Cre gene (villin-Cre x LRH-1 L2L2) were the IEC KO and termed LRH-$1^{IEC\ KO}$ hereafter, whereas mice lacking the Cre expression while expressing the floxed LRH-1 allele are referred to as LRH-$1^{fl/fl}$ and used as controls.

3.2.1.3 Cyp11b1 intestine specific knockout mice

The mice line was generated in house at the animal facility of the University of Konstanz. A conditional Cyp11b1 allele with loxP sites flanking exons 3–5 was generated by homologous recombination. Consequently, Cyp11b1 floxed mice (Cyp11b1 L2L2) were generated using C57BL/6 embryonic stem cells. Cyp11b1 IEC KO mice were generated following Cre-

recombination as described in section 3.2.1.2. Thus, Cyp11b1 L2/L2 mice were crossed with Villin-Cre transgenic mice resulting in Cyp11b1$^{IEC\ KO}$ and Cyp11b1$^{fl/fl}$ mice.

3.2.1.4 Mice genotyping

Genotypes of mice were verified via PCR using genomic DNA extracted from tail biopsies of 4-5 weeks old mice. Tail biopsies were lysed in 400 µl of tail lysis buffer and incubated overnight at 55°C on shaker. After that, Proteinase K was inactivated for 10 min at 95°C. 5 µl of the supernatant was used as DNA template. Standard genotyping protocol was performed using Tag DNA polymerase on peQlab PCR cycler.

For SHP -/- genotyping, 3x reaction master mixes were used:

1: Primer 1 and 2 for genotyping of the first loxP site.

2: Primer 3 and 4 for genotyping of the second loxP site.

3: Primer 1 and 4 for genotyping of the recombined allele.

Expected PCR product of the SHP knockout allele is at 500 bp, of the first loxP site is 225 bp and of the second loxP site is 365 bp.

Genotyping PCR for SHP -/-

Temperature	Time	
95°C	5 min	
95°C	30 sec	35 X
62°C	30 sec	
72°C	30 sec	
72°C	5 min	
4°C	∞	

Intestine specific LRH-1 and intestine specific Cyp11b1 knockout mice lines were genotyped for Cre/Myogenin. Mice positive for the Cre gene at 320 bp were referred to as the IEC KO.

Genotyping PCR for Cre/Myogenein

Temperature	Time	
95°C	10 sec	
95°C	30 sec	5X pre-cycle
62°C	60 sec	
72°C	45 sec	
95°C	30 sec	35 X
62°C	60 sec	
72°C	45 sec	
95°C	30 sec	
4°C	∞	

3.2.2 AOM/DSS colon carcinogenesis model

The inflammation-driven AOM/DSS colon carcinogenesis model was established as described previously (Neufert et al., 2007). Therefore, 7-11 weeks old age and sex- matched mice were injected intraperitoneally (i.p.) with 12µg/g body weight AOM dissolved in phosphate buffered saline (PBS) 5 days before the first cycle of DSS. Then, 2.2% (w/v) DSS (colitis grade: 36-50 kDa) was given in the drinking water for 5 consecutive days followed by 16 days normal drinking water. This cycle was repeated 3 times. Body weights were measured every day after DSS administration in the acute colitis phase and every second day in the recovery phase. Besides body weight, mice were also observed for clinical signs of illness, persistent distress or pain as well as general behavior and activity, accordingly a score is recorded. Mice were humanely euthanized according to stop criteria when a certain score is reached as described in the German guidelines of the Care and Use of Laboratory Animals.

Mice were sacrificed by CO_2 euthanasia at the indicated time points after the first DSS treatment for macroscopic examination, histologic analysis and total RNA extraction.

Upon sacrifice, colons were collected from the anal verge to the caecum to maintain consistent measurement of the colon length, and then colon length was measured. Colons were opened longitudinally and washed with ice cold PBS several times. Afterwards pictures were taken, tumor numbers and size were recorded. Tumor diameter was measured with a sliding caliper and the volume was calculated using the following formula: $V = 4/3\ \pi r^3$. (v: volume, π constant = 3.14 and r: radius = diameter/2).

For RNA extraction tumors and adjacent normal mucosa were collected using sharp surgical blades, washed with cold DEPC H_2O and immediately snap frozen in liquid nitrogen, afterwards stored at -80° C for further analysis. The colon tissue was then “Swiss rolled” and fixed overnight at freshly prepared 10% formalin in PBS for histological examination.
In some experiments colon tumors as well as normal mucosa from SHP -/- and SHP +/+ mice were collected at day 64 following DSS treatment and *ex vivo* cultured for measurement of glucocorticoid synthesis.

3.2.3 DSS acute colitis

Female mice were treated with 2.2% DSS in drinking water for 5 days followed by normal drinking water, then mice were sacrificed as indicated in the respective experiments at days 5, 7 and 10, or at day 7 only, after DSS treatment for histologic analysis (Swiss rolls), *ex vivo*

culture of colon tissue and total RNA extraction. Control mice received normal drinking water for this experiment. Body weights were measured every day after DSS administration.

3.2.4 Histology

3.2.4.1 Tissue preparation

Freshly resected tissues were fixed overnight in 10% formalin at RT for paraffin embedding. Tissues were dehydrated in ascending ethanol series and embedded in paraffin using the spin tissue processor Microm STP 120. Paraffin-embedded sections were cut with a rotary microtome at 4 µm thickness and mounted on glass slides (Superfrost plus for H&E and F4/80 (macrophage) staining, or Histobond for CD3 (T cell) and Ki-67 (proliferation) staining).

3.2.4.2 Hematoxylin and eosin (H&E) staining

Slide sections were heated on a warm plate at 60°C to liquify the paraffin, then sections were deparaffinized in xylene (3x for 5 min) and rehydrated using graded ethanol series (3x 100%, 90%, 80% then 70% for 5 min each) followed by washing in running tap water for 5min. Afterwards sections were stained for 5 min with hematoxylin, washed for 5 min in running tap water, then stained for 4 min with eosin and washed again for 5 min in running water. Finally, sections were dehydrated in ascending ethanol series (70%, 90% and 2x 100%, 20 sec each) followed by 3x immersion in xylene for 5 min. Slides were subsequently coverslipped with mounting medium (Organo/Limonene Mount^{TM}) and dried overnight.
H&E stained slides were used to examine intestinal pathology and colon adenoma development.

3.2.4.3 Histological colitis score

Hematoxylin and eosin stained Swiss roll sections were scored microscopically for colitis using a scoring method as previously described (Horino et al., 2008). The colitis score was graded according to 4 parameters: inflammation severity, inflammation extent, crypt damage as well as the percent involvement. Minimum total colitis score was set to 0 and maximum total colitis score was 40.

3.2.4.4 Immunohistochemistry (IHC)

Sections were deparaffinized in xylene (3x, 5 min) and rehydrated in graded ethanol series (3x 100%, 90%, 80% then 70%, 5 min each) followed by washing in running tap water for 5

min then washed in 1x TBS or 1x TBST for 5 min for immunohistochemical detection of F4/80-, CD3-, and Ki67-positive cells.

F4/80 staining

F4/80 as a macrophage marker was detected via IHC. Therefore, following rehydration of the sections, antigen retrieval was performed via incubation with 1x Proteinase K in TE buffer for 3 min at RT. Afterwards, slides were washed with 1x TBS for 5 min. Endogenous peroxidase activity was blocked by 1% H_2O_2 for 10 min, washed by immersion in 1x TBS, followed by incubation with the antibody dilution buffer (5% goat serum + 5% mouse serum) for 1 h at RT to block non-specific staining. The slides were dried carefully and incubated with the primary antibody (rat anti-mouse F4/80 diluted 1:100 in antibody dilution buffer) overnight at 4°C in a humified chamber, one control section was stained with anti-rat IgG2a isotype control diluted 1:100 in antibody dilution buffer to confirm the staining specificity. Next morning, sections were immersed briefly in 1x TBS then washed 3x with 1x TBS for 10 min on a shaker. For detection of F4/80 immunostaining, sections were incubated with the secondary antibody (biotinylated goat anti rat diluted 1:100 in antibody dilution buffer) in the dark for 2 h in a humified chamber. Afterwards sections were washed 3x with 1x TBS for 10 min on a shaker. Immune complexes were amplified using horseradish peroxidase coupled avidin-biotin conjugate (Vectastain ABC Kit, Vector Laboratories) according to manufacturer's protocol, accordingly ABC reagent was incubated on the section for 30 min at RT. After that sections were washed 3x with 1x TBS for 10 min on a shaker. Immune complexes were developed and visualized with peroxidase Substrate 3,3´-diaminobenzidine (DAB) using Peroxidase substrate Kit (ImmPACT DAB, Vector Laboratories) according to the manufacturer's instructions. Next, sections were washed with tap water for 5 min. The slides were counterstained with hematoxylin for 10 sec, rinsed with water for 5 min and dehydrated in ascending ethanol gradient (70%, 90%, then 2x 100% for 20 sec each) followed by 3x immersion in xylene for 5 min. Lastly slides were coverslipped with mounting medium and dried overnight.

CD3 staining

For the staining of the T cell marker CD3, slides were placed in a glass container filled with 10 mM sodium citrate buffer (pH 6.0) and containing 6 boiling chips. Antigen retrieval was mediated by boiling the sections 3x for 5 min at a microwave (400 W) as described before (Jakob et al., 2008). Afterwards, the sections were let to cool down for 30 min at RT. Next,

slides were washed with 1x TBS for 5 min. Endogenous peroxidase activity was blocked as described above. Nonspecific bonds were also blocked as described above by incubation in the antibody dilution buffer (5% goat serum + 5% BSA in 1x TBS). Then, the sections were incubated with the primary antibody (rabbit anti-mouse CD3 diluted 1:100 or 1:400 in antibody dilution buffer) overnight at 4°C in a humified chamber. Anti-rabbit IgG was used as isotype control. Next morning, sections were immersed briefly in 1x TBS then washed 3x with 1x TBS for 10 min on a shaker. For detection of CD3-positive cells, sections were incubated with the secondary antibody (biotinylated goat anti rabbit diluted 1:100 in antibody dilution buffer) in the dark for 2h in a humified chamber.

Afterwards signal amplification, development, counter staining as well as dehydration were performed as described above. Then, sections were coverslipped and dried overnight

Ki67 staining

Proliferative status was assessed by performing IHC for the nuclear proliferation marker Ki-67 (Schlüter et al., 1993). Antigen retrieval was performed as described for CD3 staining. Next, slides were washed 3x with running water for 5 min. Nonspecific bonds were blocked as described above by incubation with 3% H_2O_2 followed by antibody dilution buffer (5% goat serum in 1x TBST). Then, sections were incubated with the primary antibody (rabbit anti-mouse Ki-67 diluted 1:400 in antibody dilution buffer) overnight at 4°C in a humified chamber. Anti-rabbit IgG was used as isotype control. Next morning, sections were immersed briefly in 1x TBST then washed 3x with 1x TBST for 10 min on a shaker. For detection of Ki-67-positive cells, sections were incubated with the secondary antibody (biotinylated goat anti rabbit diluted 1:100 in antibody dilution buffer) in the dark for 2h in a humified chamber. After that sections were washed 3x in TBST for 10 min on a shaker. Signal amplification, development, counter staining, dehydration and slides covering were performed as described above.

3.2.4.5 Microscopy

Pictures were acquired at a laser capture microdissection (LCMD) device (Zeiss) using palmRobo v 4.6. software via AxioCamICcl1 camera.

3.2.5 Measurement of intestinal corticosterone synthesis

Ex vivo corticosterone synthesis in the intestinal mucosa or tumors and normal mucosa was assessed by radioimmunoassay (RIA) as described previously (Cima et al., 2004).

Tissue preparation for ex vivo culture

Mice were euthanized with CO_2 and a third of the colons or total number of isolated tumors and adjacent normal mucosal tissue, as indicated for the respective experiments, were isolated, cutted into 5-mm pieces, washed extensively in ice cold PBS, then pieces were equally distributed in a 24 well plate and cultured in RPMI medium supplemented with 10 % steroid free FBS and 1 ml gentamicin. Tissues were cultured in the absence or presence of 400 µg/ml metyrapone; the GC synthesis inhibitor. After 6- 16 hours of incubation, cell-free supernatant was harvested, and corticosterone was measured by radioimmunoassay. To correct for contamination from serum GCs i.e to present only locally synthesized GCs, results were expressed as the metyrapone-blockable corticosterone in nanogram per gram tissue weight (ng/g).

Radioimmunoassay (RIA)

Samples were boiled at 90° C for 15 min to separate the bound corticosterone from corticosteroid-binding globulins. Then samples were centrifuged at 14.000 RPM for 10 min at 4° C and the supernatant was used for the assay. Duplicate samples (100 µl) were incubated with 100 µl anti-corticosterone antibody (working dilution 1:20.000 in 0.1% BSA in RIA buffer) for 15 min at 4° C on a shaker. Next, 100 µl hot corticosterone (working dilution: 2 µl/ml in RIA buffer) was added to the samples and incubated overnight at 4° C on a shaker. Next morning 100 µl 1x dextran/charcoal was added to the samples followed by vigorous vortex mixing, then samples were incubated for 10 min at 4° C. Afterwards the samples were centrifuged at 2500 x g for 15 min at 4° C. Meanwhile scintillation tubes containing 1.5 ml of scintillation liquid were prepared, then 300 µl samples were added to the tubes and the mixture was vortexed vigorously. Lastly, the radioactivity was measured using a Scintillation and Luminescence Counter.

Preparation of the steroid free FBS

In order to reduce the contamination of steroids from the culture medium, tissues were cultured in RPMI medium containing charcoal-stripped FBS prepared as previously described (Cao et al., 2009). Firstly charcoal/dextran mix containing 0.25% activated charcoal, 0.0025% dextran, 0.25 M sucrose, 1.5 mM $MgCl_2*6H_2O$ and 10 mM HEPES in H_2O was prepared.

To activate the charcoal, the mixture was transferred to 50 ml tubes and incubated overnight at 4 °C while shaking. Subsequently, the activated charcoal was pelleted by centrifugation at 500 x g for 10 min. Afterwards, the supernatant was decanted and replaced by an equal

amount of heat-inactivated serum and vortexed. Then the mixture was incubated overnight at 4 °C while shaking. The charcoal was pelleted by centrifugation at 500 x g for 10 min and the steroid-free FBS was sterile filtered and stored at -20 °C.

3.2.6 Colorectal tumor organoids transplant

3.2.6.1 Colorectal tumor isolation, digestion and culture

Colon tumors were isolated as described previously (Xue and Shah, 2013) with minor modifications. Colorectal tumors were isolated from mice at day 56 following first DSS treatment. The mice were euthanized with CO_2. Colons were collected, opened longitudinally and washed with ice cold PBS, colon tumors were dissected using scissor and sharp surgical blades and washed 3 times with ice cold PBS. Tumors were then incubated in 10 ml digestion buffer (2.5% fetal bovine serum, 1 unit/ml penicillin, 1 µg/ml streptomycin, 200 U/ml type IV collagenase, 125 µg/ml type 1 dispase in Dulbecoo's Modified Eagle Medium) for 1 hr at 37 °C with gentle shaking at 15 min intervals. The tumor fragments were allowed to settle under gravity for 1 min, and then supernatant was collected in a 15 ml falcon. The supernatant containing tumor cell suspension was pelleted by centrifugation at 200 x g for 3 min at 4 °C and washed once with 10 ml PBS. Then filtered through a 70-µm followed by a 40-µm cell strainer to obtain single cells. Cells were pelleted by centrifugation at 200 x g for 3 min and supernatant was discarded.

For culture, tumor cells were resuspended with 500 µl PBS. Isolated single cells were counted using a hemocytometer. Tumor cells were then resuspended in BME diluted 3:4 with crypt basal culture medium (Advanced DMEM/F12 medium containing 0.1% bovine serum albumin, 2 mM L-glutamine, 10 mM HEPES, 100 U/ml penicillin, 100 µg/ml streptomycin and 1mM N-acetyl cysteine stored at -20 in 48.5 ml aliquots, after thawing of one aliquot, medium was freshly supplemented with 1x N2 (500 µl), 1x B27(1 ml), stored at 4°C and used within 4 weeks). Tumor cells were seeded at a density of 15.000 cells per 50 µl BME in 24 well plate at 37° C, 5% CO_2 incubator.

The BME was let to polymerize for 20 min at 37 °C. After polymerization, 500 µl/well colon tumor organoid culture medium was added (crypt basal culture medium containing 50 ng/ml EGF, 20% R-Spondin conditioned medium, 100 ng/ml mNoggin, 10µM Y-27632 (ROCK inhibitor), 500 nM A83-01 (TGFβ inhibitor), 3 µM Chir99021 (GSK3 inhibitor) and 10 mM Nicotinamide) as described previously (Canli et al., 2017). Then the plate was incubated at 37° C, 5% CO_2 incubator. Culture medium was changed every 2 days.

3.2.6.2 Colorectal tumor organoid passage and storage

To passage organoids, the organoids and the BME were mechanically disrupted using a P1000 pipette with cutted tips and transferred to a 50 ml falcon. The suspension was centrifuged at 200 x g for 3 min. Afterwards the supernatant was removed, and the pellet was incubated with 5 ml phenol red free TrypLE Express for 5 min at 37 °C with shaking every 2 min to digest the BME and the organoids into small cells clusters. Afterwards 10 ml of DMEM medium was added and the cells were pelleted by centrifugation at 200 x g for 3 min. The supernatant was aspirated, and cells were washed with PBS and pelleted by centrifugation at 200 x g for 3 min. Cells were then passaged at a 1:4 ratio and seeded as described above.
To freeze the organoids, they were recovered from BME plugs and dissociated as described above, then the cell pellet was resupended in DMEM medium containing 40% FBS and 10% DMSO and transferred into 1.5 ml cryo tubes. The tubes were stored immediately in a Nalgene Mr. frosty freezing container and stored at -80°C. After overnight incubation, tubes were transferred to liquid N2 tank for long-term storage.

3.2.6.3 Recovery of established organoids

To recover the organoids; frozen cells were recovered from N2 tank and kept at room temperature until the sides are thawn while the center is still frozen, then immediately transferred to a 50 ml falcon containing pre-warmed DMEM medium and washed. The tube was then centrifuged at 200 x g for 3 min and medium was removed, cells were seeded as described above (3.2.6.1).

3.2.6.4 Generation of R-spondin conditioned medium for organoid culture

HEK293 T cells were seeded at a density of 4.6 x 10^6 cells in DMEM medium containing 10% FBS, 2 mM L-glutamine and 1 ml Gentamicin in T175 cell culture flask and let to grow overnight at 37° C, 5% CO_2 incubator. Cells were then transiently transfected with 10 µg myc tagged hR-spondin expression plasmid (pcDNA3.1 (+) hRspoI mh (kl.9)) using Calcium-Phosphate method. For transfection 2 tubes of transfection solutions were prepared: Tube 1 containing 100µl $CaCl_2$ (2.5M) and 10µg plasmid DNA in 300 µl H_2O, while tube 2 contained 400 µl 2x HBS buffer. DNA/$CaCl_2$ solution was added drop wise to tube 2 while gently vortexing and then incubated for 30 min at room temperature to form the fine precipitates of calcium phosphate- DNA complexes. Meanwhile medium was removed from cells and cells were washed with PBS. Fresh medium (20 ml) was added, and the complexes were then added to the cells drop wise. After overnight incubation, supernatants were collected in 50

ml falcon and new medium was added to the cells. Next morning, supernatants were collected at the same 50 ml falcon and tested for functionality on organoid growth, moreover cells were lysed, and western blot was performed using Myc antibody to confirm the transfection efficiency.

3.2.6.5 Colorectal tumor organoids subcutaneous transplantation

Subcutaneous transplantation was performed as described previously with minor modification (Melo et al., 2017). Organoids were collected from BME and dissociated into small clusters of cells as descried for passaging. Approximately 2 x 10^5 cells were resuspended in organoid basal media, admixed with 50% BME to a final volume of 200 µl, and injected subcutaneously in the flanks of C57BL/6 wild-type mice; the knockout tumor organoids were injected in the right flank while the control tumor organoids were injected in the left flank of the same mouse. Tumor dimensions were measured using sliding caliper every three days and tumor volume was calculated as 0.523 × length × width × width. Animals were humanely euthanized according to the following criteria: clinical signs of persistent distress or pain, significant body weight loss (>20%), tumor size exceeding 2.500 mm^3, or when tumors ulcerated. In none of the transplant experiments the stop criteria was reached. At day 12 or 24 after subcutaneous transplant, mice were euthanized with CO_2. Subcutaneous tumors were collected, and individual tumor weight and volume was measured. Afterwards, tumors were fixed overnight at freshly prepared 10% formalin for histological analysis and stained with H&E as described previously.

3.2.7 Quantitative real-time PCR (qPCR)

To analyze gene expression quantitative polymerase chain reaction (qPCR), also known as real time polymerase chain reaction (RT-PCR) was performed.

RNA isolation

Total RNA was extracted from tissues using TriFast reagent according to the manufacturer's instructions. 1 ml of TriFast was added to tissue sample in a 2 ml tube containing homogenizing beads and homogenized at a frequency of 300 Hz for 4 min in a tissue lyser. The lysates were transferred into a 1.5 ml tube, incubated for 10 min at RT and shaken. Afterwards to separate phases 200 µl of chloroform was added and the tube was shaken

strongly for 1 min followed by incubation at RT for 3 min and shaken again. Samples were then centrifuged at 12.000 x g, 4° C for 15 min.

For RNA precipitation, the aqueous phase was transferred into a new 1.5 ml tube and equal volumes of isopropanol (500 µl) were added and pipetted up and down. Samples were incubated for 15 min on ice, then centrifuged at 12.000 x g, 4 °C for 15 min. For RNA washing, the supernatant was removed, and the pellet was washed twice with 1 ml ice-cold 75% ethanol in DEPC H_2O and centrifuged at 7.600 x g, 4 °C for 5 then 8 min).
To solubilize the RNA, the RNA pellet was air-dried for 10 min at 56 °C and subsequently dissolved in 20 µl pre-warmed DEPC H_2O (56 °C) and incubated at 56 °C for 15 min.
For DSS-treated tissue, RNA was isolated using SV Total RNA isolation kit according to manufacturer's instructions.
RNA quality and concentration were determined using a NanoDrop spectrophotometer. Samples were stored at -80°C until analysis.

Reverse transcriptase PCR (RT-PCR)

For the conversion of RNA into complementary DNA (cDNA), a High Capacity cDNA reverse transcription kit was used according to the manufacturer's protocol. A total amount of 1 µg RNA in 10 µl H_2O was combined with 10 µl reverse transcription master mix (2 µl 10x RT-buffer, 0.8 µl 25x dNTP mix, 2 µl 10x RT random primer mix, 1 µl transcriptase and 4.2 µl H_2O) in a 0.2 ml PCR tube. The reaction was run in a peqStar PCR machine using the following settings: lid 110 °C, 25 °C for 10 min, 37 °C for 120 min, 85 °C for 5 min. Obtained cDNA samples were stored a -20 °C.
1 µl of the resultant cDNA was used to amplify mGAPDH control gene combined with 19 µl PCR master mix (2 µl 10x buffer, 0.5 µl dNTP mix, 2.5 µl primer mix, 0.125 µl Taq DNA Polymerase and 13.875 H_2O) using the following settings: lid 110 °C, 95 °C for 30 sec, 55 °C for 30 sec, and 72 °C for 30 sec 72°C for 5 min. The PCR products were fractionated on 1.5% agarose gel and visualized by red safe staining.

qPCR

Quantitative real time PCR was performed to quantify mRNA levels of the desired genes in comparison to β-actin as an internal control using SYBR Green (a fluorescent dye that has an excitation of 485 nm, SYBR Green binds double stranded DNA; upon binding the fluorescence is enhanced >1.000-fold (Dragan et al., 2012)) on Applied Biosystems StepOne Real-Time PCR System that detects the fluorescence emitted by the excited SYBR Green at real-time.

To each well of 96 well PCR plate, duplicates of 2 µl diluted cDNA was added to 18 µl master mix (for all primers except quantitect: 7 µl H_2O, 1 µl primer mix, since quantitect primers were provided as 10x stocks, 2 µl from the primer mix and 6 µl H_2O were used instead, then 10 µl Fast SYBR®Green Master Mix was added). Plates were sealed with polyolefin film and centrifuged at 1000 x g for 10 sec. Afterwards the qPCRs were run in a StepOnePlus Real-Time PCR System and analyzed using StepONE software. The threshold cycles (CT) were determined for each gene and gene expression was calculated by the comparative CT quantization method, therefore CT values of β-actin were subtracted from CT values of the target genes (Δ CT) (Schmittgen and Livak, 2008) and relative gene expression was calculated as $2^{-\Delta CT}$.

3.2.8 Western Blot

Western blot was used to quantify and detect proteins from cell lysates. Following extraction, proteins were separated by their size and detected with specific antibodies before they were visualized with a chemiluminescence reaction.

Protein extraction for western blot

HEK293 T cells were lysed in ice cold NP-40 lysis buffer. The lysates were incubated with the lysis buffer for 10 min on ice. Next, lysates were centrifuged at 13.000 RPM for 10 min at 4° C. Then supernatant was transferred into a fresh tube and protein concentration was measured using the Pierce BCA protein assay kit according to manufacturers' protocol. Afterwards proteins were diluted in a 5x loading buffer and denatured by boiling at 95° C for 5 min.

Western Blot and SDS- polyacrylamide gel electrophoresis (SDS-PAGE)

Polyacrylamide gels consisting of a 5% stacking gel and a 12% resolving gel were prepared. After gels polymerized, they were transferred to electrophoresis chamber and filled with SDS running buffer. Equal amounts of proteins were loaded into the gels, moreover a protein standard (PageRuler Prestained Protein Ladder) was loaded with the samples to determine the molecular size of the proteins. Afterwards samples were run at 70 V through the stacking gel until the resolving (separation) gel was reached, then the voltage was increased to 120 V. The separated proteins were then transferred by wet blotting onto polyvinylidene difluoride (PVDF) membranes. For protein transfer, an assembly of a sponge, 2 whatman papers, the PVDF membrane, the SDS-PAGE gel, 2 Whatman papers and another sponge on top was

prepared and fixed, then transferred to a running chamber filled with transfer buffer and placed on ice. Western blot was performed for 1.5 h at 350 mA.

Immunoassay

Following protein transfer, the membranes were blocked in 5% milk powder in TBS-T for 1 h. Subsequently; the membranes were incubated with the primary antibodies for the detection of Myc and Tubulin as a loading control diluted in 5% milk powder in TBS-T. After overnight incubation at 4° C on a shaker, membranes were washed 3x for 5 min in TBS-T. Then incubated with a horse radish-coupled secondary antibody diluted in 5% milk powder in TBS-T for 1 h at RT. Afterwards, membranes were washed 3x in TBS-T on a shaker. Finally, the development of the specific bands was achieved by chemiluminescence after addition of 1 ml ECL solution containing H_2O_2 directly to the membranes. Chemiluminescent signals were detected with an Image Quant LAS 4000 (GE Healthcare).

3.2.9 Statistical analysis

Results are expressed as means ± SD. Alternatively, individual values and the mean of the group are shown. Statistical parameters including the exact value of n, dispersion and precision measures (mean ± SD) and statistical significance and the tests used are reported in the figure legends. GraphPad PRISM 6 software was used for statistical analysis. Statistical tests used were unpaired student's t-test when comparing two groups and two-way ANOVA followed by Tukey's multiple comparison test when comparing multiple groups. The Kaplan-Meier method was used to estimate survival distribution between the groups and log-rank tests were applied to compare survival rates.

A p value < 0.05 was set as the level of significance. The p values were represented in the figures and indicated in the legends as * $p < 0.05$, ** $p < 0.01$, *** $p < 0.001$, **** $p < 0.0001$.

4 Results

4.1 Conditional deletion of LRH-1 in the intestinal mucosa exacerbates DSS induced colitis

Accumulating evidence has shown that intestinal inflammation and subsequent immune cell activation promotes the local synthesis of glucocorticoids (GCs), which in turn suppress intestinal immune cells and associated inflammatory processes (Cima et al., 2004; Huang et al., 2018; Noti et al., 2010b, 2010a). It is also known that intestinal GCs synthesis and steroidogenic enzyme expression is regulated by LRH-1 (Mueller et al., 2006, 2007). Moreover, LRH-1-mediated GCs synthesis protects against intestinal inflammation (Coste et al., 2007). Hence, in order to further investigate the role of LRH-1-induced steroidogenic enzymes in the regulation of intestinal inflammation, we used a well-established murine model of experimental colitis, the dextran sodium sulphate (DSS) colitis model, in mice with a conditional deletion of LRH-1 in the intestinal epithelial cells (LRH-$1^{IEC\ KO}$). Consequently, conditional LRH-1-deleted mice and wild type control mice (LRH-$1^{fl/fl}$) were exposed to 2.2% dextran sodium sulfate (DSS) in the drinking water for 5 days followed by 2 days of normal drinking water, while untreated control LRH-$1^{IEC\ KO}$ and LRH-$1^{fl/fl}$ mice received normal drinking water (Figure 8A).

DSS is an inflammatory agent that causes damage in the epithelium compromising the barrier integrity (Egger et al., 2000; Kim et al., 2012), thus exposing the epithelium immune cells to the luminal microbiome. Consequently, an acute inflammation occurs that peaks at day 7 and subsequently resolves (Noti et al., 2010a).

Supporting previous findings (Coste et al., 2007) a significantly increased inflammatory response following DSS treatment at day 7 was observed in the LRH-$1^{IEC\ KO}$ mice compared to their LRH-$1^{fl/fl}$ counterparts. This was evidenced by increased shortening of the colons (Figure 8B and C) and paralleled by increased colitis score (Figure 8D). Histological analysis of the Swiss-rolled colon sections from DSS-treated mice at day 7 revealed severe tissue damage in the LRH-$1^{IEC\ KO}$ mice, characterized by crypt loss and complete destruction of the mucosa and accompanied by massive immune cells infiltrating into mucosal layers (Figure 8E, right panel). In contrast, LRH-$1^{fl/fl}$ mice suffered from moderate signs of inflammation, with restored crypt architecture and reduced inflammation in the mucosa (Figure 8E, left panel). Our results clearly indicate that LRH-1 is required for intestinal epithelium homeostasis, as the loss of LRH-1 in the IECs exacerbated intestinal inflammation.

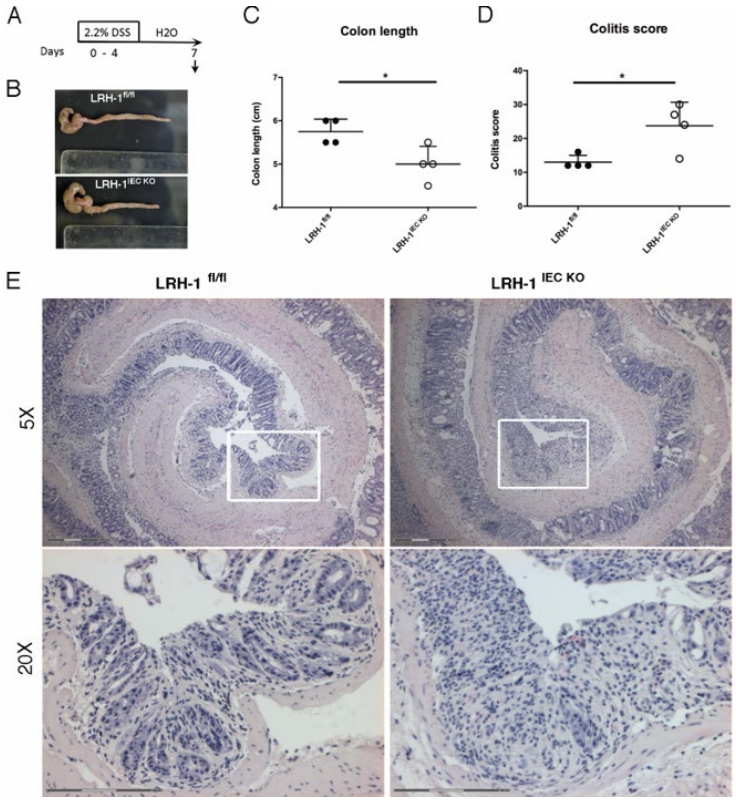

Figure 8 LRH-1 deletion exacerbates intestinal inflammation
(A) Scheme of colitis induction. Colitis was induced in 8-9 weeks old LRH-1$^{fl/fl}$ and LRH-1$^{IEC\ KO}$ female mice (n = 4 per group) by administration of 2.2% (w/v) DSS in the drinking water for 5 days followed by normal drinking water for 2 days. Control mice received normal drinking water (n = 6 per group), mice were analysed at day 7. **(B)** Representative macroscopic pictures from colon samples of DSS-treated mice at day 7. **(C)** Colon length and **(D)** Histological colitis score of DSS-treated mice at day 7. **(E)** Representative H&E staining of Swiss-rolled colon sections of mice treated with DSS at day 7. Scale bars: 300 µm overview, 150 µm inlay. Data are mean ± SD. Statistical analyses were performed using unpaired student's t-test with p value: *<0.05.

Next, in order to investigate the role of LRH-1 in the regulation of basal and colitis-induced expression of steroidogenic enzymes, we isolated colon tissue from DSS-treated LRH-1$^{IEC\ KO}$ and LRH-1$^{fl/fl}$ mice at the peak of inflammation (day 7) and from untreated mice. mRNA was extracted and the expression of the steroidogenic enzymes and their key transcriptional regulator, LRH-1, was analyzed. Consistent with LRH-1 deletion in the intestinal epithelium, decreased expression of LRH-1 was shown in colons from LRH-1$^{IEC\ KO}$ mice (Figure 9A). In agreement with increased LRH-1 activation and function upon inflammation (Coste et al., 2007), significant upregulation of the steroidogenic enzymes required for the *de novo* synthesis of corticosterone including Cyp11a1 (Figure 9B), Cyp11b1 (Figure 9C) and Cyp21 (Figure 9D) was observed in LRH-1$^{fl/fl}$ mice upon induction of inflammation. However, due to the deletion of LRH-1, LRH-1$^{IEC\ KO}$ mice failed to upregulate these normally colitis-induced enzymes (Figure 9B-D).

Recently, it has been shown that in IBD patients, the GCs metabolism pathway is dysregulated. This has been demonstrated by a significant downregulation in the expression of HSD11B2 (the inactivating enzyme of cortisol). Whereas, a trend towards a higher expression of HSD11B1 (the reactivating enzyme of cortisol from the inactive form cortisone) was observed in colon samples from IBD patients (Hussey et al., 2017). These results suggest a potential role of the dysregulation of GCs metabolism in the pathogenesis of IBD. Supporting this notion, we were able to monitor a significant colitis-induced upregulation of Hsd11b1 expression that appears to be lower in the LRH-1$^{IEC\ KO}$ mice (Figure 9E), while a downregulation of Hsd11b2 in both mice lines was observed (Figure 9F). Thus far, we have shown that colitis-induced expression of steroidogenic enzymes in the colon is dependent on LRH-1, since intestinal deletion of LRH-1 strongly reduced Cyp11a1, Cyp11b1 and Cyp21 colitis-induced expression. Moreover, the colitis experiment clearly showed that LRH-1 activity is critical for suppressing inflammation and maintaining epithelial homeostasis after acute tissue damage, as evidenced by increased inflammatory response and tissue damage in LRH-1 conditional knockout mice.

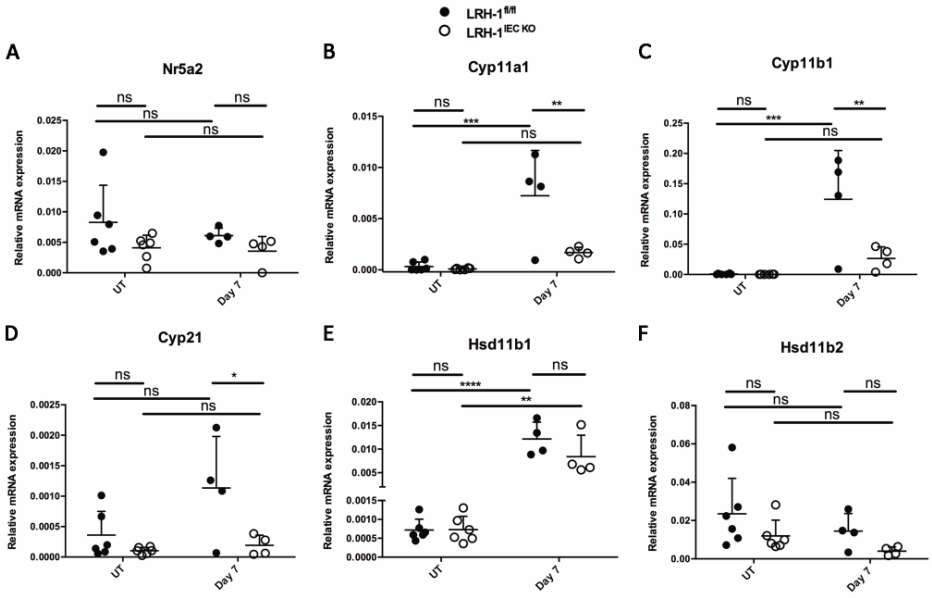

Figure 9 LRH-1-dependent regulation of steroidogenic enzymes
Gene expression of **(A)** LRH-1, **(B)** Cyp11a1, **(C)** Cyp11b1, **(D)** Cyp21, **(E)** Hsd11b1 and **(F)** Hsd11b2 from colons of LRH-1$^{fl/fl}$ and LRH-1$^{IEC\ KO}$ untreated mice (n = 6 per group) or mice treated for 5 days with 2.2% DSS followed by 2 days of normal drinking water and analysed at day 7 (n = 4 per group). Data was measured by quantitative PCR and normalized to the level of β-actin mRNA. Data are mean ± SD. Statistical analyses were performed using Two-way ANOVA followed by Tukey's multiple comparison test with p values: * <0.05, ** <0.01, *** <0.001, **** <0.0001. UT = untreated. ns = not significant.

4.2 LRH-1 intestine-specific knockout mice develop reduced incidence and size of inflammation-driven colon tumors

LRH-1 has also been described as an oncogene that derives intestinal tumorigenesis by affecting cell cycle and proliferation in synergy with the β-catenin/TCF4 signaling pathway. This was evident by the fact that heterozygous LRH-1 mice develop less intestinal tumors (Schoonjans et al., 2005). Considering the fact that colon cancer development is linked to chronic inflammation (Lasry et al., 2016) and since we have seen a critical role of LRH-1 in controlling inflammation, we next aimed at investigating the role of LRH-1 in inflammation-derived tumorigenesis. Therefore, we applied an inflammation-driven colon carcinogenesis model, the chemically induced Azoxymethane (AOM)/DSS model (Neufert et al., 2007), to induce tumors in the LRH-1 intestine-specific knockout mice.

Firstly, due to differences in strain susceptibility to AOM/DSS colitis-induced colon carcinogenesis in mice (Suzuki, 2005), we aimed at optimizing the dose of AOM and DSS for our inbred strains. Therefore, we treated wild type C57BL/6 mice with a single intraperitoneal (i.p.) injection of 12 µg/g AOM followed by 2 cycles of 2.2% DSS in the drinking water for 5 days with intermittent normal drinking water for 16 days and observed the tumor growth. AOM/DSS treatment resulted in the development of dysplastic lesions or microadenoma (< 1 mm) extended in the proximal to distal part of the colons of wild type mice at day 28 (data not shown), as described previously for the AOM/DSS treatment (Robertis et al., 2011).

According to the published histopathological scoring system (Boivin et al., 2007)., histological and immunohistochemical analyses of the Swiss-rolled colon sections at day 28 after AOM/DSS treatment revealed excessive inflammation characterized by crypt loss, epithelial erosion, hyperplasia and the development of focal areas of high-grade dysplasia also known as carcinoma *in situ* (Figure 10A). Development of dysplasia represents the first step in carcinoma development after chronic colitis (De Lerma Barbaro et al., 2014). These microadenomas were characterized by excessive proliferation as evidenced by the positive staining for the proliferation marker Ki-67 (Figure 10B). Furthermore, the microadenomas were infiltrated with massive numbers of mononuclear inflammatory cells (Figure 10A). Solid tumors including colon tumors are typically infiltrated with leukocytes, mostly lymphocytes and macrophages, which account for up to 50% of the tumor mass (Sica et al., 2008a). Indeed, we observed mainly F4/80-positive macrophages (Figure 10C) and CD3-positive T cells (Figure 10D) infiltrating the inflamed tissue especially the microadenoma.

This experiment clearly showed that the AOM/DSS doses used are optimum for the development of colon neoplasia in our inbred mice.

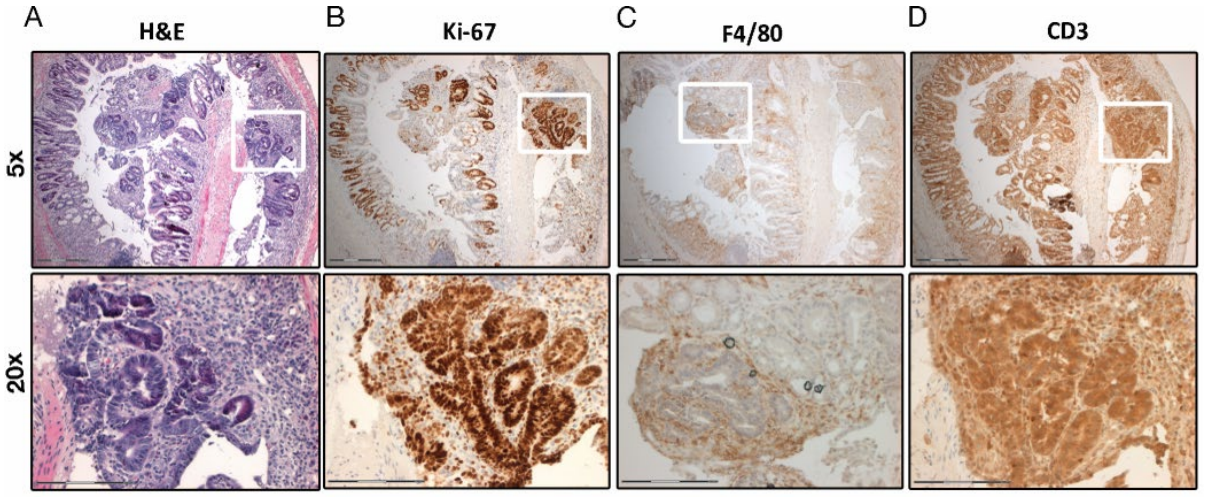

Figure 10 AOM/DSS treatment induced colon tumor formation in wild type mice characterized by massive immune cell infiltration
Wild type C57BL/6 mice (7-8 weeks old) were treated with i.p. injection of 12 µg/g AOM, followed by two cycles of 2.2% DSS for 5 days in the drinking water which was interrupted by 16 days normal drinking water. Colons were collected at day 28 following AOM/DSS treatment. Swiss-rolled colon sections stained for **(A)** H&E and IHC for **(B)** Ki-67, **(C)** F4/80 and **(D)** CD3. Representative result from 3 independent mice is shown. Scale bars: overview 300 µm, inlay 150 µm.

After optimization of the AOM/DSS treatment for our inbred mice, we next aimed at investigating the role of LRH-1 in inflammation-derived tumorigenesis at a later time point of the AOM/DSS treatment, namely day 56, at which multiple macroscopic colorectal tumor development was reported (Neufert et al., 2007). Consequently, we treated LRH-1$^{IEC\ KO}$ and LRH-1$^{fl/fl}$ control mice with 12 µg/g AOM followed by 3 cycles of 2.2% DSS in the drinking water for 5 days with intermittent normal drinking water for 16 days and then analyzed the tumor growth at day 56 following AOM/DSS treatment (Figure 11A). In line with the previous results, LRH-1$^{IEC\ KO}$ mice suffered from exacerbated colitis compared to LRH-1$^{fl/fl}$ mice during DSS treatment that persisted in all the 3 cycles, as evidenced by an increased weight loss and a delayed recovery (Figure 11B). Supporting the role of LRH-1-mediated proliferation and consequent tumorigenesis (Schoonjans et al., 2005), LRH-1$^{IEC\ KO}$ mice developed reduced number of colitis-associated colorectal tumors at day 56 (Figure 11C and D) that were significantly smaller in size compared to LRH-1$^{fl/fl}$ (Figure 11E and F). Since we analyzed the mice after they recovered from the chronic inflammation at day 56, and as both mice lines

recovered to almost 100% of initial body weight (Figure 11B), no differences in colon length were detectable as expected (Figure 11G).

Our results clearly indicate that chronic inflammation is not the only driver of colon carcinogenesis, since although the LRH-1$^{IEC\ KO}$ mice suffered from severe colitis, yet they developed significantly smaller tumors compared to control mice.

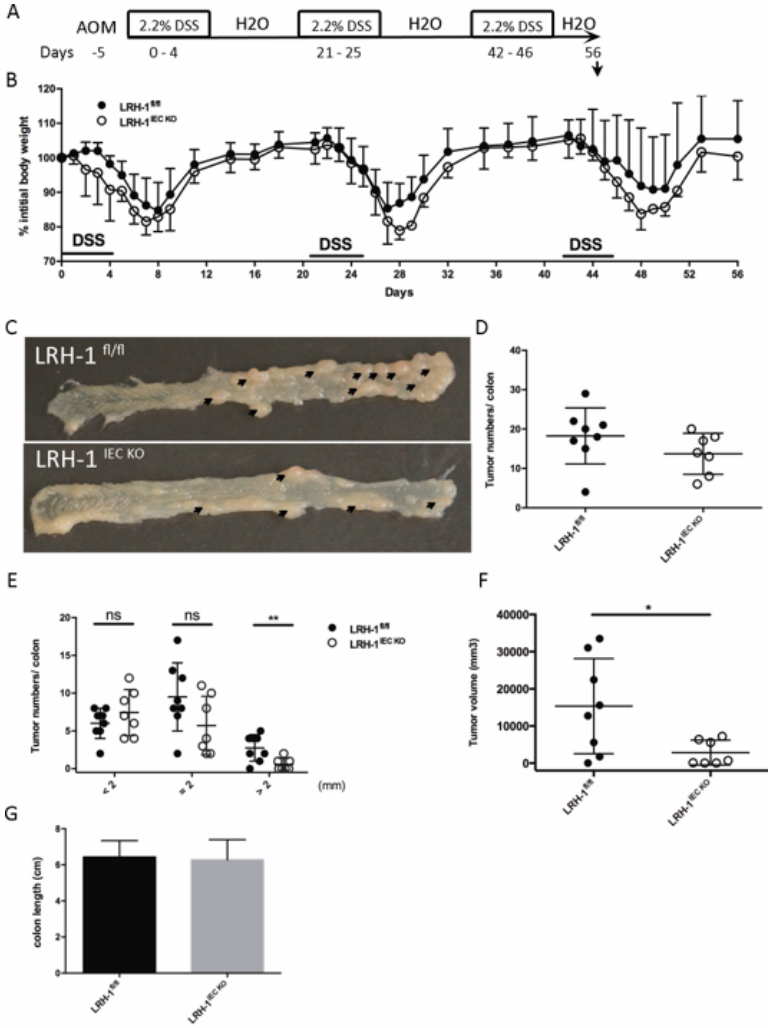

Figure 11 Deletion of LRH-1 in the intestinal epithelium attenuates colitis-associated colorectal cancer development

(A) Scheme of the AOM/DSS treatment is shown. Colitis-associated cancer was induced in 8-11 weeks old LRH-1$^{fl/fl}$ and LRH-1$^{IEC\ KO}$ mice by i.p. injection of 12 µg/g AOM, followed by three cycles of 2.2% DSS for 5 days in the drinking water which was interrupted by 16 days of normal drinking water. **(B)** Percent body weight change normalized to initial body weight at day 0 of mice treated as in A, (n = 5 per genotype). Data show representative results from 3 independent experiments. **(C)** Macroscopic pictures of colonic tumor development (arrows) in representative mice at day 56 following AOM/DSS treatment. **(D)** Total tumor numbers, **(E)** Tumor numbers according to size, **(F)** Tumor volume and **(G)** Colon length of AOM/DSS treated mice at day 56. **(D-G)** n = 7-8 mice per group. Data are mean ± SD from 3 independent experiments. Statistical analyses were performed using unpaired student's t-test with p values: * <0.05, ** <0.01. ns: not significant.

Our previous result suggests a more dominant role of LRH-1-induced proliferation in this phenotype. Confirming this hypothesis, histopathological and immunohistochemical analyses of Swiss-rolled colon sections from AOM/DSS-treated mice at day 56 revealed that LRH-1$^{fl/fl}$ mice exhibited increased Ki-67 staining further supporting the increased tumor formation in these mice (Figure 12B, left panel). Moreover, LRH-1$^{fl/fl}$ mice displayed severe tissue pathology as shown by massive formation of high-grade tubular adenoma mostly accompanied by mucosal hyperplasia and increased immune cell infiltration into the mucosal layers (Figure 12A, left panel). In contrast, LRH-1$^{IEC\ KO}$ mice suffered from moderate intestinal pathology as shown by low-grade adenoma, mucosal hyperplasia with more prominent aberrant crypt foci (ACF) and a few normal crypt structures, we also monitored immune cell infiltration into mucosal layers (Figure 12A, right panel). Moreover, due to the loss of LRH-1, colons from LRH-1 $^{IEC\ KO}$ mice exhibited reduced proliferation (Figure 12B, right panel). Our findings emphasize an important role of LRH-1-induced proliferation in the development of colorectal tumors, since LRH-1 deletion resulted in reduced proliferation and subsequent tumor formation despite the increased inflammation during the three DSS cycles (Figure 11B).

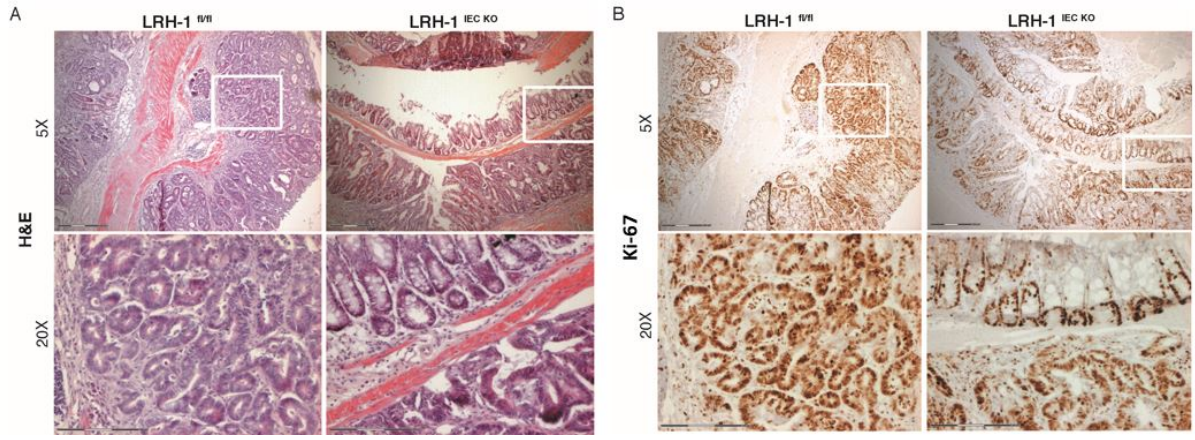

Figure 12 Deletion of LRH-1 in the intestinal epithelium results in reduced proliferation and associated colorectal tumor development

Colitis-associated cancer was induced in 8-11 weeks old LRH-1$^{fl/fl}$ and LRH-1$^{IEC\ KO}$ mice by i.p. injection of 12 µg/g AOM, followed by three cycles of 2.2% DSS for 5 days in the drinking water which was interrupted by 16 days of normal drinking water. Swiss-rolled colon sections stained for **(A)** H&E and **(B)** IHC for Ki-67. Representative results from AOM/DSS treated mice at day 56 are shown. n = 7-8 mice per genotype. Scale bars: overview 300 µm, inlay 150 µm.

4.3 SHP-deficiency abrogates inflammation-driven colorectal tumor development

We have clearly seen that LRH-1 is required for colon tumor development. Therefore, an exciting question came along: what will happen if we have an enhanced activity of LRH-1 utilizing the same inflammation-driven colon carcinogenesis model? In an attempt to answer this valid and very interesting question we next used the AOM/DSS model to induce colitis-associated colorectal cancer in mice deficient for the nuclear receptor and the potent inhibitor of LRH-1, SHP (Lee and Moore, 2002). Recently, it has been shown that deficiency of SHP results in increased intestinal GC synthesis following viral infection (Huang et al., 2018). Furthermore, unpublished data from C. Reinhold at the group of Prof. Dr. Brunner (University of Konstanz, Department of Biochemical Pharmacology) demonstrated that SHP-deficient mice have an enhanced LRH-1 activity at the intestinal epithelium, as evidenced by increased target genes expression, such as cyclin D1 and E1 (Unpublished data, data not shown). Therefore, wild type control mice (SHP +/+) as well as SHP-deficient mice (SHP -/-) were treated with AOM/DSS as described previously and the mice were analyzed at days 56 and 64 following treatment (Figure 13A).

In line with potentiated LRH-1 activity and given the role of LRH-1 in intestinal homeostasis after inflammation, indeed SHP-/- mice displayed more resistance to DSS-induced colitis compared to their wild type counterparts. This was evident by significant protection of the SHP-/- mice from weight loss. This protection was already shown after the first cycle of DSS accompanied by improved recovery. The differences in body weight loss were even more pronounced after the third DSS cycle (Figure 13B). The severity of the weight loss in wild type mice required us to humanely euthanize some mice before the end point (days 56 and 64). As a consequence of attenuated chronic colitis, SHP-/- mice showed extended survival (Figure 13H). Surprisingly and contrary to our expectations, SHP-/- mice developed remarkably reduced inflammation-driven colorectal tumors, which were also smaller in size when compared to the wild type counterpart (Figure 13C-G). Interestingly, some SHP-/- mice were completely protected from tumor development (Figure 13C). Noteworthy to mention, a very interesting finding was that among the few tumors that developed in the SHP-/- mice, there were extremely big tumors with a diameter of 5 mm (Figure 13C, lower panel), whereas the biggest tumor diameter from wild type observed was 3 mm.

Although we did not except differences in colon length in the recovery phase at days 56 and 64 where both mice lines recovered to almost 100% of initial body weight (Figure 13B), increased shortening of the colons of control mice was monitored (Figure 13I).

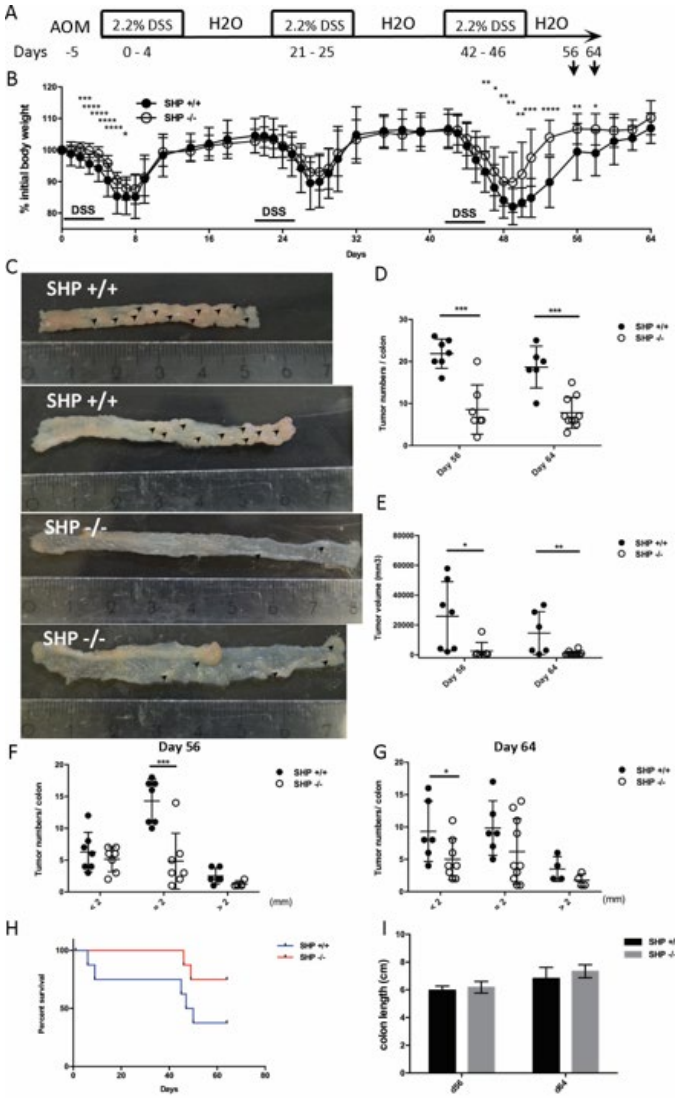

Figure 13 SHP- deficiency abrogates inflammation-driven colorectal tumor development
(A) Colitis-associated cancer was induced in 7-11 weeks SHP +/+ and SHP -/- mice by i.p. injection of 12 µg/g AOM, followed by three cycles of 2.2% DSS for 5 days in the drinking water which was interrupted by 16 days of normal drinking water. Scheme of the AOM/DSS treatment is shown. **(B)** Percent body weight change normalized to initial body weight at day 0 of mice treated as in A, results from 4 independent experiments. **(C)** Macroscopic pictures of colonic tumor development (arrows) in representative mice at day 64 following AOM/DSS treatment. Quantification of **(D)** Total tumor numbers and **(E)** Tumor volume in mice at days 56 and 64 following AOM/DSS treatment. Quantification of tumor numbers according to size in AOM/DSS treated mice at days **(F)** 56 and **(G)** 64. **(H)** Survival curve describing the percentage of mice survived until the end point of the experiment at day 64 (n = 8 per group), representative result of 3 independent experiments. **(I)** Colon length of mice at days 56 and 64 following AOM/DSS treatment. **(D-G, I)** day 56 (n = 7 mice per group), day 64 (n = 6-10 mice per group). Data are mean ± SD from 3 independent experiments. Statistical analyses were performed using unpaired student's t-test with p values: * <0.05, ** <0.01, *** <0.001, **** <0.0001.

Histopathological analysis of H&E stained Swiss-rolled sections showed a massive tumor development in wild type mice at days 64 (Figure 14), and 56 (Figure 15A) following AOM/DSS treatment. The wild type tumors showed prominent high-grade tubular adenomas, extensive mucosal hyperplasia and immune cell infiltration in all epithelial layers (Figure14 and 15A). In contrast, a striking protection of the SHP-/- mice epithelium from AOM/DSS-induced tissue damage and subsequent tumor formation was observed. This was evidenced by moderate inflammation of the mucosa and more prominent normal crypt structures, while few ACF, dysplastic epithelium and low-grade adenomas was shown in SHP-/- mice (Figure 14 and 15A). In line with the increased tumor formation in wild type mice, immunohistochemical analyses of stained sections from AOM/DSS-treated mice at day 56, revealed increased proliferation as visualized by higher numbers of Ki-67-positive cells in sections from wild type mice compared to SHP-/- mice (Figure 15B). Additionally, a remarkable proportion of cells infiltrating the tumors from wild type were CD3-positive T lymphocytes that was reduced in sections from SHP-/- mice (Figure 15C), further confirming the increased inflammatory state in colons from wildtype mice compared to SHP-/- upon AOM/DSS treatment. However, due to technical issues we were not able to detect macrophages.

Taken all together, SHP-deficiency abrogates inflammation-driven colon carcinogenesis by suppressing inflammation and associated tumorigenesis.

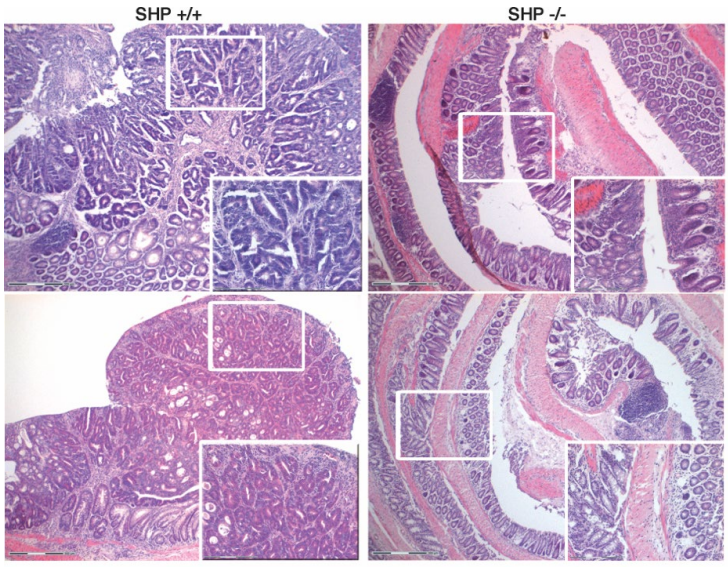

Figure 14 SHP-deficient mice exhibit mild intestinal pathology following AOM/DSS treatment
Colitis-associated cancer was induced in 7-11 weeks SHP +/+ and SHP -/- mice by i.p. injection of 12 µg/g AOM, followed by three cycles of 2.2% DSS for 5 days in the drinking water which was interrupted by 16 days of normal drinking water. Representative H&E stained Swiss-rolled colon sections from AOM/DSS treated mice at day 64 are shown. n= 6-10 mice per group. Scale bars: overview 300 µm, inlay 150 µm.

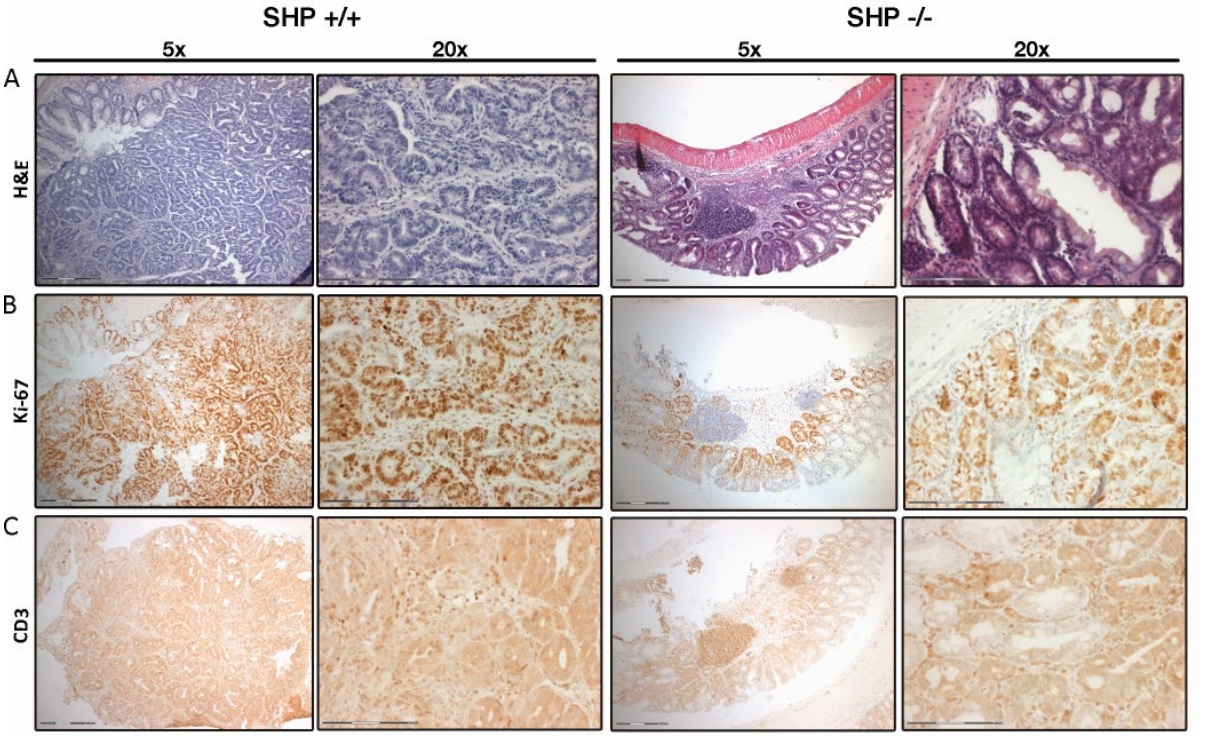

Figure 15 SHP-deficient mice show reduced AOM/DSS-induced tumor formation and immune cell infiltration Colitis-associated cancer was induced in 7-11 weeks SHP +/+ and SHP -/- mice by i.p. injection of 12 µg/g AOM, followed by three cycles of 2.2% DSS for 5 days in the drinking water which was interrupted by 16 days of normal drinking water. Representative results of Swiss-rolled colon sections stained for **(A)** H&E and IHC for **(B)** Ki-67 and **(C)** CD3 from AOM/DSS treated mice at day 56. n = 7 mice per group. Scale bars: 5x overview (left panels) 300 µm, 20x inlay (right panels) 150 µm.

4.4 SHP-deficient mice are protected from chronic colitis

We have now seen that SHP-/- mice are protected from colitis-associated cancer. Therefore, we next aimed at investigating an earlier time point of the AOM/DSS treatment, namely day 49 since it represents the peak of chronic inflammation, as evidenced by the highest weight loss that mice exhibited during the three cycles of DSS exposure (Figure 13B). Consequently, SHP-/- and wild type control mice were treated with AOM/DSS as described previously and analyzed at day 49 (Figure 16A). Supporting previous results (Figure 13A), SHP-/- mice exhibited ameliorated DSS-chronic colitis (data not shown) and subsequent tumorigenesis (Figure 16B). This was evident by a significant reduction in the shortening of colon length (Figure 16C) and colorectal tumor formation (Figure 16D) compared to wild type. Furthermore, although histopathological analysis of H&E stained Swiss-rolled sections revealed excessive tissue damage and inflammatory cells infiltrating the mucosa, submucosa

and muscularis in both mice lines, SHP-/- mice showed few ACF and carcinoma *in situ*. In contrast, wild type mice showed formation of high-grade tubular adenomas (Figure 16E).

These results confirm that SHP-deficiency protects mice from the formation of colonic neoplasia by resisting tissue damage even after chronic colitis and thereby suppressing tumor initiation and progression.

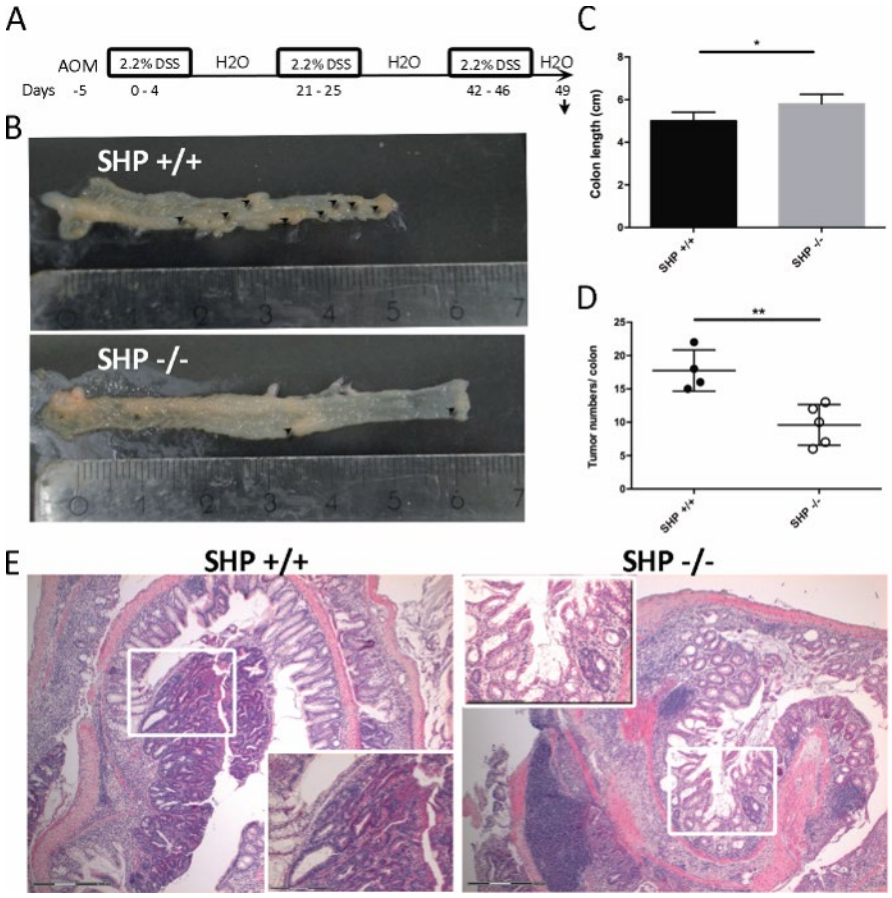

Figure 16 SHP-deficiency protects mice from chronic colitis and associated tumorigenesis following AOM/DSS treatment

(A) Colitis-associated cancer was induced in 7-11 weeks SHP +/+ and SHP -/- mice by i.p. injection of 12 µg/g AOM, followed by three cycles of 2.2% DSS for 5 days in the drinking water which was interrupted by 16 days of normal drinking water. Scheme of the AOM/DSS treatment is shown, mice were analysed at day 49. **(B)** Macroscopic pictures of colonic tumor development (arrows) in representative mice at day 49 following AOM/DSS treatment. **(C)** Colon length and **(D)** Total tumor numbers of mice at day 49 following AOM/DSS treatment. **(E)** Representative H&E stained swiss-rolled colon sections from AOM/DSS-treated mice at day 49**.** Scale bars: overview 300 µm, inlay 150 µm. n= 4-5 mice per group. Data are mean ± SD. Statistical analyses were performed using unpaired student's t-test with p values: * <0.05, ** <0.01.

4.5 SHP-deficient mice develop ameliorated colitis

In order to investigate the mechanism underlying the resistance of SHP-/- mice to chronic colitis and associated carcinogenesis, we performed an acute colitis experiment to investigate the effect of SHP-deficiency on inflammatory processes. Therefore, colitis was induced in SHP-/- and wild type control mice by 2.2% DSS in the drinking water for 5 days followed by 5 days of normal drinking water, colons were collected from mice at days 5,7 and 10 following DSS exposure for analysis (Figure 17A). These time points represent the peak of inflammation and GC synthesis (days 5 and 7), and recovery from inflammation (day 10) following DSS treatment (Noti et al., 2010a). As before, control mice received normal drinking water. In line with previous results, SHP-/- mice developed ameliorated colitis compared to wild type mice (Figure 17B-E). This was evidenced by significant resistance to DSS-induced weight loss (Figure 17C), reduced colon shortening (Figure 17D) and colitis score (Figure 17E).

The intestinal mucosa is a potent source for the production of immunoregulatory GCs upon inflammation (Cima et al., 2004). Furthermore, unpublished data from C. Reinhold at the Brunner lab. demonstrated an increased expression of LRH-1 target genes (Cyclin D1 and E1) in SHP-/- intestinal mucosa, suggesting an increased LRH-1 activity (Unpublished data). In line with this, it has recently been shown that SHP-/- mice exhibit increased LRH-1-induced GC production upon viral infection compared to control mice (Huang et al., 2018). Therefore, we hypothesized that SHP-/- mucosa resist inflammation due to increase of LRH-1-induced GC production upon DSS treatment, leading to reduced inflammation and associated tissue damage. In order to test this hypothesis, we proceed to measure the local GC produced during the DSS treatment as described previously (Cima et al., 2004). Consequently, a third part of the colons from untreated or DSS-treated mice at days 5,7 and 10 were *ex vivo* cultured in the presence or absence of the GC synthesis inhibitor metyrapone, to correct for serum GC contamination. Supporting our hypothesis, indeed SHP-/- mucosa produced significantly higher levels of immunoregulatory GCs at the peak of inflammation (day 7) compared to wild type mice (Figure 17F).

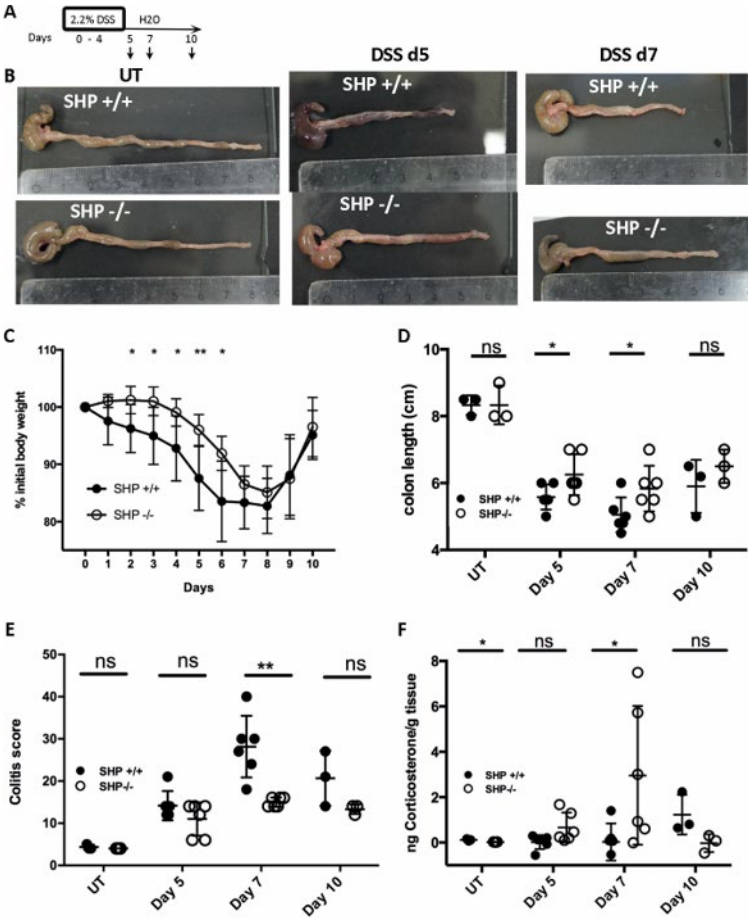

Figure 17 SHP-deficient mice develop ameliorated colitis due to increased local GC synthesis
(A) Scheme of colitis induction. Colitis was induced in 7-11 weeks old SHP +/+ and SHP -/- female mice by administration of 2.2% (w/v) DSS in the drinking water for 5 days followed by normal drinking water for 5 days. Control mice received normal drinking water, mice were analysed at days 5, 7 and 10. **(B)** Representative macroscopic pictures from colon samples of untreated and DSS-treated mice at days 5 and 7. **(C)** Percent body weight change normalized to initial body weight at day 0 of mice treated as in A, results from 2 independent experiments. **(D)** Colon length and **(E)** Histological colitis score of untreated and DSS-treated mice at days 5,7 and 10. **(F)** Colons from untreated and DSS-treated mice at days 5,7 and 10 were cultured ex vivo for 6 h in the presence or absence of metyrapone. Corticosterone in the cell-free supernatant was measured by RIA. n = 3-6 mice per group. Data are mean ± SD. Statistical analyses were performed using unpaired student's t-test with p values: * <0.05, ** <0.01. UT = untreated. ns = not significant.

Analysis of the Swiss-rolled H&E stained sections revealed nicely that SHP-/- mice suffered from moderate inflammation compared to wild type mice following DSS treatment, characterized by few altered crypts and inflammation in the mucosa and the submucosa with restored crypts architecture at days 5, 7 and 10 (Figure 18, right panels). Instead, wild type mice suffered from severe tissue damage at day 5 evidenced by complete destruction of the mucosa and crypt loss accompanied by massive immune cells infiltrating all the mucosal

layers in some parts of the colon, which was even more pronounced at the peak of inflammation (day 7) and persisted at day 10 (Figure 18, left panels).

We conclude that SHP-deficient mice are protected from colitis due to increased local GC production upon inflammation compared to wild type.

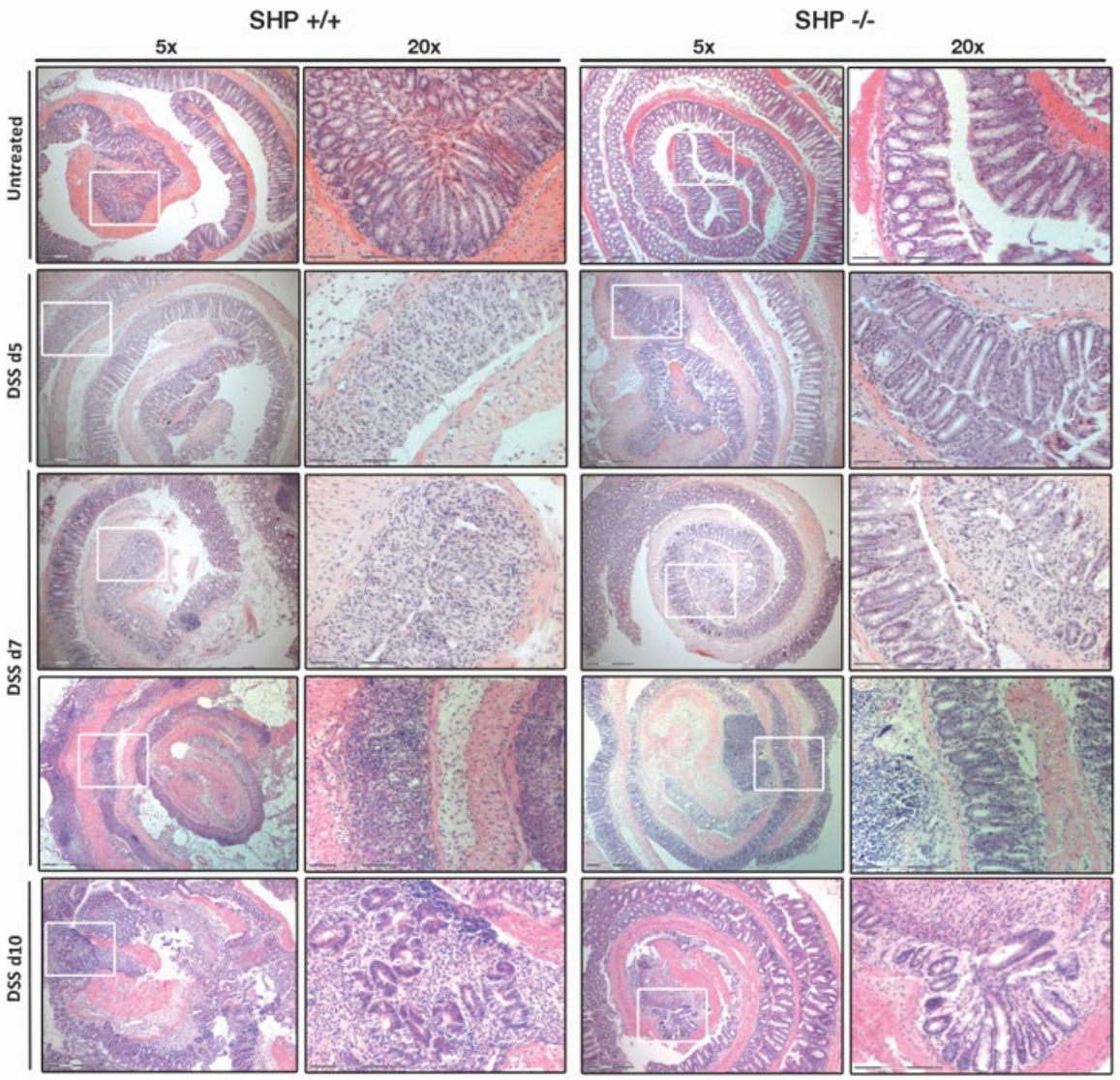

Figure 18 SHP-deficiency protects mice from acute colitis

Colitis was induced in 7-11 weeks old SHP +/+ and SHP -/- female mice by administration of 2.2% (w/v) DSS in the drinking water for 5 days followed by normal drinking water for 5 days. Control mice received normal drinking water, mice were analysed at days 5, 7 and 10 following DSS treatment. Representative H&E stained Swiss-rolled colon sections are shown**.** Scale bars: overview 300 µm, inlay 150 µm. n= 3-6 mice per group.

Next, in order to investigate the effect of SHP deficiency in the expression of steroidogenic and inflammatory factors upon colitis induction, we proceed to isolate colon tissue from SHP-/- and wild type DSS-treated mice at days 5,7 and 10 and from untreated mice, then mRNA was extracted, and the expression of steroidogenic and inflammatory factors was analyzed. As shown previously (Coste et al., 2007), LRH-1 expression was not changed upon DSS-induced inflammation in both genotypes (Figure 19A). However, in line with increased LRH-1 activity and associated GC synthesis (Figure 17F), we monitored significant increased expression of the steroidogenic enzymes Cyp11a1 (Figure 19B) and Cyp11b1 (Figure 19C) in colons from DSS-treated SHP-/- mice at day 7 compared to wild type mice. It has been described previously that the pro-inflammatory cytokines Tnf and Il-6 are elevated following DSS colitis (Coste et al., 2007). Indeed, we observed upregulation of Tnf and Il-6 in both genotypes upon colitis induction (Figure 19D and E). Consistent with reduced inflammation, reduced expression of Tnf and Il-6, while a significant increase in the expression of the anti-inflammatory cytokine Il-10 was observed in colons from SHP-/- DSS-treated mice at day 7 (Figure 19D-F).

Taken together, SHP-/- mucosa produce more immunoregulatory GCs upon inflammation due to increased LRH-1 activity, and thereby suppress inflammatory immune responses and subsequent tissue damage.

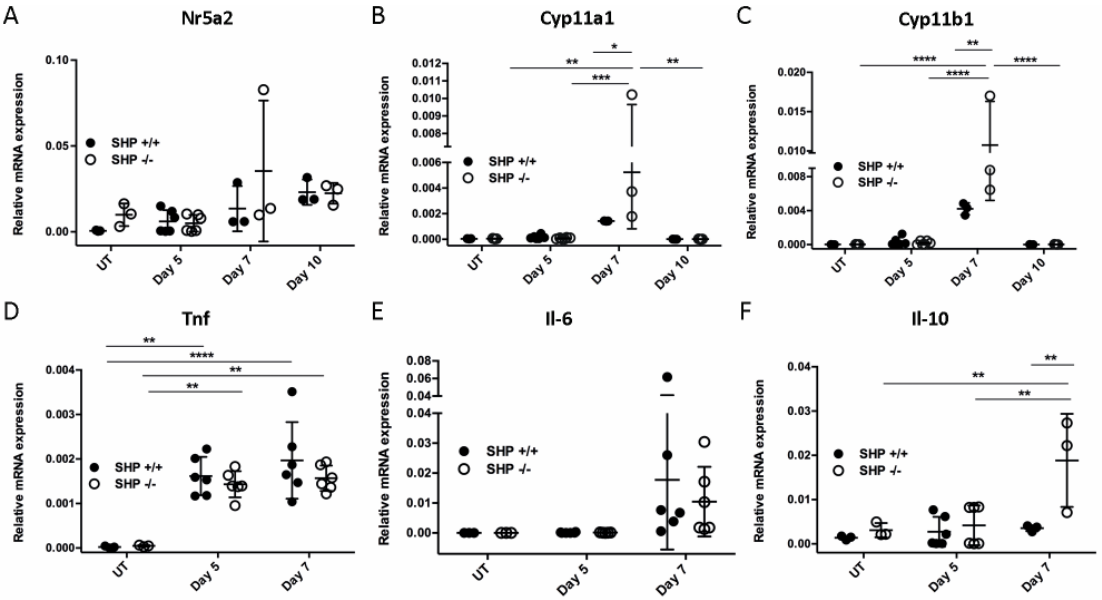

Figure 19 SHP-deficient colonic mucosa exhibit increased steroidogenic enzymes expression and reduced inflammatory responses upon colitis induction
Gene expression of **(A)** LRH-1, **(B)** Cyp11a1, **(C)** Cyp11b1, **(D)** Tnf, **(E)** Il-6 and **(F)** Il10 from colons of SHP +/+ and SHP -/- mice treated for 5 days with 2.2% DSS followed by 5 days of normal drinking water and analysed at days 5,7 and 10. Data was measured by quantitative PCR and normalized to the level of β-actin mRNA. n =3-6 per group. Data are mean ± SD. Statistical analyses were performed using Two-way ANOVA followed by Tukey's multiple comparison test with p values: * <0.05, ** <0.01, *** <0.001, **** <0.0001. UT = untreated.

4.6 SHP-deficient tumors produce more immunoregulatory GCs

Recently Sidler et al. described a previously unrecognized LRH-1-dependent *de novo* GC synthesis by colorectal tumor cell lines as well as primary tumors. Moreover, they could show that the tumor-derived GCs exerted immunoregulatory function by suppressing T cell activation and inducing T cell apoptosis (Sidler et al., 2011). The interesting observation we made that some of the SHP-deficient tumors developed were extremely big, prompted us to ask whether this increased growth is due to i) LRH-1-induced proliferation, ii) and/or as a consequence of an enhanced resistance of these tumors to anti-tumor immune responses. We assumed that resistance to anti-tumor immune responses might be mediated via LRH-1-dependent GCs synthesis, as we have seen an increased GC production in the SHP-/- mucosa upon inflammation (Figure 17F). Therefore, we aimed at investigating the local GC synthesis by AOM/DSS-induced tumors. Consequently, we collected tumors and adjacent normal mucosa from SHP-/- and wild type mice at day 64 following AOM/DSS then *ex vivo* cultured the tissues for 6 h, as described previously (Cima et al., 2004). Due to the few numbers of the tumors from SHP-/- mice, we pooled tumors from 2 mice in each group for the culture. As expected and consistent with an LRH-1 enhanced activity in SHP-/- tumors, a two-fold induction of GC synthesis was observed compared to wild type (Figure 20). Furthermore, tumors from both genotypes exhibited increased GC synthesis compared to adjacent non-tumor tissue (Figure 20). This result suggests that tumors synthesize immunoregulatory GCs as a possible immune escape mechanism, since increased GC production was observed in SHP-/- tumors showing increased tumor size than the wild type counterparts.

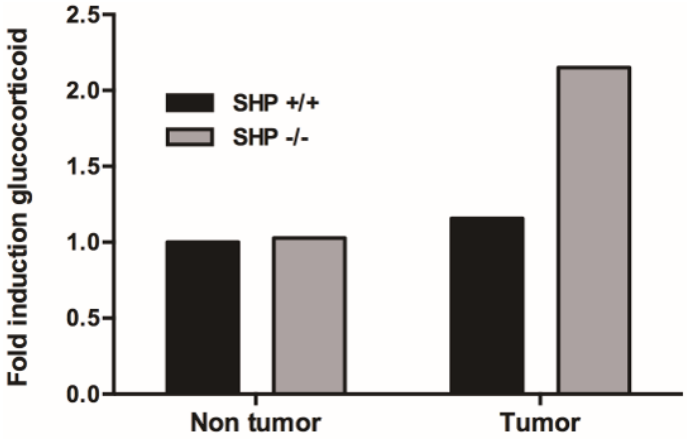

Figure 20 SHP-deficient mice tumors produce more immunoregulatory glucocorticoids
Colon tumors and adjacent non tumor tissue from SHP +/+ and SHP -/- mice at day 64 following AOM/DSS treatment (n=2 per group) were *ex vivo* cultured for 6 h in the presence or absence of metyrapone. Corticosterone in the cell-free supernatant was measured by RIA. Results are expressed as fold induction of GC from SHP +/+ non tumor tissue.

4.7 LRH-1 gene expression is reduced in tumors that express elevated levels of the proinflammatory cytokine TNF

TNF has been shown to be associated with colitis-induced colon carcinogenesis (Popivanova et al., 2008), moreover, it was reported to be upregulated in tumor tissues compared to adjacent normal mucosa (Schoonjans et al., 2005). Thus, next we investigated the expression of TNF in tumor tissues from SHP-/- and wild type mice. Therefore, we isolated adenoma tissue and adjacent normal mucosa from SHP-/- and wild type mice at day 64 following AOM/DSS treatment. mRNA was extracted, and the expression of TNF was analyzed. Consistent with previous reports (Schoonjans et al., 2005), we observed upregulation of TNF expression in tumors from both genotypes compared to adjacent normal mucosa (Figure 21A). Interestingly, tumors from SHP-/- exhibited significantly reduced TNF expression compared to wild type tumors (Figure 21A), suggesting less inflammation. As shown previously (Schoonjans et al., 2005), LRH-1 expression was reduced in tumors that express elevated levels of TNF (Figure 21B). Additionally, increased levels of Cyclin E1 and D1 was shown in tumors from both genotypes with a tendency to reduced expression from SHP-/- tumors suggesting less tumor development (Figure 21C and D). These findings indicate reduced inflammation and TNF expression in tumors from SHP-/- mice compared to wild type that correlated with reduced LRH-1 expression.

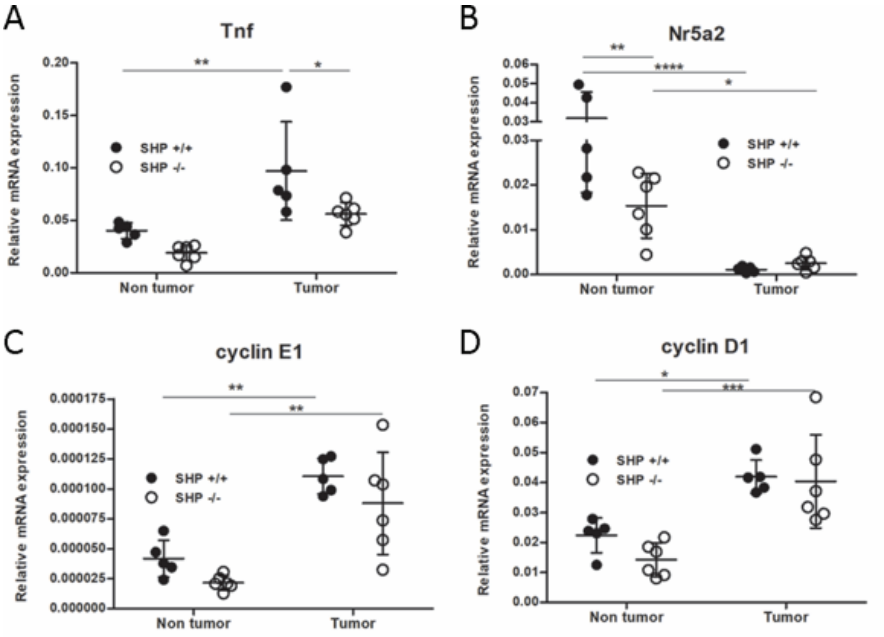

Figure 21 The proinflammatory cytokine TNF decreases LRH-1 expression in AOM/DSS-induced tumors
Colitis-associated cancer was induced in 7-11 weeks SHP +/+ and SHP -/- mice by i.p. injection of 12 µg/g AOM, followed by three cycles of 2.2% DSS for 5 days in the drinking water which was interrupted by 16 days of normal drinking water. Gene expression of **(A)** TNF, **(B)** LRH-1, **(C)** Cyclin E1 and **(D)** Cyclin D1 from colon tumors and adjacent non tumor tissue from SHP +/+ and SHP -/- mice at day 64 following AOM/DSS treatment. Data was measured by quantitative PCR and normalized to the level of β-actin mRNA. n =5-6 per group. Data are mean ± SD. Statistical analyses were performed using Two-way ANOVA followed by Tukey's multiple comparison test with p values: * <0.05, ** <0.01, *** <0.001, **** <0.0001.

4.8 Conditional deletion of Cyp11b1 in the intestinal mucosa sensitizes mice to colitis-associated tumor initiation

Our previous results clearly indicate a critical role of LRH-1-induced GCs in the initiation and progression of inflammation-driven colorectal cancer. However, besides LRH-1 role in the regulation of GC synthesis (Mueller et al., 2006), it also regulate epithelial proliferation (Botrugno et al., 2004). Therefore, in order to investigate the direct role of local GC synthesis in colorectal tumor initiation and progression, we utilized a mouse model with a conditional deletion of the enzyme that catalyzes the last step in GC synthesis, that is the conversion of 11- deoxycorticosterone to corticosterone in mice (Miller, 2008) ,Cyp11b1, in the intestinal epithelial cells ($Cyp11b1^{IEC\,KO}$), while mice with a floxed Cyp11b1 gene ($Cyp11b1^{fl/fl}$) were used as controls. Consequently, $Cyp11b1^{fl/fl}$ and $Cyp11b1^{IEC\,KO}$ mice were treated with AOM/DSS and colons were collected for analysis at different time points, namely days 28, 35 and 56, as previously described.

As a first step, we tested the initiation phase of carcinogenesis. Figure 22 showed that, Cyp11b1$^{IEC\ KO}$ mice suffered from more severe colitis and subsequent tumor development at days 28 and 35 compared to Cyp11b1$^{fl/fl}$ control mice, as evidenced by increased shortening of colons (Figure22B and E) and paralleled by increased weight loss (Figure 22G) and tumor numbers (Figure 22C and F) in Cyp11b1$^{IEC\ KO}$ compared to control mice. This observation suggested the Cyp11b1$^{IEC\ KO}$ mice were more susceptible to intestinal inflammation due to reduced colitis-induced GC production. In order to test this, colons were collected from mice at the peak of inflammation, day 28 following AOM/DSS. Third of the colons were *ex vivo* cultured for 16 h, as described previously (Cima et al., 2004). In line with the deletion of Cyp11b1 in the intestinal mucosa, Cyp11b1$^{IEC\ KO}$ mice mucosa exhibited less GC production in response to inflammation (Figure 20H).

Histopathological analysis of the Swiss-rolled H&E stained sections revealed severe inflammatory response in Cyp11b1$^{IEC\ KO}$ mice characterized by destructed mucosa infiltrated with massive numbers of immune cells and the presence of frequent crypt abscess, low-grade adenoma and mucosal hyperplasia (Figure 22I, right panels). Instead, Cyp11b1$^{fl/fl}$ mice exhibited moderate inflammation, that was shown by dysplastic epithelium, ACF with few low-grade adenomas and destructed mucosa infiltrated by immune cells (Figure 22I, left panels).

Collectively, our data provide the first evidence for the role of local GC synthesis in the initiation of inflammation-driven colon cancer, since the deletion of Cyp11b1 sensitized mice to intestinal inflammation and subsequent tumorigenesis.

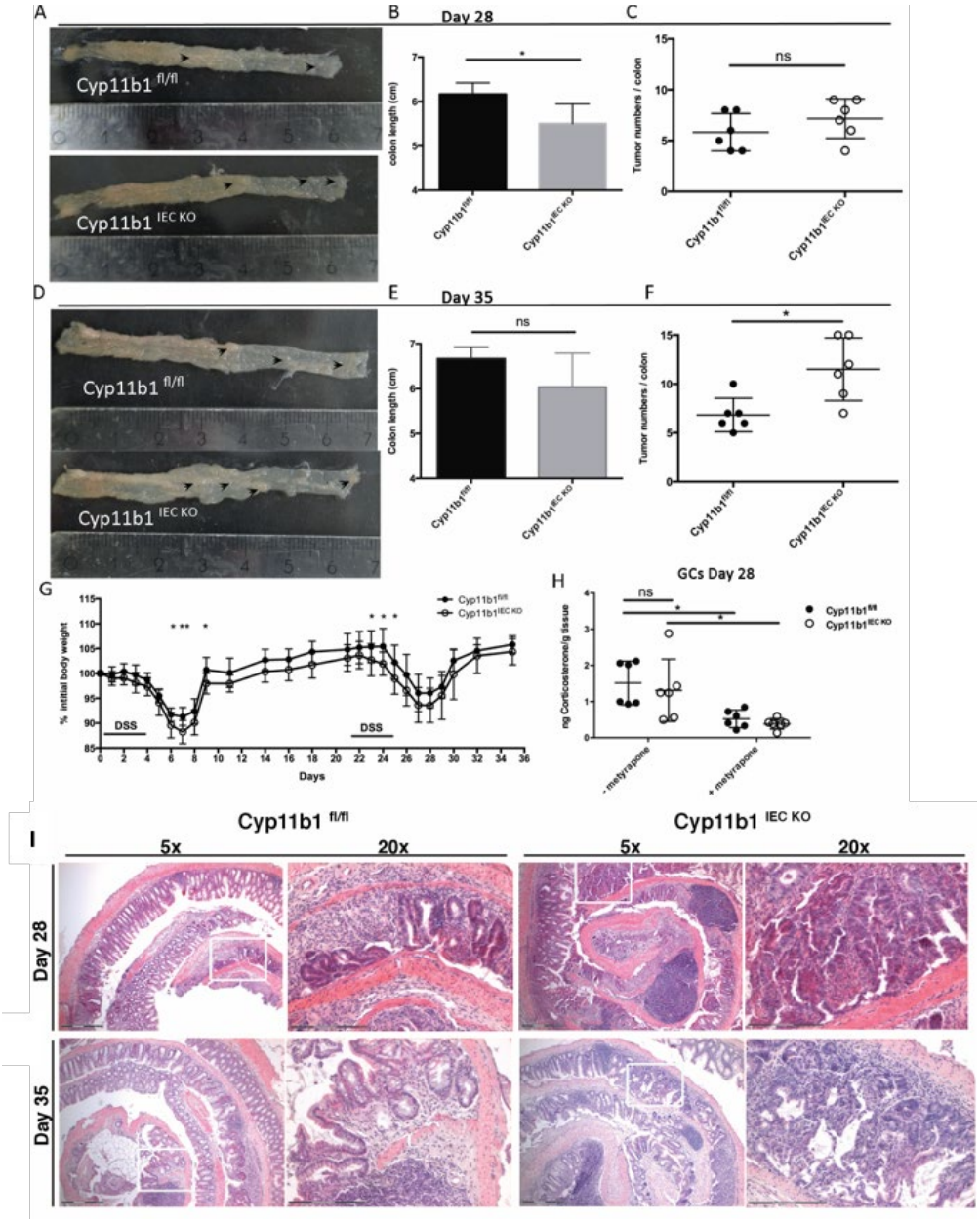

Figure 22 Deletion of Cyp11b1 in the intestinal mucosa sensitizes mice to colitis-associated colorectal cancer development

Colitis-associated cancer was induced in 7-11 weeks Cyp11b1$^{fl/fl}$ and Cyp11b1$^{IEC\ KO}$ mice by i.p. injection of 12 µg/g AOM, followed by two cycles of 2.2% DSS for 5 days in the drinking water which was interrupted by 16 days of normal drinking water, mice were analysed at days 28 and 35. **(A)** Representative macroscopic pictures of colonic tumor development (arrows) of AOM/DSS treated mice at day 28. **(B)** Colon length and **(C)** Total tumor numbers at day 28. **(D)** Representative macroscopic pictures of colonic tumor development (arrows) of AOM/DSS treated mice at day 35. **(E)** Colon length and **(F)** Total tumor numbers at day 35. **(G)** Percent body weight change normalized to initial body weight at day 0 of AOM/DSS treatment, representative result from 3 independent experiments. **(H)** Colons from mice treated with AOM/DSS at day 28 were cultured *ex vivo* for 16 h in the presence or absence of metyrapone. Corticosterone in the cell-free supernatant was measured by RIA. **(I)** Representative H&E stained Swiss-rolled colon sections from AOM/DSS-treated mice at days 28 and 35**.** Scale bars: overview 300 µm, inlay 150 µm. n= 6 mice per group. Data are mean ± SD. Statistical analyses were performed using unpaired student's t-test with p value: * <0.05, ** <0.01. ns = not significant.

4.9 Cyp11b1 intestine-specific mice develop reduced tumor burden following inflammation-driven colon carcinogenesis

In a next step, we sought to investigate the role of local GC in tumor progression in Cyp11b1$^{IEC\ KO}$ tumors hypothesizing that in the absence of Cyp11b1, tumors will have more difficulties to grow since they lack GC production and associated immune suppression. Thus, we analyzed tumor development at a later time point of AOM/DSS exposure (day 56). Supporting previous results, we monitored an increased susceptibility of Cyp11b1$^{IEC\ KO}$ mice for DSS-induced colitis in the first 2 cycles of DSS compared to their control counterparts (Cyp11b1$^{fl/fl}$), this was shown by increased weight loss in Cyp11b1$^{IEC\ KO}$. On the contrary, Cyp11b1$^{IEC\ KO}$ mice exhibited a decreased weight loss at the third DSS cycle suggesting less disease susceptibility and associated tumor burden (Figure 23A). Indeed, we observed reduced tumor development in Cyp11b1$^{IEC\ KO}$ mice at day 56 following AOM/DSS (Figure 23B), as shown by significant reduction in tumor number and tumor volume (Figure 23C and E) compared to Cyp11b1$^{fl/fl}$ mice. However, no differences in colon length were detectable (Figure 23D).

Histopathological analysis of Swiss-rolled colon sections from AOM/DSS-treated mice at day 56 revealed that CYP11b1$^{fl/fl}$ mice displayed severe tissue pathology characterized by massive formation of high-grade adenoma in addition to mucosal hyperplasia and increased immune cell infiltration into the mucosal layers (Figure 23F, left panel). Instead, Cyp11b1$^{IEC\ KO}$ mice showed moderate intestinal pathology as shown by frequent ACF, mucosal hyperplasia while less high-grade adenomas and the presence of few normal crypt structures and increased immune cell infiltration into the mucosal layers (Figure 23F, right panel). In line with the increased tumor burden, Cyp11b1$^{fl/fl}$ mice exhibited increased Ki-67-positive cells in the adenoma tissue indicating increased proliferation compared to Cyp11b1$^{IEC\ KO}$ mice (Figure 23G). Interestingly, although Cyp11b1$^{IEC\ KO}$ mice developed less tumors, these tumors were infiltrated with increased numbers of CD3-positive T cells (Figure 23H) probably due to the lack of GC-induced T cell apoptosis in these mice.

Taken all together, our findings provide the first evidence for the role of local GC synthesis in the progression of colitis-associated carcinogenesis, as seen by decreased tumor burden in mice with a conditional deletion of Cyp11b1 enzyme in the intestinal epithelium.

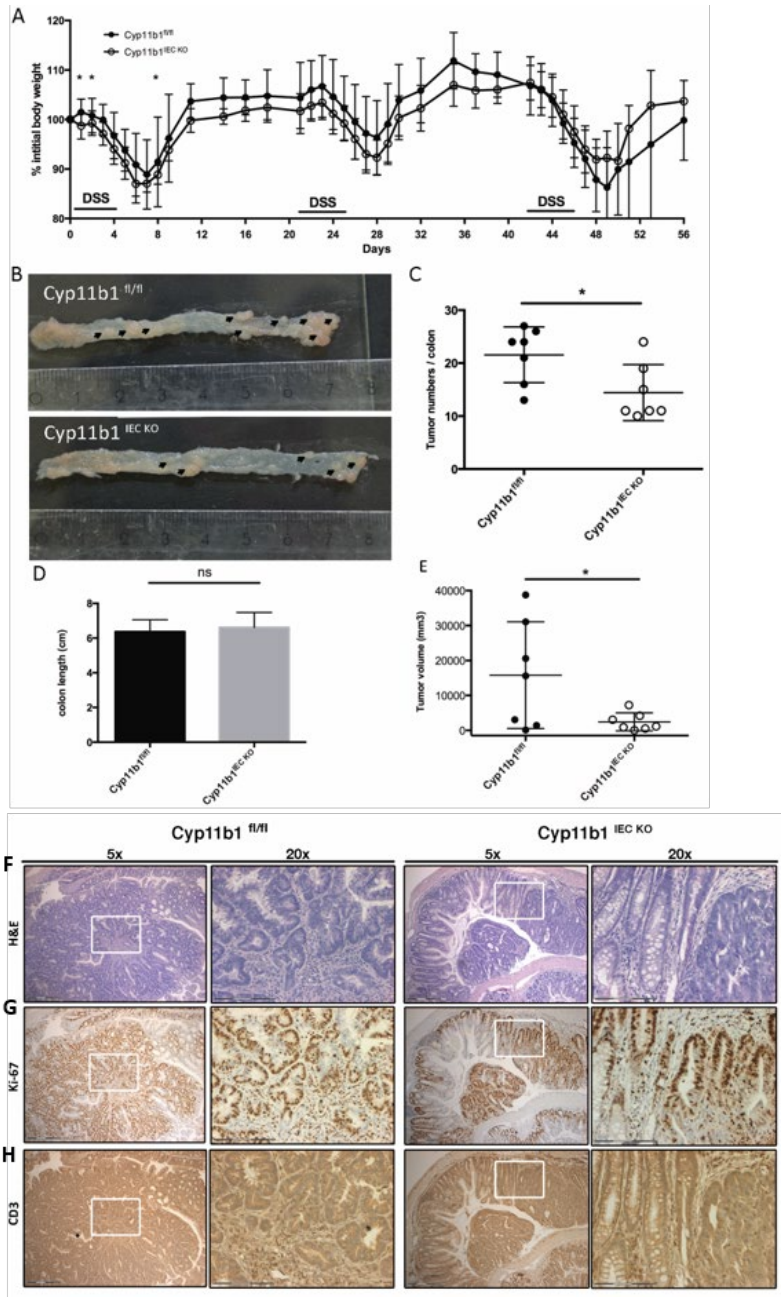

Figure 23 Cyp11b1 intestine-specific knockout mice suffer from reduced tumor burden at later time points of inflammation-driven colon carcinogenesis

Colitis-associated cancer was induced in 7-11 weeks Cyp11b1$^{fl/fl}$ and Cyp11b1$^{IEC\ KO}$ mice by i.p. injection of 12 µg/g AOM, followed by three cycles of 2.2% DSS for 5 days in the drinking water which was interrupted by 16 days of normal drinking water, mice were analysed at day 56. **(A)** Percent body weight change normalized to initial body weight at day 0 of AOM/DSS treatment, representative result from 3 independent experiments. **(B)** Representative macroscopic pictures of colonic tumor development (arrows) of AOM/DSS treated mice at day 56. **(C)** Total tumor numbers, **(D)** Colon length and **(E)** Tumor volume of AOM/DSS treated mice at day 56. **(F)** H&E and IHC from Swiss-rolled colon sections stained for **(G)** Ki-67 and **(H)** CD3 from AOM/DSS treated mice at day 56**.** Representative results are shown. Scale bars: overview 300 µm, inlay 150 µm. n= 7 mice per group. Data are mean ± SD. Statistical analyses were performed using unpaired student's t-test with p value: * <0.05. ns = not significant.

4.10 Colorectal tumor organoids as a model to study tumor progression phase and tumor-derived GC as a potential immune escape mechanism

After confirming the role of LRH-1 and LRH-1-mediated GC synthesis in the development of inflammation-driven colorectal cancer, we next wanted to study the ability of these tumors to proliferate in a non-inflamed environment. And to investigate the role of tumor-derived GC synthesis as a potential immune escape mechanism. Therefore, in order to dissect the proliferation phase from the inflammation phase we isolated tumors from SHP-/-, LRH-1$^{IEC\ KO}$, Cyp11b1$^{IEC\ KO}$ mice and their respective counterparts and *ex vivo* cultured these tumors to grow tumor organoids as described previously (Xue and Shah, 2013). Briefly, tumors were isolated at day 56 following AOM/DSS treatment, digested into single cells and *ex vivo* cultured to grow organoids, tumor organoids were then injected subcutaneously (s.c.) into the flanks of immunocompetent mice where knockout tumor organoids were injected in the right flank while the wild type tumor organoids were injected in the left flank of the same mouse to control for interindividual variability, consequently the tumor growth was monitored over time (Figure 24A). Unlike organoids from normal epithelium that retain the hallmarks and cellular composition of the *in vivo* epithelium (Sato et al., 2009), tumor organoids started to grow *in vitro* already day 2 after culture and grow substantially by day 6 in an undifferentiated organoids forming a balloon-like structures with the accumulation of apoptotic cells in the lumen (Figure 24B).

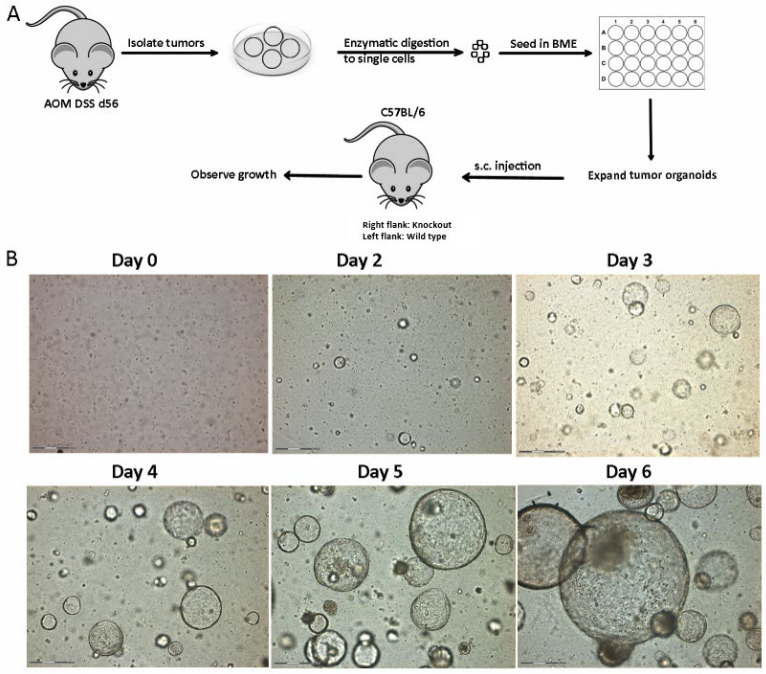

Figure 24 *Ex vivo* culture of colorectal tumor organoids
(A) Scheme of colorectal tumor organoid culture. Colitis-associated cancer was induced in 7-11 weeks old mice by i.p. injection of 12 µg/g AOM, followed by three cycles of 2.2% DSS for 5 days in the drinking water which was interrupted by 16 days of normal drinking water. Tumors were isolated from mice at day 56 following AOM/DSS treatment, underwent enzymatic digestion to single cells, then seeded in BME to grow organoids. Following growth and expansion, organoids were injected into flanks of wild type mice and the tumor growth was observed. **(B)** Representative pictures of *ex vivo* cultures of colorectal tumor organoids from wild type colorectal tumors growing *in vitro*.

As a first step, we injected tumor organoids from SHP-/- and wild type tumors in the right and left flank, respectively, of the same mouse to avoid interindividual variability. Hypothesizing that SHP-/- tumor organoids will have a growth preference over wild type tumor organoids due to increased LRH-1-mediated proliferation and GC immune suppression. As expected, following s.c. injection, tumor organoids from SHP-/- grew exponentially, indicating a higher resistance to the host immune system-mediated growth suppression. Whereas tumor organoids from wild type were not able to grow (Figure 25A-E). SHP-/- tumor organoids exhibited significant higher tumor growth rate compared to wild type as evidenced by a significant increase in tumor volume over time (Figure 25A) and significant increase in tumor weight at day 24 following s.c. injection (Figure 25E). Histological analysis of H&E stained sections from s.c. tumor organoids at day 24 following injection, revealed a remarkable growth of s.c. injected SHP-/- tumor organoids characterized by moderately differentiated phenotype that contains cellular composition, such as goblet cells in marked contrast to the tumor organoid *in vitro* phenotype (Figure 25F, right panel). This was paralleled by massive inflammatory cell infiltration surrounding the tumor organoids (Figure 25F, right panel) with more frequent eosinophils (data not shown) indicating an ongoing allergic reaction. Moreover, apoptotic cells shedding into the lumen was also observed in the s.c. injected organoids from both lines (Figure 25F, blue arrows). In contrast, few growing tumor organoids from wild type were detected that retained the same differentiated phenotype described for SHP-/- s.c. tumor organoids and the same inflammatory response (Figure 25F, left panel).
Interestingly, we could show some areas in section from both genotypes that appeared to be eliminated organoid (Figure 25F, black arrows) indicating an ongoing anti-tumor immune response that limited the growth of those organoids.

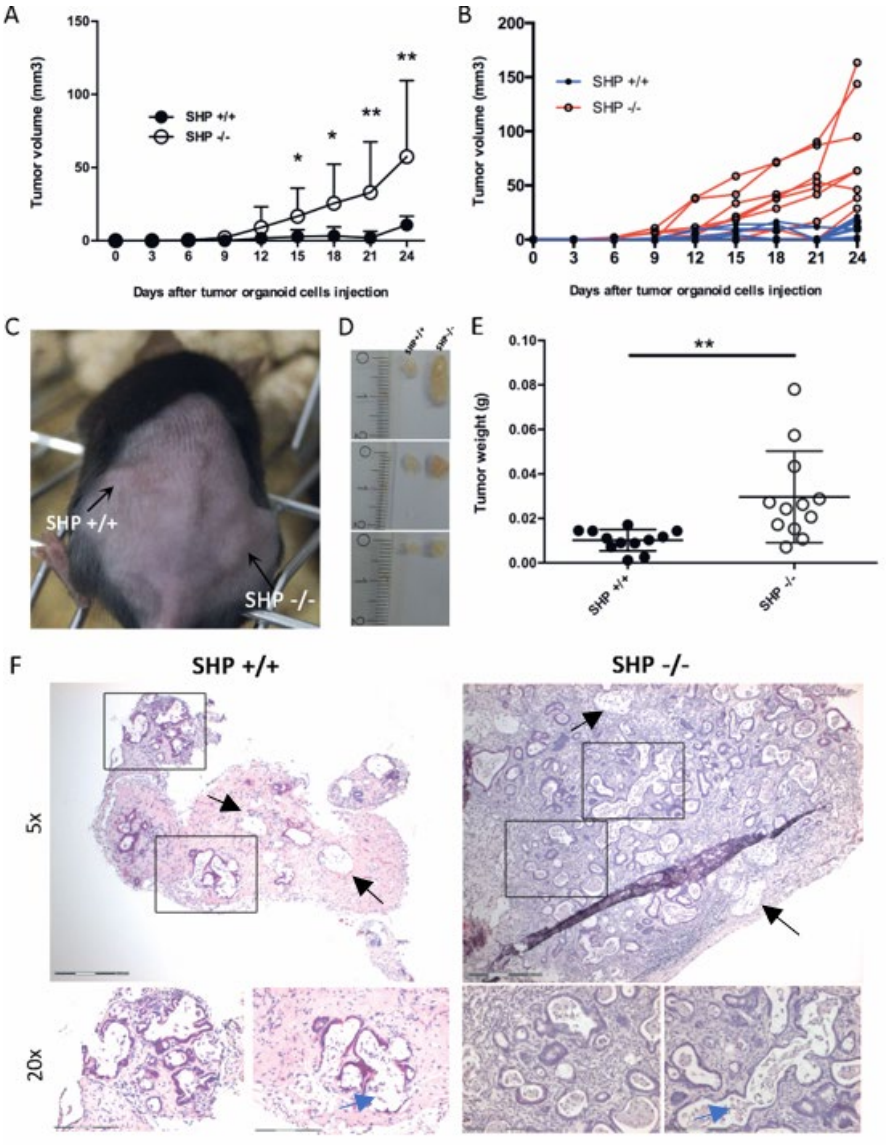

Figure 25 Increased growth rate of tumor organoids from SHP-deficient mice
Tumor organoid cells ($2*10^5$) from SHP+/+ and SHP-/- were injected subcutaneously (s.c.) into the flanks of wild type mice (n=12 mice). **(A)** Growth rate of s.c. injected tumor organoids. Mean tumor volumes ± SD (n=12 mice). **(B)** Individual growth rate (tumor volume) of s.c. injected tumor organoids. SHP+/+ (blue circles) and SHP-/- (red circles). **(C)** Representative picture of s.c. injected tumor organoids from SHP-/- (right flank) and SHP+/+ (left flank), growing in wild type mouse at day 24 following injection. **(D)** Representative pictures of s.c. tumor organoids excised at day 24 following injection. **(E)** Tumor weight at day 24 following s.c. injection. **(F)** Representative H&E stained sections of s.c. tumor organoids at day 24 following injection. Arrows indicate eliminated organoids (Black) and apoptotic cells in the lumen (Blue). Scale bars: overview 300 µm, inlay 150 µm. **(A** and **E)** Data are mean ± SD. Statistical analyses were performed using unpaired student's t-test with p value: * <0.05, ** <0.01.

Following, we aimed at investigating the growth rate of tumor organoids from LRH-1$^{IEC\ KO}$ tumors. Therefore, we injected tumor organoids from LRH-1$^{IEC\ KO}$ and LRH-1$^{fl/fl}$ tumors as before and we expected to see reduced growth rate of LRH-1$^{IEC\ KO}$ tumor organoids compared to LRH-1$^{fl/fl}$ due to the loss of LRH-1-induced proliferation and GC-synthesis. Indeed, following s.c. injection, tumor organoids from LRH-1$^{IEC\ KO}$ were not able to grow and the growth rate, as measured by tumor volume over time, started to decline already at day 12 following s.c injection, possibly due to an ongoing anti-tumor immune response that prevent the growth of these tumors. On the other hand, tumor organoids from LRH-1$^{fl/fl}$ started to grow at day 6 but the growth rate remained stable that might be due to a growth limitation by anti-tumor immune responses (Figure 26A-E). LRH-1$^{IEC\ KO}$ tumor organoids exhibited significantly reduced tumor volume (Figure 26A), in addition to significant decrease in tumor weight at day 24 following s.c. injection (Figure 26E). Histological analysis of H&E stained sections from s.c. tumor organoids at day 24 following injection revealed the detection of few growing tumor organoids from LRH-1$^{fl/fl}$ that retained the same differentiated phenotype described before for wild type s.c. tumor organoids and the same inflammatory response, the black arrows indicate eliminated organoids (Figure 26F, left panel). Instead, tumor organoids from LRH-1$^{IEC\ KO}$ were not detected in the stained sections, while immune infiltration was monitored in the stromal tissue, that could be due to increased anti-tumor immune response that prevented the growth of these tumor organoids (Figure 26F, right panel).

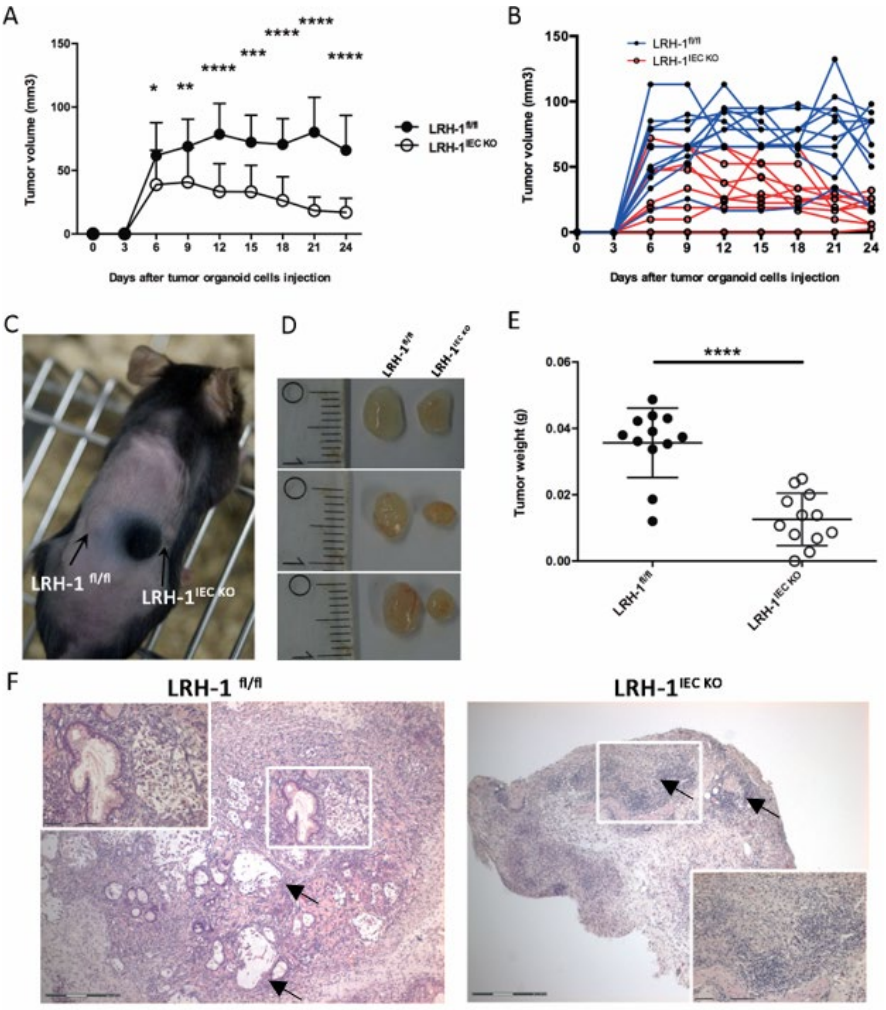

Figure 26 Reduced growth rate of tumor organoids from LRH-1 intestine-deficient mice
Tumor organoid cells ($2*10^5$) from LRH-$1^{fl/fl}$ and LRH-$1^{IEC\ KO}$ were injected subcutaneously (s.c.) into the flanks of wild type mice (n=12 mice). **(A)** Growth rate of s.c. injected tumor organoids. Mean tumor volumes ± SD (n=12 mice). **(B)** Individual growth rate (tumor volume) of s.c. injected tumor organoids. LRH-$1^{fl/fl}$ (blue circles) and LRH-$1^{IEC\ KO}$ (red circles). **(C)** Representative picture of s.c. injected tumor organoids from LRH-$1^{IEC\ KO}$ (right flank) and LRH-$1^{fl/fl}$ (left flank), growing in wild type mouse at day 24 following injection. **(D)** Representative pictures of s.c. tumor organoids excised at day 24 following injection. **(E)** Tumor weight at day 24 following s.c. injection. **(F)** Representative H&E stained sections of s.c. tumor organoids at day 24 following injection. Black arrows indicate eliminated organoids. Scale bars: overview 300 µm, inlay 150 µm. **(A** and **E)** Data are mean ± SD. Statistical analyses were performed using unpaired student's t-test with p value: * <0.05, ** <0.01, *** <0.001, **** <0.0001.

In a next experiment, in order to confirm that the observed effect is due to the direct effect of tumor-derived GC, we injected tumor organoids from Cyp11b1$^{IEC\ KO}$ and Cyp11b1$^{fl/fl}$ as we have seen previously reduced GC production upon inflammation in Cyp11b1$^{IEC\ KO}$ mice compared to Cyp11b1$^{fl/fl}$ counterparts (Figure 22H). Our hypothesis was that Cyp11b1$^{IEC\ KO}$ tumor organoids will exhibit less tumor growth compared to Cyp11b1$^{fl/fl}$ controls because they lack GC-induced immune suppression. Since we have seen a reduced tumor growth rate of LRH-1 tumor experiment starting at day 12 (Figure 26A), we sought to investigate 2 different time points namely day 12 and 24 that represent the onset and the peak of anti-tumor immune responses, respectively. Figure 27 shows reduced growth rate of tumors from Cyp11b1$^{IEC\ KO}$ compared to Cyp11b1$^{fl/fl}$ controls following s.c. injection as Evidenced by reduced tumor volume (Figure 27A) and tumor weight at days 12 (Figure 27D) and 24 (Figure 27F) following s.c. injection.

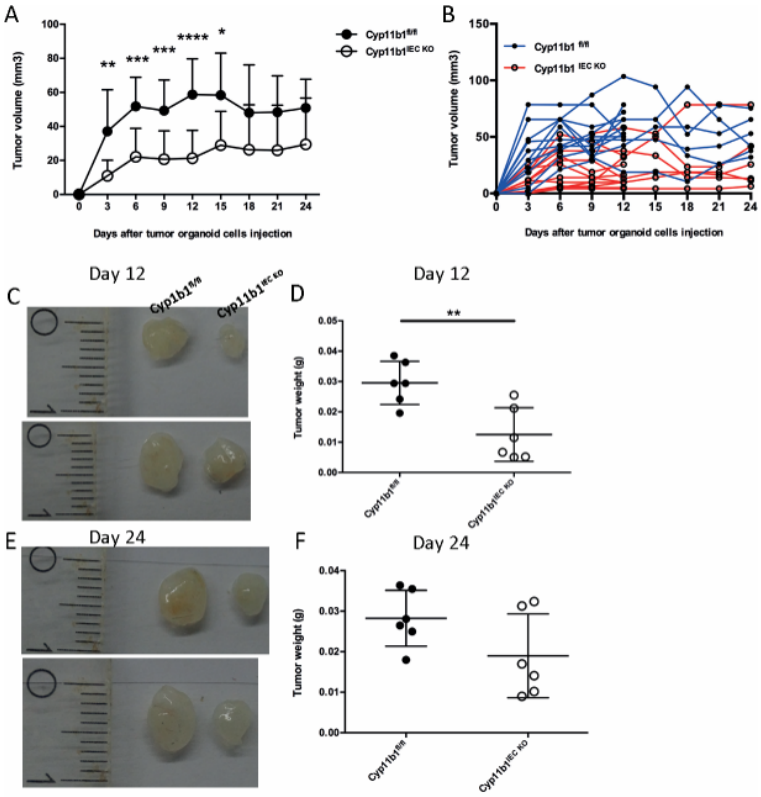

Figure 27 Reduced growth rate of tumor organoids from Cyp11b1 intestine-deficient mice
Tumor organoid cells (2*10^5) from Cyp11b1$^{fl/fl}$ and Cyp11b1$^{IEC\ KO}$ were injected subcutaneously (s.c.) into the flanks of wild type mice (n=12 mice). **(A)** Growth rate of s.c. injected tumor organoids. Mean tumor volumes ± SD (n=6-12 mice). **(B)** Individual growth rate (tumor volume) of s.c. injected tumor organoids. Cyp11b1$^{fl/fl}$ (blue circles) and Cyp11b1$^{IEC\ KO}$ (red circles). **(C)** Representative pictures of s.c. tumor organoids excised at day 12 following injection. **(D)** Tumor weight at day 12 following s.c. injection (n=6). **(E)** Representative pictures of s.c. tumor organoids excised at day 24 following injection. **(F)** Tumor weight at day 24 following s.c. injection (n=6). **(A, D** and **F)** Data are mean ± SD. Statistical analyses were performed using unpaired student's t-test with p value: * <0.05, ** <0.01, *** <0.001, **** <0.0001.

Collectively, our finding speaks for an unrecognized and important role of tumor-LRH-1-mediated proliferation and GC synthesis in counteracting anti-tumor immune responses that limit tumor growth, thus suggesting a possible role of tumor-derived GCs as tumor immune escape mechanism.

5 Discussion

GCs are steroid hormones synthesized in response to stress in order to mediate a wide range of activities, primarily anti-inflammatory and immunosuppressive. Therefore, synthetic GCs are frequently used in the treatment of wide range of inflammatory diseases (Rhen and Cidlowski, 2005) including IBD (De Iudicibus et al., 2011). GCs are predominantly produced by the adrenal glands, however increasing line of evidence has shown that various other organs are capable of not only *de novo* synthesis of bioactive GCs, but also of reactivating the inactive dehydrocorticosterone into the active form, corticosterone (Cima et al., 2004; Hostettler et al., 2012). These extra-adrenal GC-synthesizing tissues include the primary lymphoid organs, the skin, the brain, the vascular system as well as the intestine as discussed in this thesis (reviewed in (Taves et al., 2011)).

Intestinal mucosal epithelium functions as a barrier to maintain the balance between nutrient absorption while preventing the entry of pathogens and responding to harmful contents of the lumen, in order to maintain tissue homeostasis (Salim and Söderholm, 2011). This function is mediated by single layer of IECs, that separates from the underlying lamina propria and the rest of the body, the 10^{14} gut microbiota cells (Cario, 2008; Mukherji et al., 2013). The intestinal epithelium also hosts the largest number of immune cells in the body (Lee et al., 2008b). This direct contact of these immune cells with the microbiota requires fine-tuning in order to find the appropriate balance between protective immune responses and tolerance towards microbiota. The synthesis of immunoregulatory GCs has been reported to play an effective and novel role in regulating intestinal immune homeostasis under physiological as well as pathological conditions (Ballegeer et al., 2018; Cima et al., 2004; Huang et al., 2018; Noti et al., 2009). Supporting this notion, several lines of evidence indicate that local GC synthesis or metabolism in the intestinal epithelium is involved in the pathogenesis of intestinal inflammation (De Iudicibus et al., 2011; Hussey et al., 2017; Noti et al., 2010a).

The NR LRH-1 regulates intestinal homeostasis by the regulation of epithelial barrier regeneration and inducing the expression of steroidogenic enzymes and local GC synthesis (Botrugno et al., 2004; Mueller et al., 2006). Consequently, the deletion of LRH-1 renders mice more susceptible to experimental colitis induction (Coste et al., 2007). Furthermore, LRH-1 is also associated with CRC development via controlling tumor cell proliferation in synergy with the β-catenin/TCF4 signaling pathway (Botrugno et al., 2004; Schoonjans et al., 2005). Recently it has been shown that tumor-derived GCs suppress the activation of T cells,

and thus could contribute to suppression of immune surveillance, resulting in tumor immune escape (Sidler et al., 2011).

Although GC synthesis is demonstrated in the intestinal mucosa and colorectal tumors, it remains unknown whether local GCs play a role in the tumor onset. Moreover, the functional relevance of tumor-derived GC is hardly investigated. Therefore, the main goal of this study was to provide the first functional *in vivo* study for investigating the role of GC in the initiation and progression of CRC.

5.1 The role of LRH-1 in intestinal epithelium homeostasis and carcinogenesis

Confirming previous findings (Coste et al., 2007), we could show that deletion of LRH-1 in the intestinal mucosa exacerbated intestinal inflammation after colitis induction. Furthermore, in line with previous reports (Atanasov et al., 2008; Cima et al., 2004; Coste et al., 2007; Mueller et al., 2006; Noti et al., 2010a), we observed that LRH-1 and steroidogenic enzymes are detectable in colon tissue of mice, and that colitis induces the expression of the enzymes required for *de novo* GC synthesis, Cyp11a1, Cyp11b1 and Cyp21. Additionally, we could confirm that LRH-1 is a critical regulator of the mentioned enzymes since the deletion of LRH-1 significantly inhibited the induction of these enzymes. In line with previous findings (Coste et al., 2007), we have shown that LRH-1 expression was not changed upon colitis induction in both mice lines, however LRH-1 activation and function was induced as shown by the increased target genes expression.

Interestingly, LRH-1 expression was not completely absent from the colons of intestinal epithelium-specific knockout mice, suggesting another source for the expression, for example it has been shown that LRH-1 is expressed in T cells (Schwaderer et al., 2017) as well as macrophages (Lefèvre et al., 2015).

Interestingly, defective GC metabolism by HSD11B enzymes was reported in IBD patients (Hussey et al., 2017). However, whereas CYP11A1 and CYP11B1 were identified as direct transcriptional targets of LRH-1 (Sirianni et al., 2002), little is known about the role of LRH-1 in the regulation of HSD11B enzymes. Here we could show that, while the expression of Hsd11b1 was upregulated upon colitis induction, Hsd11b2 was downregulated. However, both enzymes were not affected by the deletion of LRH-1 suggesting another mechanism of regulation, possibly by inflammatory mediators such as TNF (Noti et al., 2010a).

Moreover, it is interesting to note that the intestinal mucosa aims to maintain high levels of local GC by increasing the Hsd11b1-mediated reactivation, while limiting the Hsd11b2-mediated inactivation of GC as we have seen in this study. Therefore, our findings suggest an important underlying mechanism of defective GC reactivation, as well as LRH-1-regulated GC production in the development of intestinal inflammation.

Besides regulation of GC synthesis, LRH-1 also contributes to intestinal homeostasis by regulating epithelial regeneration (Botrugno et al., 2004). Further supporting the role of LRH-1-mediated proliferation and GC synthesis in immune homeostasis (Noti et al., 2010a), Bayrer et al. recently showed that intestinal organoids lacking LRH-1 exhibit reduced expression of the LRH-1 target genes including Shp, Cyp11a1 and Cyp11b1, as well as increased crypt cell death and epithelial permeability (Bayrer et al., 2018). They also showed that overexpression of LRH-1 mitigates inflammatory damage in murine and human intestinal organoids, including those from IBD patients and decreases the disease severity in a T cell transfer model of colitis (Bayrer et al., 2018).

This study clearly underlines the druggability of LRH-1 in the treatment of intestinal inflammation. Although LRH-1 is considered an orphan NR, structural-based studies identified DLPC as a potential ligand that has been Shown to enhance LRH-1 transcriptional activity (Krylova et al., 2005). Interestingly, DLPC has been shown to exert antidiabetic effects by activating LRH-1 when used in a therapeutic setting (Lee et al., 2011; Musille et al., 2012). Similarly, LRH-1 ligands could be used in IBD models in order to activate endogenous LRH-1.

CRC is one of the most reported cancers linked to chronic inflammation. Interestingly, anti-inflammatory drugs can prevent the onset of hereditary cases that are not often preceded by inflammation (Burn et al., 2011), indicating an important role of inflammation in CRC development. Inflammation leads to DNA damage and genomic mutations that represent the first step in the adenoma formation (Hoesel and Schmid, 2013). Chronic inflammation also promotes CRC development (Lasry et al., 2016; Schwitalla et al., 2013).

Solid tumors including colon tumors are typically infiltrated with lymphocytes and macrophages, which account for up to 50% of the tumor mass (Sica et al., 2008a). Indeed, in this study we observed massive inflammation accompanied by infiltration of immune cells, these were mostly macrophages and T cells in adenomas from wild type mice treated with the AOM/DSS inflammation-driven colon carcinogenesis model.

Furthermore, we could also show that LRH-1 deletion increased the susceptibility of mice to chronic colitis using the AOM/DSS model. Remarkably, despite the exacerbated colitis during the 3 cycles of DSS exposure, yet intestine-specific LRH-1 knockout mice developed less tumors that were significantly smaller in size than their wild type counterparts. Since LRH-1 is an important mediator of CRC cell proliferation (Kramer et al., 2016) and it has been shown that LRH-1 heterozygosity significantly reduces CRC multiplicity (Schoonjans et al., 2005), we hypothesized that a predominant role of LRH-1-mediated proliferation and subsequent tumorigenesis is responsible for this phenotype. Supporting this hypothesis, Immunohistochemical analysis revealed reduced Ki-67-positive cells in tumors from the knockout mice. In line with this, expression analysis of human CRC tumors indicate a frequent overexpression of the LRH-1 target genes and cell-cycle regulators cyclin D1 (Tetsu and McCormick, 1999), cyclin E1 (Donnellan and Chetty, 1999) and c-myc (Sikora et al., 1987). Additionally, EGFR was reported to be upregulated in 60-80% of CRC tumors and it is associated with poor prognosis (Pabla et al., 2015). Of note, EGF activates LRH-1 (Lee et al., 2006; Schoonjans et al., 2005), thus it is stimulating to speculate that EGFR upregulation could activate LRH-1 that further contributes to CRC development.

Further supporting the role of LRH-1 as a driver of CRC development, it has been shown that LRH-1 inhibits the cell cycle inhibitor p21 (Kramer et al., 2016). Moreover, silencing LRH-1 in CRC cell lines impairs proliferation (Bayrer et al., 2015). Additionally, targeting LRH-1 using microRNA *in vitro* inhibits proliferation and invasion in CRC cell lines, an effect that was reversed by restoration of LRH-1 (Qu et al., 2018).

Besides, recently in two independent CRC patients cohort, a marked upregulation of LRH-1 expression was reported in colon cancer samples compared to adjacent non-cancerous tissue from the same patients (Qu et al., 2018; Wu et al., 2018). Interestingly, increased LRH-1 expression correlated with a more advanced disease stage and a significant reduction of overall survival rate (Wu et al., 2018). Consequently, LRH-1 was proposed as a possible prognostic marker in CRC patients and a novel therapeutic target (Wu et al., 2018).

Structural-based studies identified many small molecule antagonists for LRH-1 including 3d2 (Benod et al., 2013) and SR1848 (Corzo et al., 2015). Both inhibitors inhibited LRH-1 activity *in vitro* and *in vivo* and exerted antiproliferative effects on variety of cancer cell lines (Benod et al., 2013; Corzo et al., 2015; Schwaderer et al., 2017), further indicating the therapeutic potential of LRH-1 inhibition in cancer treatment.

Taken together, it is stimulating to speculate that LRH-1 inhibitors could potentially treat CRC in LRH-1-expressing tumors by inhibiting LRH-1-induced proliferation.

5.2 SHP deficiency protects mice from colitis and associated carcinogenesis

The NR SHP is a direct target and at the same time a potent inhibitor of LRH-1 (Lee et al., 1999). Several line of evidence identified SHP as a potent tumor suppressor by inhibiting cell proliferation and tumorigenesis through suppressing the transcription of the LRH-1 target cyclin D1 (Zhang et al., 2008) and activating apoptosis (Zhang et al., 2010b). Consistent with this, SHP expression is downregulated in many cancers (He et al., 2008; Kudryavtseva et al., 2018; Prestin et al., 2016).

The repressive effect of SHP on LRH-1 has been shown in intestinal epithelial cell line (Mueller et al., 2007). Furthermore, SHP-deficient mice were reported to produce increased colonic GC upon viral infection compared to wild type controls (Huang et al., 2018) indicating an increased LRH-1 activity. Besides, unpublished data from C. Reinhold demonstrated that SHP-deficient mice have an enhanced LRH-1 activity at the intestinal epithelium, as evidenced by increased expression of the LRH-1 targets cyclin D1 and cyclin E1 (Unpublished data).

As discussed before, LRH-1-induced proliferation is important for CRC tumor progression and SHP acts as a tumor suppressor by suppressing LRH-1-induced proliferation. Hence, we asked a valid question: what will be the effect of SHP deficiency on the regulation of LRH-1 activity upon inflammation-driven colon carcinogenesis induction? And the prediction was that, we would see a more tumor burden in SHP-deficient mice compared to wild type controls.

Surprisingly, we here show that SHP-deficiency substantially abrogated inflammation-driven colon carcinogenesis. In line with increased tumor formation in wild type mice, we could show formation of high-grade adenoma that showed increased Ki-67-positive cells compared to adenomas from SHP-deficient mice. Additionally, we could also show massive inflammation and immune cell infiltration in wild type adenomas, among which we were also able to detect T cells, but due to technical problems we could not detect macrophages. We have also seen that SHP-deficient mice were protected from DSS-chronic colitis and associated carcinogenesis. That indicates an increased LRH-1-mediated suppression of inflammation.

Of note, among the few tumors that developed in the SHP-deficient mice, we observed some extremely big ones compared to tumors from wild type mice. This could be due to an increased LRH-1-induced proliferation in these tumors.

We could also show by analyzing the peak of the chronic inflammation at day 49 following AOM/DSS that, although both mice lines suffered from severe inflammation, an increased formation of high-grade adenoma in wild-type mice whereas few ACF was observed in SHP-deficient mice. Interestingly, the severe inflammation at day 49 lead to the substantial growth of tumors in wild type mice by days 56 and 64, whereas this inflammation was almost resolved in SHP-deficient mice at the same time points. This result underlines a possible increased LRH-1-induced proliferation and epithelial layer regeneration in SHP-deficient mice compared to wild type.

These results confirm that SHP-deficiency protects mice from the formation of colonic neoplasia by resisting tissue damage even after chronic colitis and thereby suppressing tumor initiation and progression.

In an attempt to elucidate the mechanism by which SHP-deficient mice resist inflammation we performed DSS acute colitis experiment hypothesizing that: Due to increased LRH-1 activity, SHP-deficient mice mucosa produces more immunoregulatory GCs that suppress the inflammation and associated tissue damage, thus leading to reduced colitis-induced tumors.

Indeed, we could show that upon colitis induction, SHP-deficient mice produced more GCs compared to wild type. Furthermore, we could also show that while wild type mice suffered from severe tissue damage with complete destruction of the mucosa in some parts of the colon, SHP-deficient mice exhibited mostly moderate inflammation at the peak of DSS-induced inflammation (day 7).

Consistent with previous findings (Cima et al., 2004; Coste et al., 2007; Noti et al., 2010a) and our own results in the previous section, we observed a colitis-induced upregulation of the steroidogenic enzymes Cyp11a1 and Cyp11b1. In line with increased GC production in SHP-deficient mice, we show that these enzymes were significantly upregulated in SHP-deficient mice compared to wild type. As shown in our previous results, LRH-1 expression was not changed upon induction of colitis.

In line with previous reports (Coste et al., 2007; Huang et al., 2014; Noti et al., 2010a), we were able to show significant upregulation of the proinflammatory cytokines Tnf and Il-6 upon colitis induction, that appeared to be attenuated in the SHP-deficient mice compared to wild type controls. Interestingly, we could also show a significant upregulation of the expression of the anti-inflammatory cytokine Il-10 in SHP-deficient mice compared to wild type mice upon colitis.

The colitis experiment clearly shows that, SHP-deficient mice produce more immunoregulatory GCs upon inflammation due to increased LRH-1 activity, and thereby suppress inflammatory immune responses and subsequent tissue damage. Furthermore, this experiment further emphasizes an important role of LRH-1-mediated GC synthesis in the regulation of intestinal immune homeostasis.

In addition, TNF and IL-6 activates the pro-survival and proliferative pathways NF-κB and STAT3, respectively. Thus these cytokines are implicated in the development and progression of CRC (Grivennikov, 2013). Activation of either NF-κB or STAT3 is demonstrated in over 50% of all cancers (Grivennikov and Karin, 2010) indicating an important role in cancer onset.
Supporting this notion, reduced NF-kB activity in myeloid cells or IECs *in vivo* alters the expression of the anti-apoptotic genes Bcl-xL and Bcl2, resulting in increased levels of apoptosis and decreased CRC tumor load (Kostic et al., 2013).

Additionally, NF-κB-induced IL-6 enhances the development of CRC *in vivo* (Becker et al., 2005). Moreover, activation of STAT3 leads to the upregulation of cyclin D1 and c-myc in addition to Bcl-xL and Bcl2 as well as bFGF and VEGF (Bollrath et al., 2009; Kostic et al., 2013; Yu et al., 2009). Furthermore, It has been shown that STAT3 IEC-specific ablation results in profound reduction of colitis-induced tumor growth and multiplicity (Grivennikov et al., 2009).

Taken together, SHP-deficient mice resist intestinal inflammation by synthesizing increased levels of LRH-1-mediated GCs compared to wild type mice. Consequently, GCs suppress the proinflammatory cytokines TNF and IL-6 that are essential for the initial neoplastic transformation. Moreover, GCs also protects the SHP-deficient mice from chronic inflammation and thereby prevent inflammation-driven tumor progression.

Considering the fact that SHP acts as a potent tumor suppressor in many tumors (Zhang et al., 2008), modulation of SHP activity could represent a promising therapeutic approach for CRC treatment.

CRC are often immunogenic and therefore successful anti-tumor immune responses could limit tumor growth. However, immune escape mechanisms can significantly limit the efficacy of anti-tumor immune responses and favor tumor growth (Finn, 2008; Hanahan and Weinberg, 2011). Of note, in CRC a strong correlation between anti-tumor immune responses and patient survival has been demonstrated (Camus et al., 2009; Pagès et al., 2005).

Furthermore, as discussed previously, the type of immune responses at the TME represents a major determinant of CRC outcome.

Recently Sidler et al. described a previously unrecognized LRH-1-dependent *de novo* GC synthesis by CRC tumors. Moreover, they could show that the tumor-derived GCs exerted immunoregulatory function by suppressing T cell activation and inducing T cell apoptosis (Sidler et al., 2011). Considering the observation we made about the increased tumor size of some of the SHP-deficient tumors, and taking into account the increased GC synthesis by SHP-deficient mice compared to wild type upon inflammation, we hypothesized that: The SHP-deficient tumors produce more immunosuppressive GCs and thereby escape the anti-tumor immune responses. Indeed, we could show that *ex vivo* cultured SHP-deficient tumors exhibited 2-fold higher GC production compared to wild type tumors indicating a potential role of tumor-derived GCs in the tumor progression.

Further supporting a role of anti-tumor immune responses as an important predictor of tumor outcome, pages et al. observed a strong correlation between high expression of effector memory T cells and the survival of CRC patients (Pagès et al., 2005). Moreover, in another study increased densities of CTLs and effector memory T cells within the primary tumor of CRC patients were associated with a significant protection against tumor recurrence (Camus et al., 2009). Furthermore, patients with high expression of Th17 responses showed poor survival. This clearly indicate a critical role of the inflammatory responses at the TME in CRC development.

In line with an inflammatory response in the TME and the reported role of TNF as a tumor promoter (Grivennikov and Karin, 2010), AOM/DSS induced tumors from both SHP-deficient and wild type mice showed upregulation of TNF expression compared to adjacent non-tumor tissue. We could show that TNF expression was significantly lower in SHP-deficient tumors compared to wild type tumors confirming the reduced inflammation in SHP-deficient mice reported before. Contrary to our expectations and the role of LRH-1 in tumor development, we observed significant downregulation of LRH-1 expression compared to non-tumor tissue in both mice lines. As reported before (Schoonjans et al., 2005), we could also show an inverse correlation between LRH-1 and TNF in tumors from both lines.

Interestingly, in the intestinal mucosa TNF demonstrate a very complex functions in physiologic and pathologic conditions (Leppkes et al., 2014). While it drastically promotes epithelial cell death (Grabinger et al., 2017) and promotes CRC after sustained chronic colitis

(Popivanova et al., 2008). TNF also regulates intestinal GC synthesis (Noti et al., 2010a), which represents an important mechanism for intestinal immune homeostasis as discussed previously. In this regard, TNF plays an anti-inflammatory role. Moreover, TNF was also reported to suppress LRH-1 to sustain chronic colitis (Huang et al., 2014). Therefore, due to the complex interactions between LRH-1 and TNF, this inverse correlation remains to be further investigated.

Additionally, we could show a significant upregulation of cyclin E1 and cyclin D1 in tumors from both lines, with a reduced expression in tumors from SHP-deficient mice in line with the reported reduced tumors in these mice.

5.3 Cyp11b1 intestine-specific knockout mice exhibit biphasic tumor development following inflammation-driven colorectal carcinogenesis

We have clearly seen an important role of LRH-1 in the initiation and progression of CRC. Nevertheless, LRH-1 also regulates proliferation besides GC synthesis. The investigation of a direct role of GC synthesis in intestinal homeostasis was hampered by the availability of the proper genetically modified mouse model, hence we generated a knockout mouse with a conditional deletion of the rate limiting enzyme required for the synthesis of bioactive GCs, Cyp11b1. Therefore, in order to answer the question: Whether the observed effects described before on the tumor development are GC-mediated? we investigated CRC development in the cyp11b1 intestine-specific knockout mouse.

In line with the critical role of GCs in intestinal immune homeostasis (Cima et al., 2004; Huang et al., 2018; Noti et al., 2010a) that was also shown by us in this study, we could show that Cyp11b1 knockout mice were more susceptible to inflammation and subsequent tumor formation compared to wild type mice at days 28 and 35 of AOM/DSS treatment. We could also show that during the 2 cycles of DSS treatment, Cyp11b1 knockout mice suffered from excessive inflammation that was shown by formation of large follicles of immune cells with subsequent formation of more tumors at days 28 and 35 of AOM/DSS treatment compared to wild type mice.

These observed results suggested that, due to the loss of Cyp11b1, Cyp11b1 knockout mice are not able to synthesize immunosuppressive GCs and thereby have an increased inflammatory response compared to wild type. Indeed, following *ex vivo* culture of colons

from AOM/DSS-treated Cyp11b1 knockout and wild type mice at day 28, we could show a reduced GC production in the Cyp11b1 knockout mice compared to wild type.

We here provide the first evidence for the role of local GC synthesis in the initiation of inflammation-driven colon cancer, since the deletion of Cyp11b1 sensitized mice to intestinal inflammation and subsequent tumorigenesis.

In another study, it has been shown that intestinal epithelium-specific knockout of the P450 reductase gene (Cpr) exacerbates DSS-induced colitis (Zhu et al., 2015). Zhu et al. could also show that Cpr conditional knockout mice suffered from severe inflammation compared to wild type counterparts upon DSS-induced colitis due to reduced GC production. Interestingly, they report that oral administration of GC to Cpr conditional knockout mice abolished the hypersensitivity of these mice to DSS-induced colitis (Zhu et al., 2015).

Additionally, GCs has been shown to regulate the expression of TJs and to antagonize the TJ-destructing effect of TNF (Boivin et al., 2007). Moreover *in vitro* data suggested an important role of GCs in the maturation of the IECs (Lu et al., 2011). Furthermore, intestinal GC synthesis was also shown to control colonic PPARγ expression, a NR that regulates intestinal immune homeostasis and is impaired in IBD (Bouguen et al., 2015b).

Taken together our results further confirms the importance of a direct role of GC in intestinal epithelium homeostasis. In line with this, GCs have long been used for the treatment of IBD (De Iudicibus et al., 2011).

Next, we proceeded to investigate the role of Cyp11b1 in the progression of CRC by analyzing day 56 following AOM/DSS treatment. We hypothesized that, tumors from Cyp11b1 knockout mice will be smaller in size compared to wild type since they lack tumor-derived GC production and associated immune suppression. Indeed, although Cyp11b1 knockout mice developed more tumors in the initial phase of tumorigenesis (days 28 and 35) compared to wild type mice, we could show that these mice developed significantly reduced tumor numbers and size compared to wild type mice at an advance stage of tumorigenesis (day 56). In line with increased tumor number in Cyp11b1 knockout mice at day 56, we here showed an increased Ki-67-positive cells in tumors from Cyp11b1 knockout, that was infiltrated with less T cells compared to wild type. This could indicate a possible GC-mediated apoptosis, since T cells are sensitive to GC-induced apoptosis (Brunner et al., 2001; Mittelstadt et al., 2018).

We here report a biphasic tumor development stages in the Cyp11b1 knockout mice: an initiation phase driven by local GC and a progression phase mediated by tumor-derived GC.

Taken all together, we provide the first evidence for a direct role of local GC synthesis in the initiation and progression of CRC and propose tumor-derived GCs as a possible tumor immune escape mechanism.

5.4 Potential role of colorectal tumor-derived GCs as an immune escape mechanism

In the previous discussion we could show that LRH-1-mediated proliferation and GC synthesis plays important roles in the modulation of intestinal inflammation and associated tumorigenesis. However, because an inflammation-driven colon carcinogenesis model was used and given the dual roles of LRH-1 in the intestine i.e regulation of inflammation and proliferation, it was not possible to distinguish between these two roles in this context.

Therefore, we proceed to study the ability of the already formed AOM/DSS-induced tumors to grow in a non-inflamed environment. We also aimed at investigating the role of tumor-derived GC synthesis as a potential immune escape mechanism. For this purpose, we utilized the exciting technology of the 3D *in vitro* organoid culture (Sato et al., 2009).

The advantage of using intestinal organoids stems from the fact that these so-called mini-guts retain the cellular structure and composition of the *in vivo* epithelium (Sato et al., 2009), thus provide more relevance for the *in vivo* situation. These organoids could be applied for the identification of the molecular mechanisms of CRC development and can be used as powerful tools for drug testing.

Consistent with previous reports regarding the growth of malignant organoids (Sato et al., 2011b; Xue and Shah, 2013), we could show that AOM/DSS-induced tumors are able to grow *in vitro*. Unlike organoids from normal epithelium that retain the hallmarks of the *in vivo* epithelium (Sato et al., 2009), we could show that tumor organoids grew in an undifferentiated organoids forming a balloon-like structures. This observation further confirms that these organoids are originated from cancer stem cells that proliferate but do not differentiate (Melo et al., 2017).

Following the successful growth of tumor organoids, we next proceed to use the model as a tool to study the proliferation of the tumor organoids in a non-inflamed condition. For this purpose, tumor organoids were injected s.c. into the flanks of immunocompetent mice to study the effect of an intact immune system on the growth potential of the tumor organoids from the abovementioned genotypes. In order to avoid interindividual variability knockout tumor organoids were injected in the right flank while the wild type tumor organoids were injected in the left flank of the same mouse, consequently the growth rate was observed over time.

We firstly investigated the growth rate of tumor organoids from SHP-deficient tumors hypothesizing that SHP-/- tumor organoids will have a growth preference over wild type tumor organoids due to increased LRH-1-mediated proliferation and GC immune suppression. Supporting our hypothesis, we could show that whereas SHP-deficient organoids grew exponentially over time, tumor organoids from wild type were not able to grow. Moreover, histological analysis of the s.c. tumors 24 days following injection showed a remarkable growth of tumor organoids from SHP-deficient tumors compared to wild type. In marked contrast to the balloon-like organoid structures growing *in vitro*, we have seen differentiated organoids growing at day 24 following s.c injection in both genotypes as seen by epithelial-like organoid structure that contained cellular composition including goblet cells. This phenotype could be due to mutations acquired following the dissociation of the tumor organoids from the 3D stroma and the following s.c. injection.

Interestingly, we also observed some structures that appeared to be eliminated organoid, indicating an ongoing anti-tumor immune response that limited the growth of those organoids.

Recently, Melo et al. identified a distinct role for Lgr5+ stem cells in the development of primary and metastatic CRC using intestinal organoids as a model system (Melo et al., 2017). Unpublished data from C. Reinhold showed an increased Lgr5+ expression in the SHP-deficient intestinal mucosa compared to wild type further indicating increased proliferation (Unpublished data). Therefore, the increased growth potential of the SHP-deficient organoids could be due to an increased pool of cancer stem cells in these organoids, besides the LRH-1-induced GC production.

Next, we aimed at investigating the growth rate of tumor organoids from LRH-1 knockout tumors. We expected that due to the lack of LRH-1-induced proliferation and GC synthesis these tumors will exhibit reduced growth rate compared to wild type organoids. Indeed, we could show that although wild type tumors did not grow exponentially like SHP-deficient organoids, we could see a stable growth rate that started to decline after 12 days following s.c. injection. In contrast, LRH-1 knockout mice were not able to grow and the growth rate drastically declined after 12 days following s.c. injection. In line with this, histological analysis of sections at day 24 following injection indicated few growing organoids in wild type mice while no LRH-1 knockout organoids were detected.

LRH-1 plays vital roles in maintenance of stemness and pluripotency by regulating the expression of Oct4 (Gu et al., 2005), this fact is underlined by the embryonic lethal phenotype of the LRH-1-null mice (Paré et al., 2004). Therefore, the hindered growth phenotype of the LRH-1 knockout tumor organoid might be due to reduced LRH-1-induced proliferation.

Next, we aimed at investigating the direct effect of tumor-derived GC on the growth rate of tumor organoids. For this purpose, we used the Cyp11b1 knockout tumor organoids, since we have shown that Cyp11b1 have a defective GC production. Our hypothesis was that Cyp11b1 knockout tumor organoids would exhibit less tumor growth compared to wild type counterparts due to the loss of GC production, however since they have active LRH-1 the effect would not be as drastic as seen in LRH-1-knockout tumor organoids. Indeed, we observed that tumor organoids from Cyp11b1 knockout exhibited a reduced growth rate compared to wild type counterparts.

As discussed previously, GCs can modulate both innate and adaptive immune cells (Bereshchenko et al., 2018; Liberman et al., 2018). GCs mediate the shift of the tumor suppressive M1 macrophages to the tumor promoting M2 phenotype (Ehrchen et al., 2007). Furthermore, GCs inhibit DCs function (Baschant and Tuckermann, 2010) resulting in a reduced proliferative Th1 responses and an increase in immunosuppressive Treg (Chen et al., 2017). GCs also induce T cell apoptosis (Brunner et al., 2001; Mittelstadt et al., 2018). All these GC-mediated mechanisms are associated with suppression of anti-tumor immune responses and represent the major mechanisms by which tumors escape the immune surveillance (Vinay et al., 2015). In line with this and due to the massive macrophage and T cell infiltration we have seen in AOM/DSS-induced tumors, and since TAMs and T cells represent the majority of immune cells infiltrating CRC (Ferrone and Dranoff, 2010; Tosolini et al., 2011), it is

stimulating to propose that tumor-derived GCs could module the TME by suppressing these immune cells and thereby inhibit anti-tumor immune responses.

In summary, we provide the first functional *in vivo* study for investigating the role of GC in the initiation and progression of CRC. we could show that intact local GC synthesis regulates intestinal epithelium homeostasis and attenuates the initiation of CRC, whereas enhanced GC synthesis abrogates CRC development. Moreover, we were able to show that LRH-1-induced proliferation and tumor-derived GCs are critical for the progression of CRC. Furthermore, we could show an unexpected role of SHP deficiency in the control of CRC development, not via the control of LRH-1-promoted tumor proliferation, but rather via the regulation of intestinal inflammation and associated tumorigenesis. Additionally, we report a possible role of LRH-1-mediated GC synthesis in CRC tumors as an important immune escape mechanism.

Taken together, our data provide the first evidence for the role of local GC synthesis in the initiation and progression of CRC development. Additionally, we identified the nuclear receptors LRH-1 and SHP as important therapeutic targets for the treatment of CRC. Furthermore, we could show a critical role of tumor-derived GCs in the regulation of anti-tumor immune responses that could possibly represent an important immune escape mechanism.

6 Outlook

Although our data provide the first functional *in vivo* study that show substantial evidence for the role of local GC synthesis in the initiation and progression of CRC, many questions are still opened and remained to be answered.

In this study we show phenotypically the role of LRH-1 and LRH-1-induced GC synthesis in the development of CRC, however future studies are required to elucidate the molecular mechanisms underlying the observed phenotypes.

Most importantly, analysis of GC synthesis and the expression of the steroidogenic enzymes and regulators should be performed.

Additionally, expression of genes that correlate with T cell activity could be performed including perforin and granzyme B.

Since we have seen that immune interaction at the tumor microenvironment play a critical role in determining the fate of CRC. Immunohistochemistry for specific markers of tumor infiltrating immune cells could be performed to identify the immune responses in each mouse model.

Furthermore, tumors could be dissociated and stained for different immune cell markers and subjected to FACS analysis to identify the immune cell composition in tumors from each genotype.

Tumor organoids could also be tested for GC production, moreover co-culture experiments with activated T cells could be performed to test the potential of tumor-derived GCs to inhibit T cell activation and function.

Furthermore, since cell death at the tumor microenvironment is a critical regulator of the tumor outcome apoptosis could be tested for example by performing immunohistochemistry staining or western blot for cleaved caspase 3.

Moreover, since genetic instability is an important driver of carcinogenesis, it would be relevant to identify the mutations in tumors from different genotypes.

7 Publication

Ahmed A, Schwaderer J, Hantusch A, Kolho K-L, Brunner T. Intestinal glucocorticoid synthesis enzymes in pediatric inflammatory bowel disease patients. Genes Immun. 2019 Jan 28;1.

8 Table of Figures

Table of Figures

9 References

Alangari, A.A. (2014). Corticosteroids in the treatment of acute asthma. Ann. Thorac. Med. *9*, 187–192.

Ameyar, M., Wisniewska, M., and Weitzman, J.B. (2003). A role for AP-1 in apoptosis: the case for and against. Biochimie *85*, 747–752.

Annane, D., Bellissant, E., Bollaert, P.-E., Briegel, J., Confalonieri, M., De Gaudio, R., Keh, D., Kupfer, Y., Oppert, M., and Meduri, G.U. (2009). Corticosteroids in the treatment of severe sepsis and septic shock in adults: a systematic review. JAMA *301*, 2362–2375.

Arnold, M., Sierra, M.S., Laversanne, M., Soerjomataram, I., Jemal, A., and Bray, F. (2017). Global patterns and trends in colorectal cancer incidence and mortality. Gut *66*, 683–691.

Ashwell, J.D., Lu, F.W., and Vacchio, M.S. (2000). Glucocorticoids in T cell development and function*. Annu. Rev. Immunol. *18*, 309–345.

Atanasov, A.G., Leiser, D., Roesselet, C., Noti, M., Corazza, N., Schoonjans, K., and Brunner, T. (2008). Cell cycle-dependent regulation of extra-adrenal glucocorticoid synthesis in murine intestinal epithelial cells. FASEB J. *22*, 4117–4125.

Ballegeer, M., Looveren, K.V., Timmermans, S., Eggermont, M., Vandevyver, S., Thery, F., Dendoncker, K., Souffriau, J., Vandewalle, J., Wyngene, L.V., et al. (2018). Glucocorticoid receptor dimers control intestinal STAT1 and TNF-induced inflammation in mice. J. Clin. Invest. *128*, 3265–3279.

Barczyk, K., Ehrchen, J., Tenbrock, K., Ahlmann, M., Kneidl, J., Viemann, D., and Roth, J. (2010). Glucocorticoids promote survival of anti-inflammatory macrophages via stimulation of adenosine receptor A3. Blood *116*, 446–455.

Barker, N., van Es, J.H., Kuipers, J., Kujala, P., van den Born, M., Cozijnsen, M., Haegebarth, A., Korving, J., Begthel, H., Peters, P.J., et al. (2007). Identification of stem cells in small intestine and colon by marker gene Lgr5. Nature *449*, 1003–1007.

Baschant, U., and Tuckermann, J. (2010). The role of the glucocorticoid receptor in inflammation and immunity. J. Steroid Biochem. Mol. Biol. *120*, 69–75.

Bayrer, J.R., Mukkamala, S., Sablin, E.P., Webb, P., and Fletterick, R.J. (2015). Silencing LRH-1 in colon cancer cell lines impairs proliferation and alters gene expression programs. Proc. Natl. Acad. Sci. *112*, 2467–2472.

Bayrer, J.R., Wang, H., Nattiv, R., Suzawa, M., Escusa, H.S., Fletterick, R.J., Klein, O.D., Moore, D.D., and Ingraham, H.A. (2018). LRH-1 mitigates intestinal inflammatory disease by maintaining epithelial homeostasis and cell survival. Nat. Commun. *9*, 4055.

Becker, C., Fantini, M.C., Wirtz, S., Nikolaev, A., Lehr, H.A., Galle, P.R., Rose-John, S., and Neurath, M.F. (2005). IL-6 signaling promotes tumor growth in colorectal cancer. Cell Cycle Georget. Tex *4*, 217–220.

Benod, C., Vinogradova, M.V., Jouravel, N., Kim, G.E., Fletterick, R.J., and Sablin, E.P. (2011). Nuclear receptor liver receptor homologue 1 (LRH-1) regulates pancreatic cancer cell growth and proliferation. Proc. Natl. Acad. Sci. U. S. A. *108*, 16927–16931.

Benod, C., Carlsson, J., Uthayaruban, R., Hwang, P., Irwin, J.J., Doak, A.K., Shoichet, B.K., Sablin, E.P., and Fletterick, R.J. (2013). Structure-based Discovery of Antagonists of Nuclear Receptor LRH-1. J. Biol. Chem. *288*, 19830–19844.

Bereshchenko, O., Bruscoli, S., and Riccardi, C. (2018). Glucocorticoids, Sex Hormones, and Immunity. Front. Immunol. *9*.

Bijlsma, J.W.J., Jacobs, J.W.G., and Buttgereit, F. (2015). Glucocorticoids in the treatment of rheumatoid arthritis. Clin. Exp. Rheumatol. *33*, S34-36.

Bode, H., Schmitz, H., Fromm, M., Scholz, P., Riecken, E.-O., and Schulzke, J.-D. (1998). IL-1β AND TNF-α, BUT NOT IFN-α, IFN-γ, IL-6 OR IL-8, ARE SECRETORY MEDIATORS IN HUMAN DISTAL COLON. Cytokine *10*, 457–465.

Boivin, M.A., Ye, D., Kennedy, J.C., Al-Sadi, R., Shepela, C., and Ma, T.Y. (2007). Mechanism of glucocorticoid regulation of the intestinal tight junction barrier. Am. J. Physiol. Gastrointest. Liver Physiol. *292*, G590–G598.

Bollrath, J., Phesse, T.J., von Burstin, V.A., Putoczki, T., Bennecke, M., Bateman, T., Nebelsiek, T., Lundgren-May, T., Canli, O., Schwitalla, S., et al. (2009). gp130-mediated Stat3 activation in enterocytes regulates cell survival and cell-cycle progression during colitis-associated tumorigenesis. Cancer Cell *15*, 91–102.

Bookout, A.L., Jeong, Y., Downes, M., Yu, R.T., Evans, R.M., and Mangelsdorf, D.J. (2006). Anatomical Profiling of Nuclear Receptor Expression Reveals a Hierarchical Transcriptional Network. Cell *126*, 789–799.

Botrugno, O.A., Fayard, E., Annicotte, J.-S., Haby, C., Brennan, T., Wendling, O., Tanaka, T., Kodama, T., Thomas, W., Auwerx, J., et al. (2004). Synergy between LRH-1 and β-catenin induces G 1 cyclin-mediated cell proliferation. Mol. Cell *15*, 499–509.

Bouguen, G., Dubuquoy, L., Desreumaux, P., Brunner, T., and Bertin, B. (2015a). Intestinal steroidogenesis. Steroids.

Bouguen, G., Langlois, A., Djouina, M., Branche, J., Koriche, D., Dewaeles, E., Mongy, A., Auwerx, J., Colombel, J.-F., Desreumaux, P., et al. (2015b). Intestinal steroidogenesis controls PPARγ expression in the colon and is impaired during ulcerative colitis. Gut *64*, 901–910.

Bradley, J.R. (2008). TNF-mediated inflammatory disease. J. Pathol. *214*, 149–160.

Bray, F., Ferlay, J., Soerjomataram, I., Siegel, R.L., Torre, L.A., and Jemal, A. (2018). Global cancer statistics 2018: GLOBOCAN estimates of incidence and mortality worldwide for 36 cancers in 185 countries. CA. Cancer J. Clin. *68*, 394–424.

Brendel, C., Gelman, L., and Auwerx, J. (2002). Multiprotein Bridging Factor-1 (MBF-1) Is a Cofactor for Nuclear Receptors that Regulate Lipid Metabolism. Mol. Endocrinol. *16*, 1367–1377.

Brenner, H., Kloor, M., and Pox, C.P. (2014). Colorectal cancer. Lancet Lond. Engl. *383*, 1490–1502.

Breuner, C.W., and Orchinik, M. (2002). Plasma binding proteins as mediators of corticosteroid action in vertebrates. J. Endocrinol. *175*, 99–112.

Brunner, T., Arnold, D., Wasem, C., Herren, S., and Frutschi, C. (2001). Regulation of cell death and survival in intestinal intraepithelial lymphocytes. Cell Death Differ. *8*.

Burn, J., Gerdes, A.-M., Macrae, F., Mecklin, J.-P., Moeslein, G., Olschwang, S., Eccles, D., Evans, D.G., Maher, E.R., Bertario, L., et al. (2011). Long-term effect of aspirin on cancer risk in carriers of hereditary colorectal cancer: an analysis from the CAPP2 randomised controlled trial. The Lancet *378*, 2081–2087.

Burris, T.P., Busby, S.A., and Griffin, P.R. (2012). Targeting orphan nuclear receptors for treatment of metabolic diseases and autoimmunity. Chem. Biol. *19*, 51–59.

Burstein, E., and Fearon, E.R. (2008). Colitis and cancer: a tale of inflammatory cells and their cytokines. J. Clin. Invest.

Busillo, J.M., and Cidlowski, J.A. (2013). The five Rs of glucocorticoid action during inflammation: ready, reinforce, repress, resolve, and restore. Trends Endocrinol. Metab. TEM *24*, 109–119.

Camus, M., Tosolini, M., Mlecnik, B., Pages, F., Kirilovsky, A., Berger, A., Costes, A., Bindea, G., Charoentong, P., Bruneval, P., et al. (2009). Coordination of Intratumoral Immune Reaction and Human Colorectal Cancer Recurrence. Cancer Res. *69*, 2685–2693.

Canli, Ö., Nicolas, A.M., Gupta, J., Finkelmeier, F., Goncharova, O., Pesic, M., Neumann, T., Horst, D., Löwer, M., Sahin, U., et al. (2017). Myeloid Cell-Derived Reactive Oxygen Species Induce Epithelial Mutagenesis. Cancer Cell *32*, 869-883.e5.

Cao, Z., West, C., Norton-Wenzel, C.S., Rej, R., Davis, F.B., Davis, P.J., and Rej, R. (2009). Effects of resin or charcoal treatment on fetal bovine serum and bovine calf serum. Endocr. Res. *34*, 101–108.

Cario, E. (2008). Innate immune signalling at intestinal mucosal surfaces: a fine line between host protection and destruction. Curr. Opin. Gastroenterol. *24*, 725–732.

Cario, E. (2013). Microbiota and innate immunity in intestinal inflammation and neoplasia. Curr. Opin. Gastroenterol. *29*, 85.

Chand, A.L., Herridge, K.A., Thompson, E.W., and Clyne, C.D. (2010). The orphan nuclear receptor LRH-1 promotes breast cancer motility and invasion. Endocr. Relat. Cancer *17*, 965–975.

Chanda, D., Park, J.-H., and Choi, H.-S. (2008). Molecular Basis of Endocrine Regulation by Orphan Nuclear Receptor Small Heterodimer Partner. Endocr. J. *55*, 253–268.

Chanda, D., Xie, Y.-B., and Choi, H.-S. (2010). Transcriptional corepressor SHP recruits SIRT1 histone deacetylase to inhibit LRH-1 transactivation. Nucleic Acids Res. *38*, 4607–4619.

Chen, L., Hasni, M.S., Jondal, M., and Yakimchuk, K. (2017). Modification of anti-tumor immunity by tolerogenic dendritic cells. Autoimmunity *50*, 370–376.

Chen, X., Oppenheim, J.J., Winkler-Pickett, R.T., Ortaldo, J.R., and Howard, O.M.Z. (2006). Glucocorticoid amplifies IL-2-dependent expansion of functional FoxP3+CD4+CD25+ T regulatory cells in vivo and enhances their capacity to suppress EAE. Eur. J. Immunol. *36*, 2139–2149.

Cheroutre, H., Lambolez, F., and Mucida, D. (2011). The light and dark sides of intestinal intraepithelial lymphocytes. Nat. Rev. Immunol. *11*, 445–456.

Ciccone, A., Beretta, S., Brusaferri, F., Galea, I., Protti, A., and Spreafico, C. (2008). Corticosteroids for the long-term treatment in multiple sclerosis. Cochrane Database Syst. Rev. CD006264.

Cima, I., Corazza, N., Dick, B., Fuhrer, A., Herren, S., Jakob, S., Ayuni, E., Mueller, C., and Brunner, T. (2004). Intestinal Epithelial Cells Synthesize Glucocorticoids and Regulate T Cell Activation. J. Exp. Med. *200*, 1635–1646.

Clevers, H. (2013). The intestinal crypt, a prototype stem cell compartment. Cell *154*, 274–284.

Clevers, H., and Batlle, E. (2013). SnapShot: The Intestinal Crypt. Cell *152*, 1198-1198.e2.

Clyne, C.D., Speed, C.J., Zhou, J., and Simpson, E.R. (2002). Liver receptor homologue-1 (LRH-1) regulates expression of aromatase in preadipocytes. J. Biol. Chem. *277*, 20591–20597.

Cobo, I., Martinelli, P., Flández, M., Bakiri, L., Zhang, M., Carrillo-de-Santa-Pau, E., Jia, J., Lobo, V.J.S.-A., Megías, D., Felipe, I., et al. (2018). Transcriptional regulation by NR5A2 links differentiation and inflammation in the pancreas. Nature.

Cohen, S.A., and Leininger, A. (2014). The genetic basis of Lynch syndrome and its implications for clinical practice and risk management. Appl. Clin. Genet. *7*, 147–158.

Corzo, C.A., Mari, Y., Chang, M.R., Khan, T., Kuruvilla, D., Nuhant, P., Kumar, N., West, G.M., Duckett, D.R., Roush, W.R., et al. (2015). Antiproliferation activity of a small molecule repressor of liver receptor homolog 1. Mol. Pharmacol. *87*, 296–304.

Coste, A., Dubuquoy, L., Barnouin, R., Annicotte, J.-S., Magnier, B., Notti, M., Corazza, N., Antal, M.C., Metzger, D., Desreumaux, P., et al. (2007). LRH-1-mediated glucocorticoid synthesis in enterocytes protects against inflammatory bowel disease. Proc. Natl. Acad. Sci. *104*, 13098–13103.

Coutinho, A.E., and Chapman, K.E. (2011). The anti-inflammatory and immunosuppressive effects of glucocorticoids, recent developments and mechanistic insights. Mol. Cell. Endocrinol. *335*, 2–13.

Croft, A.P., O'Callaghan, M.J., Shaw, S.G., Connolly, G., Jacquot, C., and Little, H.J. (2008). Effects of minor laboratory procedures, adrenalectomy, social defeat or acute alcohol on regional brain concentrations of corticosterone. Brain Res. *1238*, 12–22.

Crowder, M.K., Seacrist, C.D., and Blind, R.D. (2017). Phospholipid Regulation of the Nuclear Receptor Superfamily. Adv. Biol. Regul. *63*, 6–14.

Davies, R.J., Miller, R., and Coleman, N. (2005). Colorectal cancer screening: prospects for molecular stool analysis. Nat. Rev. Cancer *5*, 199–209.

De Iudicibus, S., Franca, R., Martelossi, S., Ventura, A., and Decorti, G. (2011). Molecular mechanism of glucocorticoid resistance in inflammatory bowel disease. World J. Gastroenterol. WJG *17*, 1095–1108.

De Lerma Barbaro, A., Perletti, G., Bonapace, I.M., and Monti, E. (2014). Inflammatory cues acting on the adult intestinal stem cells and the early onset of cancer (Review). Int. J. Oncol. *45*, 959–968.

Delgado, M.E., Grabinger, T., and Brunner, T. (2016). Cell death at the intestinal epithelial front line. FEBS J. *283*, 2701–2719.

Donnellan, R., and Chetty, R. (1999). Cyclin E in human cancers. FASEB J. Off. Publ. Fed. Am. Soc. Exp. Biol. *13*, 773–780.

Dragan, A.I., Pavlovic, R., McGivney, J.B., Casas-Finet, J.R., Bishop, E.S., Strouse, R.J., Schenerman, M.A., and Geddes, C.D. (2012). SYBR Green I: fluorescence properties and interaction with DNA. J. Fluoresc. *22*, 1189–1199.

Dubuquoy, L., Rousseaux, C., Thuru, X., Peyrin-Biroulet, L., Romano, O., Chavatte, P., Chamaillard, M., and Desreumaux, P. (2006). PPARγ as a new therapeutic target in inflammatory bowel diseases. Gut *55*, 1341–1349.

Dunn, G.P., Bruce, A.T., Ikeda, H., Old, L.J., and Schreiber, R.D. (2002). Cancer immunoediting: from immunosurveillance to tumor escape. Nat. Immunol. *3*, 991–998.

Eaden, J., Abrams, K., and Mayberry, J. (2001). The risk of colorectal cancer in ulcerative colitis: a meta-analysis. Gut *48*, 526–535.

Egger, B., Bajaj-Elliott, M., MacDonald, T.T., Inglin, R., Eysselein, V.E., and Büchler, M.W. (2000). Characterisation of acute murine dextran sodium sulphate colitis: cytokine profile and dose dependency. Digestion *62*, 240–248.

Ehrchen, J., Steinmüller, L., Barczyk, K., Tenbrock, K., Nacken, W., Eisenacher, M., Nordhues, U., Sorg, C., Sunderkötter, C., and Roth, J. (2007). Glucocorticoids induce differentiation of a specifically activated, anti-inflammatory subtype of human monocytes. Blood *109*, 1265–1274.

El Marjou, F., Janssen, K.-P., Hung-Junn Chang, B., Li, M., Hindie, V., Chan, L., Louvard, D., Chambon, P., Metzger, D., and Robine, S. (2004). Tissue-specific and inducible Cre-mediated recombination in the gut epithelium. Genesis *39*, 186–193.

Erhardt, J.G., Kreichgauer, H.P., Meisner, C., Bode, J.C., and Bode, C. (2002). Alcohol, cigarette smoking, dietary factors and the risk of colorectal adenomas and hyperplastic polyps--a case control study. Eur. J. Nutr. *41*, 35–43.

Erlacher, M., Labi, V., Manzl, C., Böck, G., Tzankov, A., Häcker, G., Michalak, E., Strasser, A., and Villunger, A. (2006). Puma cooperates with Bim, the rate-limiting BH3-only protein in cell death during lymphocyte development, in apoptosis induction. J. Exp. Med. *203*, 2939–2951.

Fayard, E., Auwerx, J., and Schoonjans, K. (2004). LRH-1: an orphan nuclear receptor involved in development, metabolism and steroidogenesis. Trends Cell Biol. *14*, 250–260.

Fazio, V., Robertis, M., Massi, E., Poeta, M., Carotti, S., Morini, S., Cecchetelli, L., and Signori, E. (2011). The AOM/DSS murine model for the study of colon carcinogenesis: From pathways to diagnosis and therapy studies. J. Carcinog. *10*, 9.

Fearon, E.R. (2011). Molecular Genetics of Colorectal Cancer. Annu. Rev. Pathol. Mech. Dis. *6*, 479–507.

Fearon, E.R., and Vogelstein, B. (1990). A genetic model for colorectal tumorigenesis. Cell *61*, 759–767.

Ferlay, J., Parkin, D.M., and Steliarova-Foucher, E. (2010). Estimates of cancer incidence and mortality in Europe in 2008. Eur. J. Cancer *46*, 765–781.

Fernandez-Marcos, P.J., Auwerx, J., and Schoonjans, K. (2011). Emerging actions of the nuclear receptor LRH-1 in the gut. Biochim. Biophys. Acta BBA - Mol. Basis Dis. *1812*, 947–955.

Ferrone, C., and Dranoff, G. (2010). Dual roles for immunity in gastrointestinal cancers. J. Clin. Oncol. Off. J. Am. Soc. Clin. Oncol. *28*, 4045–4051.

Finn, O.J. (2008). Cancer immunology. N. Engl. J. Med. *358*, 2704–2715.

Fleet, J.C. (2014). Animal models of gastrointestinal and liver diseases. New mouse models for studying dietary prevention of colorectal cancer. Am. J. Physiol. - Gastrointest. Liver Physiol. *307*, G249–G259.

van der Flier, L.G., and Clevers, H. (2009). Stem cells, self-renewal, and differentiation in the intestinal epithelium. Annu. Rev. Physiol. *71*, 241–260.

França, M.M., Ferraz-de-Souza, B., Lerario, A.M., Fragoso, M.C.B.V., and Lotfi, C.F.P. (2015). POD-1/TCF21 Reduces SHP Expression, Affecting LRH-1 Regulation and Cell Cycle Balance in Adrenocortical and Hepatocarcinoma Tumor Cells.

Fries, W., Muja, C., Crisafulli, C., Costantino, G., Longo, G., Cuzzocrea, S., and Mazzon, E. (2008). Infliximab and etanercept are equally effective in reducing enterocyte APOPTOSIS in experimental colitis. Int. J. Med. Sci. *5*, 169–180.

Gaifulina, R., Maher, A.T., Kendall, C., Nelson, J., Rodriguez-Justo, M., Lau, K., and Thomas, G.M. (2016). Label-free Raman spectroscopic imaging to extract morphological and chemical information from a formalin-fixed, paraffin-embedded rat colon tissue section. Int. J. Exp. Pathol. *97*, 337–350.

Galarneau, L., Paré, J.F., Allard, D., Hamel, D., Levesque, L., Tugwood, J.D., Green, S., and Bélanger, L. (1996). The alpha1-fetoprotein locus is activated by a nuclear receptor of the Drosophila FTZ-F1 family. Mol. Cell. Biol. *16*, 3853–3865.

Gerbe, F., Legraverend, C., and Jay, P. (2012). The intestinal epithelium tuft cells: specification and function. Cell. Mol. Life Sci. *69*, 2907–2917.

Gillen, C.D., Walmsley, R.S., Prior, P., Andrews, H.A., and Allan, R.N. (1994). Ulcerative colitis and Crohn's disease: a comparison of the colorectal cancer risk in extensive colitis. Gut *35*, 1590–1592.

Gomez-Sanchez, C.E. (2009). Glucocorticoid Production and Regulation in Thymus: Of Mice and Birds. Endocrinology *150*, 3977–3979.

Goodwin, B., Jones, S.A., Price, R.R., Watson, M.A., McKee, D.D., Moore, L.B., Galardi, C., Wilson, J.G., Lewis, M.C., Roth, M.E., et al. (2000). A regulatory cascade of the nuclear receptors FXR, SHP-1, and LRH-1 represses bile acid biosynthesis. Mol. Cell *6*, 517–526.

Grabinger, T., Luks, L., Kostadinova, F., Zimberlin, C., Medema, J.P., Leist, M., and Brunner, T. (2014). Ex vivo culture of intestinal crypt organoids as a model system for assessing cell death induction in intestinal epithelial cells and enteropathy. Cell Death Dis. *5*, e1228.

Grabinger, T., Bode, K.J., Demgenski, J., Seitz, C., Delgado, M.E., Kostadinova, F., Reinhold, C., Etemadi, N., Wilhelm, S., Schweinlin, M., et al. (2017). Inhibitor of Apoptosis Protein-1 Regulates Tumor Necrosis Factor-Mediated Destruction of Intestinal Epithelial Cells. Gastroenterology *152*, 867–879.

Granados-Romero, J.J., Valderrama-Treviño, A.I., Contreras-Flores, E.H., Barrera-Mera, B., Enríquez, M.H., Uriarte-Ruíz, K., Ceballos-Villalba, J.C., Estrada-Mata, A.G., Rodríguez, C.A., and Arauz-Peña, G. (2017). Colorectal cancer: a review. Int. J. Res. Med. Sci. *5*, 4667–4676.

Greten, F.R., Eckmann, L., Greten, T.F., Park, J.M., Li, Z.-W., Egan, L.J., Kagnoff, M.F., and Karin, M. (2004). IKKbeta links inflammation and tumorigenesis in a mouse model of colitis-associated cancer. Cell *118*, 285–296.

Grivennikov, S.I. (2013). Inflammation and colorectal cancer: colitis-associated neoplasia. Semin. Immunopathol. *35*, 229–244.

Grivennikov, S.I., and Karin, M. (2010). Inflammation and oncogenesis: a vicious connection. Curr. Opin. Genet. Dev. *20*, 65.

Grivennikov, S., Karin, E., Terzic, J., Mucida, D., Yu, G.-Y., Vallabhapurapu, S., Scheller, J., Rose-John, S., Cheroutre, H., Eckmann, L., et al. (2009). IL-6 and STAT3 are required for survival of intestinal epithelial cells and development of colitis associated cancer. Cancer Cell *15*, 103–113.

Grizzi, F., Basso, G., Borroni, E.M., Cavalleri, T., Bianchi, P., Stifter, S., Chiriva-Internati, M., Malesci, A., and Laghi, L. (2018). Evolving notions on immune response in colorectal cancer and their implications for biomarker development. Inflamm. Res. Off. J. Eur. Histamine Res. Soc. Al *67*, 375–389.

Gu, P., Goodwin, B., Chung, A.C.-K., Xu, X., Wheeler, D.A., Price, R.R., Galardi, C., Peng, L., Latour, A.M., Koller, B.H., et al. (2005). Orphan Nuclear Receptor LRH-1 Is Required To Maintain Oct4 Expression at the Epiblast Stage of Embryonic Development. Mol. Cell. Biol. *25*, 3492–3505.

Gupta, R.A., and Dubois, R.N. (2001). Colorectal cancer prevention and treatment by inhibition of cyclooxygenase-2. Nat. Rev. Cancer *1*, 11–21.

Haegebarth, A., and Clevers, H. (2009). Wnt Signaling, Lgr5, and Stem Cells in the Intestine and Skin. Am. J. Pathol. *174*, 715–721.

Haggar, F.A., and Boushey, R.P. (2009). Colorectal Cancer Epidemiology: Incidence, Mortality, Survival, and Risk Factors. Clin. Colon Rectal Surg. *22*, 191–197.

Hanahan, D., and Weinberg, R.A. (2011). Hallmarks of Cancer: The Next Generation. Cell *144*, 646–674.

Hankey, W., Chen, Z., Bergman, M.J., Fernandez, M.O., Hancioglu, B., Lan, X., Jegga, A.G., Zhang, J., Jin, V.X., Aronow, B.J., et al. (2018). Chromatin-associated APC regulates gene expression in collaboration with canonical WNT signaling and AP-1. Oncotarget *9*, 31214–31230.

Haramis, A.-P.G., Begthel, H., van den Born, M., van Es, J., Jonkheer, S., Offerhaus, G.J.A., and Clevers, H. (2004). De novo crypt formation and juvenile polyposis on BMP inhibition in mouse intestine. Science *303*, 1684–1686.

Harris, S.L., and Levine, A.J. (2005). The p53 pathway: positive and negative feedback loops. Oncogene *24*, 2899–2908.

Hawkey, C.J. (1999). COX-2 inhibitors. The Lancet *353*, 307–314.

He, N., Park, K., Zhang, Y., Huang, J., Lu, S., and Wang, L. (2008). Epigenetic Inhibition of Nuclear Receptor Small Heterodimer Partner Is Associated With and Regulates Hepatocellular Carcinoma Growth. Gastroenterology *134*, 793–802.

He, T.-C., Sparks, A.B., Rago, C., Hermeking, H., Zawel, L., Costa, L.T. da, Morin, P.J., Vogelstein, B., and Kinzler, K.W. (1998). Identification of c-MYC as a Target of the APC Pathway. Science *281*, 1509–1512.

Heldin, C.H., Miyazono, K., and ten Dijke, P. (1997). TGF-beta signalling from cell membrane to nucleus through SMAD proteins. Nature *390*, 465–471.

Hoeke, M.O., Heegsma, J., Hoekstra, M., Moshage, H., and Faber, K.N. (2014). Human FXR Regulates SHP Expression through Direct Binding to an LRH-1 Binding Site, Independent of an IR-1 and LRH-1. PLoS ONE *9*, e88011.

Hoesel, B., and Schmid, J.A. (2013). The complexity of NF-κB signaling in inflammation and cancer. Mol. Cancer *12*, 86.

Hooper, L.V., and Macpherson, A.J. (2010). Immune adaptations that maintain homeostasis with the intestinal microbiota. Nat. Rev. Immunol. *10*, 159–169.

Horino, J., Fujimoto, M., Terabe, F., Serada, S., Takahashi, T., Soma, Y., Tanaka, K., Chinen, T., Yoshimura, A., Nomura, S., et al. (2008). Suppressor of cytokine signaling-1 ameliorates dextran sulfate sodium-induced colitis in mice. Int. Immunol. *20*, 753–762.

Hostettler, N., Bianchi, P., Gennari-Moser, C., Kassahn, D., Schoonjans, K., Corazza, N., and Brunner, T. (2012). Local glucocorticoid production in the mouse lung is induced by immune cell stimulation. Allergy *67*, 227–234.

Huang, J., Jia, R., and Brunner, T. (2018). Local synthesis of immunosuppressive glucocorticoids in the intestinal epithelium regulates anti-viral immune responses. Cell. Immunol.

Huang, P., Chandra, V., and Rastinejad, F. (2010). Structural Overview of the Nuclear Receptor Superfamily: Insights into Physiology and Therapeutics. Annu. Rev. Physiol. *72*, 247–272.

Huang, S.-C., Lee, C., and Chung, B. (2014). Tumor necrosis factor suppresses NR5A2 activity and intestinal glucocorticoid synthesis to sustain chronic colitis. Sci. Signal. *7*, ra20.

Humphries, A., and Wright, N.A. (2008). Colonic crypt organization and tumorigenesis. Nat. Rev. Cancer *8*, 415–424.

Hung, C.-C.C., Farooqi, I.S., Ong, K., Luan, J., Keogh, J.M., Pembrey, M., Yeo, G.S.H., Dunger, D., Wareham, N.J., and O' Rahilly, S. (2003). Contribution of variants in the small heterodimer partner gene to birthweight, adiposity, and insulin levels: mutational analysis and association studies in multiple populations. Diabetes *52*, 1288–1291.

Hussey, M., Holleran, G., Smith, S., Sherlock, M., and McNamara, D. (2017). The Role and Regulation of the 11 Beta-Hydroxysteroid Dehydrogenase Enzyme System in Patients with Inflammatory Bowel Disease. Dig. Dis. Sci. *62*, 3385–3390.

Huxley, R.R., Ansary-Moghaddam, A., Clifton, P., Czernichow, S., Parr, C.L., and Woodward, M. (2009). The impact of dietary and lifestyle risk factors on risk of colorectal cancer: a quantitative overview of the epidemiological evidence. Int. J. Cancer *125*, 171–180.

Ikeda, S., Kishida, S., Yamamoto, H., Murai, H., Koyama, S., and Kikuchi, A. (1998). Axin, a negative regulator of the Wnt signaling pathway, forms a complex with GSK-3beta and beta-catenin and promotes GSK-3beta-dependent phosphorylation of beta-catenin. EMBO J. *17*, 1371–1384.

Ilyas, M., Straub, J., Tomlinson, I.P.M., and Bodmer, W.F. (1999). Genetic pathways in colorectal and other cancers1Reprinted from Eur J Cancer 1999, 35(3), 335–351. Please use this reference when citing this article.1. Eur. J. Cancer *35*, 1986–2002.

Jakob, S., Corazza, N., Diamantis, E., Kappeler, A., and Brunner, T. (2008). Detection of apoptosis in vivo using antibodies against caspase-induced neo-epitopes. Methods San Diego Calif *44*, 255–261.

Janakiram, N.B., and Rao, C.V. (2014). The Role of Inflammation in Colon Cancer. In Inflammation and Cancer, B.B. Aggarwal, B. Sung, and S.C. Gupta, eds. (Basel: Springer Basel), pp. 25–52.

Jess, T., Rungoe, C., and Peyrin-Biroulet, L. (2012). Risk of colorectal cancer in patients with ulcerative colitis: a meta-analysis of population-based cohort studies. Clin. Gastroenterol. Hepatol. Off. Clin. Pract. J. Am. Gastroenterol. Assoc. *10*, 639–645.

Johansson, L., Båvner, A., Thomsen, J.S., Färnegårdh, M., Gustafsson, J.-Å., and Treuter, E. (2000). The Orphan Nuclear Receptor SHP Utilizes Conserved LXXLL-Related Motifs for Interactions with Ligand-Activated Estrogen Receptors. Mol. Cell. Biol. *20*, 1124–1133.

Johansson, M.E.V., Sjövall, H., and Hansson, G.C. (2013). The gastrointestinal mucus system in health and disease. Nat. Rev. Gastroenterol. Hepatol. *10*, 352–361.

Kaminski, R.M., and Rogawski, M.A. (2011). 11β-Hydroxylase inhibitors protect against seizures in mice by increasing endogenous neurosteroid synthesis. Neuropharmacology *61*, 133–137.

Kerber, R.A., Neklason, D.W., Samowitz, W.S., and Burt, R.W. (2005). Frequency of familial colon cancer and hereditary nonpolyposis colorectal cancer (Lynch syndrome) in a large population database. Fam. Cancer *4*, 239–244.

Kim, J.J., Shajib, M.S., Manocha, M.M., and Khan, W.I. (2012). Investigating Intestinal Inflammation in DSS-induced Model of IBD. J. Vis. Exp.

Kim, M.J., Lee, K.J., Hwang, J.-Y., Lee, H.S., Chio, S.H., Lim, S., Jang, H.C., and Park, Y.J. (2013). Loss of small heterodimer partner protects against atherosclerosis in apolipoprotein E-deficient mice. Endocr. J. *60*, 1171–1177.

Kim, Y.S., Han, C.-Y., Kim, S.-W., Kim, J.-H., Lee, S.-K., Jung, D.-J., Park, S.-Y., Kang, H., Choi, H.-S., Lee, J.W., et al. (2001). The Orphan Nuclear Receptor Small Heterodimer Partner as a Novel Coregulator of Nuclear Factor-κB in Oxidized Low Density Lipoprotein-treated Macrophage Cell Line RAW 264.7. J. Biol. Chem. *276*, 33736–33740.

Kinnebrew, M.A., and Pamer, E.G. (2012). Innate immune signaling in defense against intestinal microbes. Immunol. Rev. *245*, 113–131.

Kinzler, K.W., and Vogelstein, B. (1996). Lessons from Hereditary Colorectal Cancer. Cell *87*, 159–170.

Kinzler, K.W., Nilbert, M.C., Su, L.K., Vogelstein, B., Bryan, T.M., Levy, D.B., Smith, K.J., Preisinger, A.C., Hedge, P., McKechnie, D., et al. (1991). Identification of FAP locus genes from chromosome 5q21. Science *253*, 661–665.

Kojetin, D.J., and Burris, T.P. (2013). Small Molecule Modulation of Nuclear Receptor Conformational Dynamics: Implications for Function and Drug Discovery. Mol. Pharmacol. *83*, 1–8.

Korinek, V., Barker, N., Morin, P.J., Wichen, D. van, Weger, R. de, Kinzler, K.W., Vogelstein, B., and Clevers, H. (1997). Constitutive Transcriptional Activation by a β-Catenin-Tcf Complex in APC−/− Colon Carcinoma. Science *275*, 1784–1787.

Korniluk, A., Koper, O., Kemona, H., and Dymicka-Piekarska, V. (2017). From inflammation to cancer. Ir. J. Med. Sci. *186*, 57–62.

Kosinski, C., Li, V.S.W., Chan, A.S.Y., Zhang, J., Ho, C., Tsui, W.Y., Chan, T.L., Mifflin, R.C., Powell, D.W., Yuen, S.T., et al. (2007). Gene expression patterns of human colon tops and basal crypts and BMP antagonists as intestinal stem cell niche factors. Proc. Natl. Acad. Sci. U. S. A. *104*, 15418–15423.

Kostadinova, F., Schwaderer, J., Sebeo, V., and Brunner, T. (2014). Why does the gut synthesize glucocorticoids? Ann. Med. *46*, 490–497.

Kostadinova, F.I., Hostettler, N., Bianchi, P., and Brunner, T. (2012). Extra-Adrenal Glucocorticoid Synthesis in Mucosal Tissues and Its Implication in Mucosal Immune Homeostasis and Tumor Development. Glucocorticoids - New Recognit. Our Fam. Friend.

Kostic, A.D., Chun, E., Meyerson, M., and Garrett, W.S. (2013). Microbes and Inflammation in Colorectal Cancer. Cancer Immunol. Res. *1*, 150–157.

Kovacic, A., Speed, C.J., Simpson, E.R., and Clyne, C.D. (2004). Inhibition of aromatase transcription via promoter II by short heterodimer partner in human preadipocytes. Mol. Endocrinol. Baltim. Md *18*, 252–259.

Kramer, H.B., Lai, C.-F., Patel, H., Periyasamy, M., Lin, M.-L., Feller, S.M., Fuller-Pace, F.V., Meek, D.W., Ali, S., and Buluwela, L. (2016). LRH-1 drives colon cancer cell growth by repressing the expression of the *CDKN1A* gene in a p53-dependent manner. Nucleic Acids Res. *44*, 582–594.

Krylova, I.N., Sablin, E.P., Moore, J., Xu, R.X., Waitt, G.M., MacKay, J.A., Juzumiene, D., Bynum, J.M., Madauss, K., Montana, V., et al. (2005). Structural Analyses Reveal Phosphatidyl Inositols as Ligands for the NR5 Orphan Receptors SF-1 and LRH-1. Cell *120*, 343–355.

Kudryavtseva, A.V., Nyushko, K.M., Zaretsky, A.R., Shagin, D.A., Sadritdinova, A.F., Fedorova, M.S., Savvateeva, M.V., Guvatova, Z.G., Pudova, E.A., Alekseev, B.Y., et al. (2018). [Suppression of NR0B2 gene in Clear Cell Renal Cell Carcinoma Is Associated with Hypermethylation of Its Promoter]. Mol. Biol. (Mosk.) *52*, 482–488.

Kuhnert, F., Davis, C.R., Wang, H.-T., Chu, P., Lee, M., Yuan, J., Nusse, R., and Kuo, C.J. (2004). Essential requirement for Wnt signaling in proliferation of adult small intestine and colon revealed by adenoviral expression of Dickkopf-1. Proc. Natl. Acad. Sci. U. S. A. *101*, 266–271.

Larsson, S.C., Rafter, J., Holmberg, L., Bergkvist, L., and Wolk, A. (2005). Red meat consumption and risk of cancers of the proximal colon, distal colon and rectum: the Swedish Mammography Cohort. Int. J. Cancer *113*, 829–834.

Lascorz, J., Hemminki, K., and Försti, A. (2011). Systematic enrichment analysis of gene expression profiling studies identifies consensus pathways implicated in colorectal cancer development. J. Carcinog. *10*.

Lasry, A., Zinger, A., and Ben-Neriah, Y. (2016). Inflammatory networks underlying colorectal cancer. Nat. Immunol. *17*, 230–240.

Lazarus, K.A., Wijayakumara, D., Chand, A.L., Simpson, E.R., and Clyne, C.D. (2012a). Therapeutic potential of Liver Receptor Homolog-1 modulators. J. Steroid Biochem. Mol. Biol. *130*, 138–146.

Lazarus, K.A., Wijayakumara, D., Chand, A.L., Simpson, E.R., and Clyne, C.D. (2012b). Therapeutic potential of Liver Receptor Homolog-1 modulators. J. Steroid Biochem. Mol. Biol. *130*, 138–146.

Lechner, O., Wiegers, G.J., Oliveira-Dos-Santos, A.J., Dietrich, H., Recheis, H., Waterman, M., Boyd, R., and Wick, G. (2000). Glucocorticoid production in the murine thymus. Eur. J. Immunol. *30*, 337–346.

Leclerc, D., Deng, L., Trasler, J., and Rozen, R. (2004). ApcMin/+ mouse model of colon cancer: Gene expression profiling in tumors. J. Cell. Biochem. *93*, 1242–1254.

Lee, Y.-K., and Moore, D.D. (2002). Dual mechanisms for repression of the monomeric orphan receptor liver receptor homologous protein-1 by the orphan small heterodimer partner. J. Biol. Chem. *277*, 2463–2467.

Lee, H., Herrmann, A., Deng, J.-H., Kujawski, M., Niu, G., Li, Z., Forman, S., Jove, R., Pardoll, D.M., and Yu, H. (2009a). Persistently activated Stat3 maintains constitutive NF-kappaB activity in tumors. Cancer Cell *15*, 283–293.

Lee, J., Gonzales-Navajas, J.M., and Raz, E. (2008a). The “polarizing-tolerizing” mechanism of intestinal epithelium: its relevance to colonic homeostasis. Semin. Immunopathol. *30*, 3–9.

Lee, J.M., Lee, Y.K., Mamrosh, J.L., Busby, S.A., Griffin, P.R., Pathak, M.C., Ortlund, E.A., and Moore, D.D. (2011). A nuclear-receptor-dependent phosphatidylcholine pathway with antidiabetic effects. Nature *474*, 506–510.

Lee, K.-M., Seo, H.-Y., Kim, M., Min, A.-K., Ryu, S.Y., Kim, Y.-N., Park, Y.J., Choi, H.-S., Lee, K., Park, W.J., et al. (2009b). Orphan nuclear receptor small heterodimer partner inhibits angiotensin II-stimulated PAI-1 expression in vascular smooth muscle cells. Exp. Mol. Med. *42*, 21–29.

Lee, Y.-K., Parker, K.L., Choi, H.-S., and Moore, D.D. (1999). Activation of the Promoter of the Orphan Receptor SHP by Orphan Receptors That Bind DNA as Monomers. J. Biol. Chem. *274*, 20869–20873.

Lee, Y.-K., Choi, Y.-H., Chua, S., Park, Y.J., and Moore, D.D. (2006). Phosphorylation of the Hinge Domain of the Nuclear Hormone Receptor LRH-1 Stimulates Transactivation. J. Biol. Chem. *281*, 7850–7855.

Lee, Y.-K., Schmidt, D.R., Cummins, C.L., Choi, M., Peng, L., Zhang, Y., Goodwin, B., Hammer, R.E., Mangelsdorf, D.J., and Kliewer, S.A. (2008b). Liver Receptor Homolog-1 Regulates Bile Acid Homeostasis but Is Not Essential for Feedback Regulation of Bile Acid Synthesis. Mol. Endocrinol. *22*, 1345–1356.

Lee, Y.-S., Chanda, D., Sim, J., Park, Y.-Y., and Choi, H.-S. (2007). Structure and function of the atypical orphan nuclear receptor small heterodimer partner. Int. Rev. Cytol. *261*, 117–158.

Lefèvre, L., Authier, H., Stein, S., Majorel, C., Couderc, B., Dardenne, C., Eddine, M.A., Meunier, E., Bernad, J., Valentin, A., et al. (2015). LRH-1 mediates anti-inflammatory and antifungal phenotype of IL-13-activated macrophages through the PPARγ ligand synthesis. Nat. Commun. *6*.

Lengauer, C., Kinzler, K.W., and Vogelstein, B. (1997). Genetic instability in colorectal cancers. Nature *386*, 623–627.

Leppkes, M., Roulis, M., Neurath, M.F., Kollias, G., and Becker, C. (2014). Pleiotropic functions of TNF-α in the regulation of the intestinal epithelial response to inflammation. Int. Immunol. *26*, 509–515.

Levin, B. (1992). Inflammatory bowel disease and colon cancer. Cancer *70*, 1313–1316.

Li, M., Xie, Y.-H., Kong, Y.-Y., Wu, X., Zhu, L., and Wang, Y. (1998). Cloning and Characterization of a Novel Human Hepatocyte Transcription Factor, hB1F, Which Binds and Activates Enhancer II of Hepatitis B Virus. J. Biol. Chem. *273*, 29022–29031.

Li, Y., Choi, M., Suino, K., Kovach, A., Daugherty, J., Kliewer, S.A., and Xu, H.E. (2005). Structural and biochemical basis for selective repression of the orphan nuclear receptor liver receptor homolog 1 by small heterodimer partner. Proc. Natl. Acad. Sci. U. S. A. *102*, 9505–9510.

Liberman, A.C., Budziñski, M.L., Sokn, C., Gobbini, R.P., Steininger, A., and Arzt, E. (2018). Regulatory and Mechanistic Actions of Glucocorticoids on T and Inflammatory Cells. Front. Endocrinol. *9*, 235.

Liu, X., Ory, V., Chapman, S., Yuan, H., Albanese, C., Kallakury, B., Timofeeva, O.A., Nealon, C., Dakic, A., Simic, V., et al. (2012). ROCK inhibitor and feeder cells induce the conditional reprogramming of epithelial cells. Am. J. Pathol. *180*, 599–607.

Liyanage, C.K., Galappatthy, P., and Seneviratne, S.L. (2017). Corticosteroids in management of anaphylaxis; a systematic review of evidence. Eur. Ann. Allergy Clin. Immunol. *49*, 196–207.

Lu, L., Li, T., Williams, G., Petit, E., Borowsky, M., and Walker, W.A. (2011). Hydrocortisone induces changes in gene expression and differentiation in immature human enterocytes. Am. J. Physiol. Gastrointest. Liver Physiol. *300*, G425-432.

Lu, T.T., Makishima, M., Repa, J.J., Schoonjans, K., Kerr, T.A., Auwerx, J., and Mangelsdorf, D.J. (2000). Molecular basis for feedback regulation of bile acid synthesis by nuclear receptors. Mol. Cell *6*, 507–515.

Lynch, H.T., and de la Chapelle, A. (2003). Hereditary Colorectal Cancer. N. Engl. J. Med. *348*, 919–932.

Marchand, L.L., Wilkens, L.R., Kolonel, L.N., Hankin, J.H., and Lyu, L.-C. (1997). Associations of Sedentary Lifestyle, Obesity, Smoking, Alcohol Use, and Diabetes with the Risk of Colorectal Cancer. Cancer Res. *57*, 4787–4794.

Marini, M., Bamias, G., Rivera-Nieves, J., Moskaluk, C.A., Hoang, S.B., Ross, W.G., Pizarro, T.T., and Cominelli, F. (2003). TNF-alpha neutralization ameliorates the severity of murine Crohn's-like ileitis by abrogation of intestinal epithelial cell apoptosis. Proc. Natl. Acad. Sci. U. S. A. *100*, 8366–8371.

Markowitz, S., Wang, J., Myeroff, L., Parsons, R., Sun, L., Lutterbaugh, J., Fan, R.S., Zborowska, E., Kinzler, K.W., Vogelstein, B., et al. (1995). Inactivation of the type II TGF-beta receptor in colon cancer cells with microsatellite instability. Science *268*, 1336–1338.

Mármol, I., Sánchez-de-Diego, C., Pradilla Dieste, A., Cerrada, E., and Rodriguez Yoldi, M.J. (2017). Colorectal Carcinoma: A General Overview and Future Perspectives in Colorectal Cancer. Int. J. Mol. Sci. *18*, 197.

McCart, A.E., Vickaryous, N.K., and Silver, A. (2008). Apc mice: Models, modifiers and mutants. Pathol. - Res. Pract. *204*, 479–490.

McEwan, I.J., Wright, A.P., and Gustafsson, J.A. (1997). Mechanism of gene expression by the glucocorticoid receptor: role of protein-protein interactions. BioEssays News Rev. Mol. Cell. Dev. Biol. *19*, 153–160.

McGuckin, M.A., Eri, R., Simms, L.A., Florin, T.H.J., and Radford-Smith, G. (2009). Intestinal barrier dysfunction in inflammatory bowel diseases. Inflamm. Bowel Dis. *15*, 100–113.

Meira, L.B., Bugni, J.M., Green, S.L., Lee, C.-W., Pang, B., Borenshtein, D., Rickman, B.H., Rogers, A.B., Moroski-Erkul, C.A., McFaline, J.L., et al. (2008). DNA damage induced by chronic inflammation contributes to colon carcinogenesis in mice. J. Clin. Invest. *118*, 2516–2525.

Melo, F. de S. e, Kurtova, A.V., Harnoss, J.M., Kljavin, N., Hoeck, J.D., Hung, J., Anderson, J.E., Storm, E.E., Modrusan, Z., Koeppen, H., et al. (2017). A distinct role for Lgr5+ stem cells in primary and metastatic colon cancer. Nature *543*, 676–680.

Miller, W.L. (2008). Steroidogenic Enzymes. In Endocrine Development, C.E. Flück, and W.L. Miller, eds. (Basel: KARGER), pp. 1–18.

Mittelstadt, P.R., Taves, M.D., and Ashwell, J.D. (2018). Cutting Edge: De Novo Glucocorticoid Synthesis by Thymic Epithelial Cells Regulates Antigen-Specific Thymocyte Selection. J. Immunol. *200*, 1988–1994.

Modica, S., Gofflot, F., Murzilli, S., D'Orazio, A., Salvatore, L., Pellegrini, F., Nicolucci, A., Tognoni, G., Copetti, M., Valanzano, R., et al. (2010). The intestinal nuclear receptor signature with epithelial localization patterns and expression modulation in tumors. Gastroenterology *138*, 636–648, 648.e1-12.

Mueller, M., Cima, I., Noti, M., Fuhrer, A., Jakob, S., Dubuquoy, L., Schoonjans, K., and Brunner, T. (2006). The nuclear receptor LRH-1 critically regulates extra-adrenal glucocorticoid synthesis in the intestine. J. Exp. Med. *203*, 2057–2062.

Mueller, M., Atanasov, A., Cima, I., Corazza, N., Schoonjans, K., and Brunner, T. (2007). Differential Regulation of Glucocorticoid Synthesis in Murine Intestinal Epithelial Versus Adrenocortical Cell Lines. Endocrinology *148*, 1445–1453.

Mukherji, A., Kobiita, A., Ye, T., and Chambon, P. (2013). Homeostasis in Intestinal Epithelium Is Orchestrated by the Circadian Clock and Microbiota Cues Transduced by TLRs. Cell *153*, 812–827.

Musille, P.M., Pathak, M., Lauer, J.L., Hudson, W.H., Griffin, P.R., and Ortlund, E.A. (2012). Antidiabetic Phospholipid – Nuclear Receptor Complex Reveals the Mechanism for Phospholipid Driven Gene Regulation. Nat. Struct. Mol. Biol. *19*, 532-S2.

Nadolny, C., and Dong, X. (2015). Liver receptor homolog-1 (LRH-1): a potential therapeutic target for cancer. Cancer Biol. Ther. *16*, 997–1004.

Nagamine, C.M., Rogers, A.B., Fox, J.G., and Schauer, D.B. (2008). Helicobacter hepaticus promotes azoxymethane-initiated colon tumorigenesis in BALB/c-IL10-deficient mice. Int. J. Cancer *122*, 832–838.

Neufert, C., Becker, C., and Neurath, M.F. (2007). An inducible mouse model of colon carcinogenesis for the analysis of sporadic and inflammation-driven tumor progression. Nat. Protoc. *2*, 1998–2004.

Ng, K., Meyerhardt, J.A., Chan, A.T., Sato, K., Chan, J.A., Niedzwiecki, D., Saltz, L.B., Mayer, R.J., Benson, A.B., Schaefer, P.L., et al. (2015). Aspirin and COX-2 inhibitor use in patients with stage III colon cancer. J. Natl. Cancer Inst. *107*, 345.

Nicolaides, N.C., Pavlaki, A.N., Maria Alexandra, M.A., and Chrousos, G.P. (2000). Glucocorticoid Therapy and Adrenal Suppression. In Endotext, L.J. De Groot, G. Chrousos, K.

Dungan, K.R. Feingold, A. Grossman, J.M. Hershman, C. Koch, M. Korbonits, R. McLachlan, M. New, et al., eds. (South Dartmouth (MA): MDText.com, Inc.), p.

Nicolaides, N.C., Charmandari, E., Kino, T., and Chrousos, G.P. (2017). Stress-Related and Circadian Secretion and Target Tissue Actions of Glucocorticoids: Impact on Health. Front. Endocrinol. *8*.

Nikolakis, G., and Zouboulis, C.C. (2014). Skin and glucocorticoids: effects of local skin glucocorticoid impairment on skin homeostasis. Exp. Dermatol. *23*, 807–808.

Nishigori, H., Tomura, H., Tonooka, N., Kanamori, M., Yamada, S., Sho, K., Inoue, I., Kikuchi, N., Onigata, K., Kojima, I., et al. (2001). Mutations in the small heterodimer partner gene are associated with mild obesity in Japanese subjects. Proc. Natl. Acad. Sci. U. S. A. *98*, 575–580.

Nishizawa, H., Yamagata, K., Shimomura, I., Takahashi, M., Kuriyama, H., Kishida, K., Hotta, K., Nagaretani, H., Maeda, N., Matsuda, M., et al. (2002). Small heterodimer partner, an orphan nuclear receptor, augments peroxisome proliferator-activated receptor gamma transactivation. J. Biol. Chem. *277*, 1586–1592.

Nitta, M., Ku, S., Brown, C., Okamoto, A.Y., and Shan, B. (1999). CPF: An orphan nuclear receptor that regulates liver-specific expression of the human cholesterol 7α-hydroxylase gene. Proc. Natl. Acad. Sci. U. S. A. *96*, 6660–6665.

Noti, M., Sidler, D., and Brunner, T. (2009). Extra-adrenal glucocorticoid synthesis in the intestinal epithelium: more than a drop in the ocean? Semin. Immunopathol. *31*, 237–248.

Noti, M., Corazza, N., Mueller, C., Berger, B., and Brunner, T. (2010a). TNF suppresses acute intestinal inflammation by inducing local glucocorticoid synthesis. J. Exp. Med. *207*, 1057–1066.

Noti, M., Corazza, N., Tuffin, G., Schoonjans, K., and Brunner, T. (2010b). Lipopolysaccharide induces intestinal glucocorticoid synthesis in a TNFalpha-dependent manner. FASEB J. Off. Publ. Fed. Am. Soc. Exp. Biol. *24*, 1340–1346.

Nusse, R., and Clevers, H. (2017). Wnt/β-Catenin Signaling, Disease, and Emerging Therapeutic Modalities. Cell *169*, 985–999.

Oakley, R.H., and Cidlowski, J.A. (2013). The Biology of the Glucocorticoid Receptor: New Signaling Mechanisms in Health and Disease. J. Allergy Clin. Immunol. *132*, 1033.

Okayasu, I., Hatakeyama, S., Yamada, M., Ohkusa, T., Inagaki, Y., and Nakaya, R. (1990). A novel method in the induction of reliable experimental acute and chronic ulcerative colitis in mice. Gastroenterology *98*, 694–702.

O'Rourke, K.P., Ackerman, S., Dow, L.E., and Lowe, S.W. (2016). Isolation, Culture, and Maintenance of Mouse Intestinal Stem Cells. Bio-Protoc. *6*.

O'Rourke, K.P., Loizou, E., Livshits, G., Schatoff, E.M., Baslan, T., Manchado, E., Simon, J., Romesser, P.B., Leach, B., Han, T., et al. (2017). Transplantation of engineered organoids enables rapid generation of metastatic mouse models of colorectal cancer. Nat. Biotechnol. *35*, 577–582.

Ortlund, E.A., Lee, Y., Solomon, I.H., Hager, J.M., Safi, R., Choi, Y., Guan, Z., Tripathy, A., Raetz, C.R.H., McDonnell, D.P., et al. (2005). Modulation of human nuclear receptor LRH-1 activity by phospholipids and SHP. Nat. Struct. Mol. Biol. *12*, 357–363.

Pabla, B., Bissonnette, M., and Konda, V.J. (2015). Colon cancer and the epidermal growth factor receptor: Current treatment paradigms, the importance of diet, and the role of chemoprevention. World J. Clin. Oncol. *6*, 133–141.

Pagès, F., Berger, A., Camus, M., Sanchez-Cabo, F., Costes, A., Molidor, R., Mlecnik, B., Kirilovsky, A., Nilsson, M., Damotte, D., et al. (2005). Effector Memory T Cells, Early Metastasis, and Survival in Colorectal Cancer. N. Engl. J. Med. *353*, 2654–2666.

Paré, J.-F., Malenfant, D., Courtemanche, C., Jacob-Wagner, M., Roy, S., Allard, D., and Bélanger, L. (2004). The Fetoprotein Transcription Factor (FTF) Gene Is Essential to Embryogenesis and Cholesterol Homeostasis and Is Regulated by a DR4 Element. J. Biol. Chem. *279*, 21206–21216.

Pasparakis, M. (2012). Role of NF-κB in epithelial biology. Immunol. Rev. *246*, 346–358.

Passardi, A., Canale, M., Valgiusti, M., and Ulivi, P. (2017). Immune Checkpoints as a Target for Colorectal Cancer Treatment. Int. J. Mol. Sci. *18*.

Peterson, L.W., and Artis, D. (2014). Intestinal epithelial cells: regulators of barrier function and immune homeostasis. Nat. Rev. Immunol. *14*, 141–153.

Philip, M., Rowley, D.A., and Schreiber, H. (2004). Inflammation as a tumor promoter in cancer induction. Semin. Cancer Biol. *14*, 433–439.

Pinto, D., Gregorieff, A., Begthel, H., and Clevers, H. (2003). Canonical Wnt signals are essential for homeostasis of the intestinal epithelium. Genes Dev. *17*, 1709–1713.

Popivanova, B.K., Kitamura, K., Wu, Y., Kondo, T., Kagaya, T., Kaneko, S., Oshima, M., Fujii, C., and Mukaida, N. (2008). Blocking TNF-α in mice reduces colorectal carcinogenesis associated with chronic colitis. J. Clin. Invest.

Powell, S.M., Zilz, N., Beazer-Barclay, Y., Bryan, T.M., Hamilton, S.R., Thibodeau, S.N., Vogelstein, B., and Kinzler, K.W. (1992). APC mutations occur early during colorectal tumorigenesis. Nature *359*, 235–237.

Powell, S.M., Petersen, G.M., Krush, A.J., Booker, S., Jen, J., Giardiello, F.M., Hamilton, S.R., Vogelstein, B., and Kinzler, K.W. (1993). Molecular Diagnosis of Familial Adenomatous Polyposis. N. Engl. J. Med. *329*, 1982–1987.

Powrie, F. (1995). T cells in inflammatory bowel disease: protective and pathogenic roles. Immunity *3*, 171–174.

Pratt, W.B., and Toft, D.O. (1997). Steroid receptor interactions with heat shock protein and immunophilin chaperones. Endocr. Rev. *18*, 306–360.

Prestin, K., Olbert, M., Hussner, J., Isenegger, T.L., Gliesche, D.G., Böttcher, K., Zimmermann, U., and Meyer Zu Schwabedissen, H.E. (2016). Modulation of expression of the nuclear receptor NR0B2 (small heterodimer partner 1) and its impact on proliferation of renal carcinoma cells. OncoTargets Ther. *9*, 4867–4878.

Qian, B.-Z., and Pollard, J.W. (2010). Macrophage Diversity Enhances Tumor Progression and Metastasis. Cell *141*, 39–51.

Qian, J., Steigerwald, K., Combs, K.A., Barton, M.C., and Groden, J. (2007). Caspase cleavage of the APC tumor suppressor and release of an amino-terminal domain is required for the transcription-independent function of APC in apoptosis. Oncogene *26*, 4872–4876.

Qu, R., Hao, S., Jin, X., Shi, G., Yu, Q., Tong, X., and Guo, D. (2018). MicroRNA-374b reduces the proliferation and invasion of colon cancer cells by regulation of LRH-1/Wnt signaling. Gene *642*, 354–361.

Raddatz, D., Middel, P., Bockemühl, M., Benöhr, P., Wissmann, C., Schwörer, H., and Ramadori, G. (2004). Glucocorticoid receptor expression in inflammatory bowel disease: evidence for a mucosal down-regulation in steroid-unresponsive ulcerative colitis. Aliment. Pharmacol. Ther. *19*, 47–61.

Rakoff-Nahoum, S., Paglino, J., Eslami-Varzaneh, F., Edberg, S., and Medzhitov, R. (2004). Recognition of commensal microflora by toll-like receptors is required for intestinal homeostasis. Cell *118*, 229–241.

Ramírez, F., Fowell, D.J., Puklavec, M., Simmonds, S., and Mason, D. (1996). Glucocorticoids promote a TH2 cytokine response by CD4+ T cells in vitro. J. Immunol. *156*, 2406–2412.

Rawlings, J.S., Rosler, K.M., and Harrison, D.A. (2004). The JAK/STAT signaling pathway. J. Cell Sci. *117*, 1281–1283.

Reichardt, H.M., and Schütz, G. (1998). Glucocorticoid signalling—multiple variations of a common theme. Mol. Cell. Endocrinol. *146*, 1–6.

Rhen, T., and Cidlowski, J.A. (2005). Antiinflammatory Action of Glucocorticoids — New Mechanisms for Old Drugs. N. Engl. J. Med. *353*, 1711–1723.

Robertis, M.D., Massi, E., Poeta, M.L., Carotti, S., Morini, S., Cecchetelli, L., Signori, E., and Fazio, V.M. (2011). The AOM/DSS murine model for the study of colon carcinogenesis: From pathways to diagnosis and therapy studies. J. Carcinog. *10*.

Roda, G., Sartini, A., Zambon, E., Calafiore, A., Marocchi, M., Caponi, A., Belluzzi, A., and Roda, E. (2010). Intestinal epithelial cells in inflammatory bowel diseases. World J. Gastroenterol. WJG *16*, 4264–4271.

Roper, J., Tammela, T., Cetinbas, N.M., Akkad, A., Roghanian, A., Rickelt, S., Almeqdadi, M., Wu, K., Oberli, M.A., Sánchez-Rivera, F.J., et al. (2017). In vivo genome editing and organoid transplantation models of colorectal cancer and metastasis. Nat. Biotechnol. *35*, 569–576.

Rosenberg, D.W., Giardina, C., and Tanaka, T. (2009). Mouse models for the study of colon carcinogenesis. Carcinogenesis *30*, 183–196.

Rosenfeld, M.G., Lunyak, V.V., and Glass, C.K. (2006). Sensors and signals: a coactivator/corepressor/epigenetic code for integrating signal-dependent programs of transcriptional response. Genes Dev. *20*, 1405–1428.

Roulis, M., Armaka, M., Manoloukos, M., Apostolaki, M., and Kollias, G. (2011). Intestinal epithelial cells as producers but not targets of chronic TNF suffice to cause murine Crohn-like pathology. Proc. Natl. Acad. Sci. U. S. A. *108*, 5396–5401.

Rowan, A.J., Lamlum, H., Ilyas, M., Wheeler, J., Straub, J., Papadopoulou, A., Bicknell, D., Bodmer, W.F., and Tomlinson, I.P.M. (2000). APC mutations in sporadic colorectal tumors: A mutational “hotspot” and interdependence of the “two hits.” Proc. Natl. Acad. Sci. U. S. A. *97*, 3352–3357.

Rustgi, A.K. (2007). The genetics of hereditary colon cancer. Genes Dev. *21*, 2525–2538.

Salim, S.Y., and Söderholm, J.D. (2011). Importance of disrupted intestinal barrier in inflammatory bowel diseases. Inflamm. Bowel Dis. *17*, 362–381.

Sampath-Kumar, R., Yu, M., Khalil, M.W., and Yang, K. (1997). Metyrapone is a competitive inhibitor of 11beta-hydroxysteroid dehydrogenase type 1 reductase. J. Steroid Biochem. Mol. Biol. *62*, 195–199.

Sandler, R.S., Halabi, S., Baron, J.A., Budinger, S., Paskett, E., Keresztes, R., Petrelli, N., Pipas, J.M., Karp, D.D., Loprinzi, C.L., et al. (2003). A Randomized Trial of Aspirin to Prevent Colorectal Adenomas in Patients with Previous Colorectal Cancer. N. Engl. J. Med. *348*, 883–890.

Sato, T., and Clevers, H. (2013). Growing self-organizing mini-guts from a single intestinal stem cell: mechanism and applications. Science *340*, 1190–1194.

Sato, T., Vries, R.G., Snippert, H.J., van de Wetering, M., Barker, N., Stange, D.E., van Es, J.H., Abo, A., Kujala, P., Peters, P.J., et al. (2009). Single Lgr5 stem cells build crypt–villus structures in vitro without a mesenchymal niche. Nature *459*, 262–265.

Sato, T., van Es, J.H., Snippert, H.J., Stange, D.E., Vries, R.G., van den Born, M., Barker, N., Shroyer, N.F., van de Wetering, M., and Clevers, H. (2011a). Paneth cells constitute the niche for Lgr5 stem cells in intestinal crypts. Nature *469*, 415–418.

Sato, T., Stange, D.E., Ferrante, M., Vries, R.G.J., Van Es, J.H., Van den Brink, S., Van Houdt, W.J., Pronk, A., Van Gorp, J., Siersema, P.D., et al. (2011b). Long-term expansion of epithelial organoids from human colon, adenoma, adenocarcinoma, and Barrett's epithelium. Gastroenterology *141*, 1762–1772.

Schimmer, B.P., and White, P.C. (2010). Minireview: steroidogenic factor 1: its roles in differentiation, development, and disease. Mol. Endocrinol. Baltim. Md *24*, 1322–1337.

Schlüter, C., Duchrow, M., Wohlenberg, C., Becker, M.H., Key, G., Flad, H.D., and Gerdes, J. (1993). The cell proliferation-associated antigen of antibody Ki-67: a very large, ubiquitous nuclear protein with numerous repeated elements, representing a new kind of cell cycle-maintaining proteins. J. Cell Biol. *123*, 513–522.

Schmittgen, T.D., and Livak, K.J. (2008). Analyzing real-time PCR data by the comparative C_T method. Nat. Protoc. *3*, 1101–1108.

Schonthaler, H.B., Guinea-Viniegra, J., and Wagner, E.F. (2011). Targeting inflammation by modulating the Jun/AP-1 pathway. Ann. Rheum. Dis. *70 Suppl 1*, i109-112.

Schoonjans, K., Dubuquoy, L., Mebis, J., Fayard, E., Wendling, O., Haby, C., Geboes, K., and Auwerx, J. (2005). Liver receptor homolog 1 contributes to intestinal tumor formation through effects on cell cycle and inflammation. Proc. Natl. Acad. Sci. U. S. A. *102*, 2058–2062.

Schwaderer, J., Gaiser, A.-K., Phan, T.S., Delgado, Me., and Brunner, T. (2017). Liver receptor homolog-1 (NR5a2) regulates CD95/Fas ligand transcription and associated T-cell effector functions. Cell Death Dis. *8*, e2745.

Schwitalla, S., Ziegler, P.K., Horst, D., Becker, V., Kerle, I., Begus-Nahrmann, Y., Lechel, A., Rudolph, K.L., Langer, R., Slotta-Huspenina, J., et al. (2013). Loss of p53 in enterocytes generates an inflammatory microenvironment enabling invasion and lymph node metastasis of carcinogen-induced colorectal tumors. Cancer Cell *23*, 93–106.

Seol, W., Choi, H.S., and Moore, D.D. (1996). An orphan nuclear hormone receptor that lacks a DNA binding domain and heterodimerizes with other receptors. Science *272*, 1336–1339.

Shaked, H., Hofseth, L.J., Chumanevich, A., Chumanevich, A.A., Wang, J., Wang, Y., Taniguchi, K., Guma, M., Shenouda, S., Clevers, H., et al. (2012). Chronic epithelial NF-κB activation

accelerates APC loss and intestinal tumor initiation through iNOS up-regulation. Proc. Natl. Acad. Sci. U. S. A. *109*, 14007–14012.

Shaw, K.A., Cutler, D.J., Okou, D., Dodd, A., Aronow, B.J., Haberman, Y., Stevens, C., Walters, T.D., Griffiths, A., Baldassano, R.N., et al. (2018). Genetic variants and pathways implicated in a pediatric inflammatory bowel disease cohort. Genes Immun. 1–12.

Sica, A., Allavena, P., and Mantovani, A. (2008a). Cancer related inflammation: The macrophage connection. Cancer Lett. *267*, 204–215.

Sica, A., Larghi, P., Mancino, A., Rubino, L., Porta, C., Totaro, M.G., Rimoldi, M., Biswas, S.K., Allavena, P., and Mantovani, A. (2008b). Macrophage polarization in tumour progression. Semin. Cancer Biol. *18*, 349–355.

Sidler, D., Renzulli, P., Schnoz, C., Berger, B., Schneider-Jakob, S., Flück, C., Inderbitzin, D., Corazza, N., Candinas, D., and Brunner, T. (2011). Colon cancer cells produce immunoregulatory glucocorticoids. Oncogene *30*, 2411–2419.

Sikora, K., Chan, S., Evan, G., Gabra, H., Markham, N., Stewart, J., and Watson, J. (1987). c-myc oncogene expression in colorectal cancer. Cancer *59*, 1289–1295.

Sirianni, R., Seely, J.B., Attia, G., Stocco, D.M., Carr, B.R., Pezzi, V., and Rainey, W.E. (2002). Liver receptor homologue-1 is expressed in human steroidogenic tissues and activates transcription of genes encoding steroidogenic enzymes. J. Endocrinol. *174*.

Slominski, A., Zbytek, B., Nikolakis, G., Manna, P.R., Skobowiat, C., Zmijewski, M., Li, W., Janjetovic, Z., Postlethwaite, A., Zouboulis, C.C., et al. (2013). Steroidogenesis in the skin: implications for local immune functions. J. Steroid Biochem. Mol. Biol. *137*, 107–123.

Smith, A.J., Stern, H.S., Penner, M., Hay, K., Mitri, A., Bapat, B.V., and Gallinger, S. (1994). Somatic APC and K-ras Codon 12 Mutations in Aberrant Crypt Foci from Human Colons. Cancer Res. *54*, 5527–5530.

Smith, G., Carey, F.A., Beattie, J., Wilkie, M.J.V., Lightfoot, T.J., Coxhead, J., Garner, R.C., Steele, R.J.C., and Wolf, C.R. (2002). Mutations in APC, Kirsten-ras, and p53—alternative genetic pathways to colorectal cancer. Proc. Natl. Acad. Sci. *99*, 9433–9438.

Smyth, M.J., Dunn, G.P., and Schreiber, R.D. (2006). Cancer Immunosurveillance and Immunoediting: The Roles of Immunity in Suppressing Tumor Development and Shaping Tumor Immunogenicity. In Advances in Immunology, (Academic Press), pp. 1–50.

Sohn, O.S., Fiala, E.S., Requeijo, S.P., Weisburger, J.H., and Gonzalez, F.J. (2001). Differential effects of CYP2E1 status on the metabolic activation of the colon carcinogens azoxymethane and methylazoxymethanol. Cancer Res. *61*, 8435–8440.

Sonoda, J., Pei, L., and Evans, R.M. (2008). Nuclear Receptors: Decoding Metabolic Disease. FEBS Lett. *582*, 2–9.

Souza, P.R. de, Sales-Campos, H., Basso, P.J., Nardini, V., Silva, A., Banquieri, F., Alves, V.B.F., Chica, J.E.L., Nomizo, A., and Cardoso, C.R. de B. (2016). Adrenal-Derived Hormones Differentially Modulate Intestinal Immunity in Experimental Colitis.

Spit, M., Koo, B.-K., and Maurice, M.M. (2018). Tales from the crypt: intestinal niche signals in tissue renewal, plasticity and cancer. Open Biol. *8*.

Steigerwald, K., Behbehani, G.K., Combs, K.A., Barton, M.C., and Groden, J. (2005). The APC Tumor Suppressor Promotes Transcription-Independent Apoptosis In vitro11NIH CA 63517 (J. Groden) and CA 53683 (M.C. Barton) and Albert J. Ryan Foundation (K. Steigerwald). Mol. Cancer Res. *3*, 78–89.

Sun, Y., Liu, W.-Z., Liu, T., Feng, X., Yang, N., and Zhou, H.-F. (2015). Signaling pathway of MAPK/ERK in cell proliferation, differentiation, migration, senescence and apoptosis. J. Recept. Signal Transduct. *35*, 600–604.

Suzuki, R. (2005). Strain differences in the susceptibility to azoxymethane and dextran sodium sulfate-induced colon carcinogenesis in mice. Carcinogenesis *27*, 162–169.

Takeda, Y., Miyamori, I., Yoneda, T., Iki, K., Hatakeyama, H., Blair, I.A., Hsieh, F.Y., and Takeda, R. (1994). Synthesis of corticosterone in the vascular wall. Endocrinology *135*, 2283–2286.

Talabér, G., Jondal, M., and Okret, S. (2013). Extra-adrenal glucocorticoid synthesis: Immune regulation and aspects on local organ homeostasis. Mol. Cell. Endocrinol. *380*, 89–98.

Tanaka, T., Kohno, H., Suzuki, R., Yamada, Y., Sugie, S., and Mori, H. (2003). A novel inflammation-related mouse colon carcinogenesis model induced by azoxymethane and dextran sodium sulfate. Cancer Sci. *94*, 965–973.

Taves, M.D., Gomez-Sanchez, C.E., and Soma, K.K. (2011). Extra-adrenal glucocorticoids and mineralocorticoids: evidence for local synthesis, regulation, and function. AJP Endocrinol. Metab. *301*, E11–E24.

Tetsu, O., and McCormick, F. (1999). Beta-catenin regulates expression of cyclin D1 in colon carcinoma cells. Nature *398*, 422–426.

Thiruchelvam, P.T.R., Lai, C.-F., Hua, H., Thomas, R.S., Hurtado, A., Hudson, W., Bayly, A.R., Kyle, F.J., Periyasamy, M., Photiou, A., et al. (2011). The liver receptor homolog-1 regulates estrogen receptor expression in breast cancer cells. Breast Cancer Res. Treat. *127*, 385–396.

Tian, H., Biehs, B., Warming, S., Leong, K.G., Rangell, L., Klein, O.D., and de Sauvage, F.J. (2011). A reserve stem cell population in small intestine renders Lgr5-positive cells dispensable. Nature *478*, 255–259.

Tong, Y., Yang, W., and Koeffler, H.P. (2011). Mouse models of colorectal cancer. Chin. J. Cancer *30*, 450–462.

Tosolini, M., Kirilovsky, A., Mlecnik, B., Fredriksen, T., Mauger, S., Bindea, G., Berger, A., Bruneval, P., Fridman, W.-H., Pagès, F., et al. (2011). Clinical impact of different classes of infiltrating T cytotoxic and helper cells (Th1, th2, treg, th17) in patients with colorectal cancer. Cancer Res. *71*, 1263–1271.

Turner, J.R. (2009). Intestinal mucosal barrier function in health and disease. Nat. Rev. Immunol. *9*, 799–809.

Ugor, E., Prenek, L., Pap, R., Berta, G., Ernszt, D., Najbauer, J., Németh, P., Boldizsár, F., and Berki, T. (2018). Glucocorticoid hormone treatment enhances the cytokine production of regulatory T cells by upregulation of Foxp3 expression. Immunobiology *223*, 422–431.

Vacchio, M.S., Papadopoulos, V., and Ashwell, J.D. (1994). Steroid production in the thymus: implications for thymocyte selection. J. Exp. Med. *179*, 1835–1846.

Vandevyver, S., Dejager, L., Tuckermann, J., and Libert, C. (2013). New Insights into the Anti-inflammatory Mechanisms of Glucocorticoids: An Emerging Role for Glucocorticoid-Receptor-Mediated Transactivation. Endocrinology *154*, 993–1007.

Vandewalle, J., Luypaert, A., Bosscher, K.D., and Libert, C. (2018). Therapeutic Mechanisms of Glucocorticoids. Trends Endocrinol. Metab. *29*, 42–54.

Vatandoust, S., Price, T.J., and Karapetis, C.S. (2015). Colorectal cancer: Metastases to a single organ. World J. Gastroenterol. *21*, 11767–11776.

Viennois, E., Chen, F., Laroui, H., Baker, M.T., and Merlin, D. (2013). Dextran sodium sulfate inhibits the activities of both polymerase and reverse transcriptase: lithium chloride purification, a rapid and efficient technique to purify RNA. BMC Res. Notes *6*, 360.

Vinay, D.S., Ryan, E.P., Pawelec, G., Talib, W.H., Stagg, J., Elkord, E., Lichtor, T., Decker, W.K., Whelan, R.L., Kumara, H.M.C.S., et al. (2015). Immune evasion in cancer: Mechanistic basis and therapeutic strategies. Semin. Cancer Biol. *35*, S185–S198.

Volle, D.H., Duggavathi, R., Magnier, B.C., Houten, S.M., Cummins, C.L., Lobaccaro, J.-M.A., Verhoeven, G., Schoonjans, K., and Auwerx, J. (2007). The small heterodimer partner is a gonadal gatekeeper of sexual maturation in male mice. Genes Dev. *21*, 303–315.

Waddell, W.R., Ganser, G.F., Cerise, E.J., and Loughry, R.W. (1989). Sulindac for polyposis of the colon. Am. J. Surg. *157*, 175–179.

Waldner, M.J., and Neurath, M.F. (2014). Mechanisms of Immune Signaling in Colitis-Associated Cancer. Cell. Mol. Gastroenterol. Hepatol. *1*, 6–16.

Walter, J., and Ley, R. (2011). The human gut microbiome: ecology and recent evolutionary changes. Annu. Rev. Microbiol. *65*, 411–429.

Wang, S., Liu, Z., Wang, L., and Zhang, X. (2009a). NF-kappaB signaling pathway, inflammation and colorectal cancer. Cell. Mol. Immunol. *6*, 327–334.

Wang, S.-L., Zheng, D.-Z., Lan, F.-H., Deng, X.-J., Zeng, J., Li, C.-J., Wang, R., and Zhu, Z.-Y. (2008). Increased expression of hLRH-1 in human gastric cancer and its implication in tumorigenesis. Mol. Cell. Biochem. *308*, 93–100.

Wang, X., Ellis, J., Pennisi, D.J., Song, X., Batra, J., Hollis, K., Bradbury, L., Li, Z., Kenna, T., and Brown, M.A. (2017). Transcriptome Analysis of Ankylosing Spondylitis Patients Before and After TNF-α Inhibitor Therapy Reveals the Pathways Affected. Genes Immun.

Wang, Z., Zang, C., Cui, K., Schones, D.E., Barski, A., Peng, W., and Zhao, K. (2009b). Genome-wide mapping of HATs and HDACs reveals distinct functions in active and inactive genes. Cell *138*, 1019–1031.

Watson, P.J., Fairall, L., and Schwabe, J.W.R. (2012). Nuclear hormone receptor co-repressors: structure and function. Mol. Cell. Endocrinol. *348*, 440–449.

Wells, A. (1999). EGF receptor. Int. J. Biochem. Cell Biol. *31*, 637–643.

Williams, C.S., Shattuck-Brandt, R.L., and DuBois, R.N. (1999). The role of COX-2 in intestinal cancer. Expert Opin. Investig. Drugs *8*, 1–12.

Woltman, A.M., de Fijter, J.W., Kamerling, S.W., Paul, L.C., Daha, M.R., and van Kooten, C. (2000). The effect of calcineurin inhibitors and corticosteroids on the differentiation of human dendritic cells. Eur. J. Immunol. *30*, 1807–1812.

Wong, V.W.Y., Stange, D.E., Page, M.E., Buczacki, S., Wabik, A., Itami, S., van de Wetering, M., Poulsom, R., Wright, N.A., Trotter, M.W.B., et al. (2012). Lrig1 controls intestinal stem-cell homeostasis by negative regulation of ErbB signalling. Nat. Cell Biol. *14*, 401–408.

Wu, C., Feng, J., Li, L., Wu, Y., Xie, H., Yin, Y., Ye, J., and Li, Z. (2018). Liver receptor homologue 1, a novel prognostic marker in colon cancer patients. Oncol. Lett. *16*, 2833–2838.

Xiao, L., Wang, Y., Xu, K., Hu, H., Xu, Z., Wu, D., Wang, Z., You, W., Ng, C.-F., Yu, S., et al. (2018). Nuclear receptor LRH-1 functions to promote castration-resistant growth of prostate cancer via its promotion of intratumoral androgen biosynthesis. Cancer Res. canres.2341.2017.

Xie, B.-Y., and Wu, A.-W. (2016). Organoid Culture of Isolated Cells from Patient-derived Tissues with Colorectal Cancer. Chin. Med. J. (Engl.) *129*, 2469–2475.

Xue, X., and Shah, Y.M. (2013). In vitro Organoid Culture of Primary Mouse Colon Tumors. J. Vis. Exp. JoVE.

Yamashita, N., Minamoto, T., Ochiai, A., Onda, M., and Esumi, H. (1995). Frequent and characteristic K-ras activation in aberrant crypt foci of colon. Is there preference among K-ras mutants for malignant progression? Cancer *75*, 1527–1533.

Yang, C.-S., Yuk, J.-M., Kim, J.-J., Hwang, J.H., Lee, C.-H., Kim, J.-M., Oh, G.T., Choi, H.-S., and Jo, E.-K. (2013). Small Heterodimer Partner-Targeting Therapy Inhibits Systemic Inflammatory Responses through Mitochondrial Uncoupling Protein 2. PLoS ONE *8*, e63435.

Yazawa, T., Inaoka, Y., Okada, R., Mizutani, T., Yamazaki, Y., Usami, Y., Kuribayashi, M., Orisaka, M., Umezawa, A., and Miyamoto, K. (2010). PPAR-γ Coactivator-1α Regulates Progesterone Production in Ovarian Granulosa Cells with SF-1 and LRH-1. Mol. Endocrinol. *24*, 485–496.

Yu, H., Pardoll, D., and Jove, R. (2009). STATs in cancer inflammation and immunity: a leading role for STAT3. Nat. Rev. Cancer *9*, 798–809.

Yu, S., Tong, K., Zhao, Y., Balasubramanian, I., Yap, G.S., Ferraris, R.P., Bonder, E.M., Verzi, M.P., and Gao, N. (2018). Paneth Cell Multipotency Induced by Notch Activation following Injury. Cell Stem Cell *23*, 46-59.e5.

Yuk, J.-M., Shin, D.-M., Lee, H.-M., Kim, J.-J., Kim, S.-W., Jin, H.S., Yang, C.-S., Park, K.A., Chanda, D., Kim, D.-K., et al. (2011). The orphan nuclear receptor SHP acts as a negative regulator in inflammatory signaling triggered by Toll-like receptors. Nat. Immunol. *12*, 742–751.

Yumoto, F., Nguyen, P., Sablin, E.P., Baxter, J.D., Webb, P., and Fletterick, R.J. (2012). Structural basis of coactivation of liver receptor homolog-1 by β-catenin. Proc. Natl. Acad. Sci. *109*, 143–148.

Zhang, Y., and Wang, L. (2011). Nuclear Receptor Small Heterodimer Partner in Apoptosis Signaling and Liver Cancer. Cancers *3*, 198–212.

Zhang, Y.-Z., and Li, Y.-Y. (2014). Inflammatory bowel disease: Pathogenesis. World J. Gastroenterol. WJG *20*, 91–99.

Zhang, B., Halder, S.K., Kashikar, N.D., Cho, Y., Datta, A., Gorden, D.L., and Datta, P.K. (2010a). Antimetastatic Role of Smad4 Signaling in Colorectal Cancer. Gastroenterology *138*, 969-980.e3.

Zhang, Y., Xu, P., Park, K., Choi, Y., Moore, D.D., and Wang, L. (2008). Orphan receptor small heterodimer partner suppresses tumorigenesis by modulating cyclin D1 expression and cellular proliferation. Hepatology *48*, 289–298.

Zhang, Y., Soto, J., Park, K., Viswanath, G., Kuwada, S., Abel, E.D., and Wang, L. (2010b). Nuclear Receptor SHP, a Death Receptor That Targets Mitochondria, Induces Apoptosis and Inhibits Tumor Growth. Mol. Cell. Biol. *30*, 1341–1356.

Zhang, Y., Hagedorn, C.H., and Wang, L. (2011). Role of nuclear receptor SHP in metabolism and cancer. Biochim. Biophys. Acta *1812*, 893–908.

Zhang, Z., Jones, S., Hagood, J.S., Fuentes, N.L., and Fuller, G.M. (1997). STAT3 Acts as a Co-activator of Glucocorticoid Receptor Signaling. J. Biol. Chem. *272*, 30607–30610.

Zhong, X., Chen, B., and Yang, Z. (2018). The Role of Tumor-Associated Macrophages in Colorectal Carcinoma Progression. Cell. Physiol. Biochem. Int. J. Exp. Cell. Physiol. Biochem. Pharmacol. *45*, 356–365.

Zhou, T., Edwards, C.K., Yang, P., Wang, Z., Bluethmann, H., and Mountz, J.D. (1996). Greatly accelerated lymphadenopathy and autoimmune disease in lpr mice lacking tumor necrosis factor receptor I. J. Immunol. *156*, 2661–2665.

Zhu, Y., Xie, F., Ding, L., Fan, X., Ding, X., and Zhang, Q.-Y. (2015). Intestinal epithelium-specific knockout of the cytochrome P450 reductase gene exacerbates dextran sulfate sodium-induced colitis. J. Pharmacol. Exp. Ther. *354*, 10–17.

Zou, W. (2006). Regulatory T cells, tumour immunity and immunotherapy. Nat. Rev. Immunol. *6*, 295–307.

Zou, A., Lehn, S., Magee, N., and Zhang, Y. (2015). New Insights into Orphan Nuclear Receptor SHP in Liver Cancer. Nucl. Recept. Res. *2*.

10 Acknowledgement

First of all, I would like to express my thanks and gratitude to Prof. Dr. Thomas Brunner for giving me the opportunity to perform my PhD thesis in his laboratory and to work in this exciting project. Thank you for believing in me and always motivating me. Thank you for your continuous support and guidance during all the phases of my project and the great scientific discussions.

My gratitude is also extended to Prof. Dr. Daniel Legler for accepting to be the second advisor of my thesis. Thank you for all the fruitful discussions and the great input.

I would like also to thank Prof. Dr. Christof Hauck for accepting to review my thesis and to attend my thesis committee.

My sincere gratitude also goes to my head department at Khartoum University in Sudan, Prof. Dr. Sania Shaddad for supporting me and believing in me.

My sincere gratitude is also extended to Julia Körner for sharing her great experience in animal experiments with me, thank you for helping me to establish the animal experiments and for your continuous guidance and advice.

I particularly want to thank all the members of the Brunner group for all the wonderful time we shared together. Without the support from all of you this work would not have been done, it was a pleasure meeting you and working as a member of such a wonderful team. My thanks are extended to Juliane, Juan, Anna Pia, San, Konstantin, Svenja, Janine, Paola, Annika, Rebekka, Leonhard, Cindy, Anne, Lea and Valentina. Moreover, my gratitude goes to Regine for handling all the administrative work during my PhD.

My sincere thanks also to Astrid for all the wonderful histological tissue preparations.

Special thanks goes to Eugenia for her continuous support and motivation and for the time she dedicated for reviewing my thesis, I will always be grateful for you.

I would like to thank all staff of the TFA at the University of Konstanz for the kind help and support.

Furthermore, my biggest gratitude and appreciation is extended to my husband Mutaz and my wonderful children Mohamed and Ayman for their unconditional love and support, for their patience during my long working hours especially during weekends and for sharing me the adventure of coming to Germany for my PhD, I will never thank you enough.

Acknowledgement

Besides I would like to thank my father Ahmed for his continuous guidance and support, I learned a lot from you. Your dedication and hard work even during your sickness gave me something to look up to and always motivated me to do my best, I feel blessed for having you as my father. I would like also to thank my mother Aisha for always being in my side, I learned from you how to be patient and to help others and most important to be a very well-organized person like you.

Additionally, I would like to thank my sisters Reem, Rasha, Arwa and Ethar and my brothers Hassan and Mohamed for supporting me during all times and motivating me to do my best.

I want also to thank my second family in Konstanz. Thank you Khawla, Fatima and Zeinab for being there for my family and me all the time.

Finally, I would like to thank all my friends and relatives for their continuous support and motivation.